

AUTOMATED TRANSIT NETWORK VEHICLE EMERGENCY EGRESS  
SYSTEM DESIGN AND ANALYSIS

A Project Presented to  
The Faculty of the Department of  
Mechanical Engineering  
San José State University

In Partial Fulfillment  
Of the Requirements for the Degree  
Master of Science  
in  
Mechanical Engineering

by  
Reza B. Khosroshahi

Dec 2018

© 2018

Reza B. Khosroshahi

ALL RIGHTS RESERVED

SAN JOSÉ STATE UNIVERSITY

The Undersigned Committee Approves

Automated Transit Network Vehicle Emergency Egress

System Design and Analysis

of

Reza B. Khosroshahi

APPROVED FOR THE DEPARTMENT OF MECHANICAL ENGINEERING

---

Dr. Burford J Furman, Committee Chair

Date

---

Dr. Kourosh Youssefi, Committee Member

Date

---

Mr. Edward Cydzik, Committee Member

Date

# ABSTRACT

## Automated Transit Network Vehicle Emergency Egress System Design and Analysis

By Reza B. Khosroshahi

The Spartan Superway is a research project at San José State University that is developing a new form of sustainable urban transportation that uses automated vehicles suspended from a network of elevated guideways. The National Fire Protection Association (NFPA) and the American Society of Civil Engineers (ASCE) require all automated network vehicles to have an emergency egress system capable of evacuating passengers in less than 15 minutes. The objective of this project was to design a means to evacuate passengers from Superway vehicles in case of an emergency. After a state-of-the-art review of the subject and research, escape chutes were found to be the most practical solution for the rapid evacuation of the vehicles. During this project, a model was designed consisting of the chute storage unit and its release mechanism. Off the shelf items were used when possible, and most of the other parts were designed using sandwich-structured composites or 1023 carbon steel. Closed cell PVC foam was used as the core of the sandwich-structured composite parts and fiberglass/epoxy for their skins. Steel parts would have to be either machined from blocks of steel or could be made from sheet metal plates. This unit is designed to be installed on the floor of the vehicles and can be deployed using egress release levers which need to be mounted on the wall of the vehicle. Pulling on the egress lever unlatches the top hatch and the bottom door using Bowden cables. Gravity forces the bottom door to be opened, and the chute gets deployed. At the same time, two gas springs force open the hatch allowing passengers to enter the chute to be lowered to the ground safely. During the design process, the chute frame, the chute support, the door, the hatch, and the housing were analyzed based on the requirements using finite element analysis (FEA). Based on the FEA results, the models were modified until they satisfied the requirements and passed the analyses with a factor of safety of greater than 1.5. Hand calculations were used to estimate the minimum required gas spring compressed force and the maximum allowable latch spring constant based on the requirements. After completion of the design, an animated movie was made to demonstrate the assembly process and the functionality of the system.

## **ACKNOWLEDGEMENTS**

I would like to thank Dr. Burford Furman, the committee chair, for meeting with me on a weekly basis and for his guidance and significant help throughout this project. He has also had a major influence on my career path and has helped me find the job of my dreams. I'll be forever grateful for the impact that he has had on my life. I would also like to thank my committee member, Dr. Kourosh Youssefi for meeting me multiple times throughout my design process. His insights and constructive advice were extremely helpful and resulted in numerous changes of direction in the design paths that were being followed. I also would like to thank Mr. Edwards Cydzik for his time and advice which has had a significant influence in helping me reach my final design.

# TABLE OF CONTENTS

ABSTRACT.....	iv
ACKNOWLEDGEMENTS.....	v
TABLE OF CONTENTS.....	vi
NOMENCLATURE .....	vii
LIST OF TABLES.....	viii
LIST OF FIGURES .....	ix
1.0 INTRODUCTION .....	1
1.1 LITERATURE REVIEW .....	2
1.2 OBJECTIVES .....	2
2.0 METHODOLOGY .....	2
3.0 DESIGN REQUIREMENTS AND SPECIFICATIONS.....	2
4.0 DESIGN DESCRIPTION .....	4
5.0 DESIGN ANALYSIS .....	14
6.0 RESULTS AND DISCUSSION .....	29
7.0 CONCLUSIONS AND RECOMMENDATIONS FOR FUTURE WORK.....	32
REFERENCES .....	33
APPENDICES .....	35
APPENDIX A: FINAL MODEL RELEVANT DOCUMENTS .....	35
APPENDIX B: PREVIOUS MODELS RELEVANT DOCUMENTS .....	56
FIRST GENERATION UNIT .....	56
SECOND GENERATION UNIT .....	57
THIRD GENERATION UNIT .....	58

## NOMENCLATURE

ATN	-	Automated Transit Network
PRT	-	Personal Rapid Transit
ASCE	-	American Society of Civil Engineers
NFPA	-	National Fire Protection Association
FEA	-	Finite Element Analysis

## LIST OF TABLES

Table 1. List of requirements. ....	3
Table 2. Material properties of E-glass fiber/epoxy unidirectional laminate (Samborsky, Mandell, & Agastra, 2017).....	9
Table 3. Material properties of AIREX C70.200 closed cell foam (3accorematerials, 2011). ....	9
Table 4. The estimated overall mass of the unit and the major component. ....	29
Table 5. FEA tabulated results. ....	30
Table 6. Hand calculated results. ....	31
Table 7. Top assembly BOM. ....	35
Table 8. 1023 carbon steel material properties. ....	44
Table 9. E-glass fiber material properties (E-Glass Fibre). ....	70
Table 10. Galvanized steel material properties (SolidWorks material properties). ....	70

## LIST OF FIGURES

Figure 1. Different ATN vehicle designs (Louw, 2016).....	2
Figure 2. Hitachi Monorail emergency egress system (Kimijima, Kim, Furuta, & Sakatsume, 2017). .....	4
Figure 3. Axel Thoms escape chute (Axel Thoms).....	2
Figure 4. Chute frame. ....	5
Figure 5. Chute Support. ....	5
Figure 6. Bottom door.....	6
Figure 7. Bottom door latches.....	6
Figure 8. Gas spring setup. ....	7
Figure 9. Coupon orientation indices and location in thick E-glass fiber/epoxy laminate (Samborsky, Mandell, & Agastra, 2017). ....	8
Figure 10. Housing and hatch design.....	10
Figure 11. Hatch latch.....	11
Figure 12. Housing installation on the vehicle. ....	11
Figure 13. Emergency egress release lever.....	12
Figure 14. Packed escape chute. ....	13
Figure 15. Deployed escape chute. ....	13
Figure 16. Chute support 5052.15 N verification test Von Mises stress and displacement fringe plots.....	15
Figure 17. 2,500 N hatch verification test displacement and Von Mises stress fringe plots. ....	16
Figure 18. 5,000 N hatch verification test displacement and Von Mises stress fringe plots. ....	17
Figure 19. 5,400 N housing verification test displacement and Von Mises stress fringe plots. ....	19
Figure 20. 5,500 N housing verification test displacement and Von Mises stress fringe plots. ....	20
Figure 21. 147.15 N bottom door verification test displacement and Von Mises stress fringe plots. ....	21
Figure 22. 5,130.63 N chute frame verification test deformation and Von Mises stress fringe plots.....	23
Figure 23. Gas spring force calculation setup.....	24
Figure 24. Hatch latch and hatch hinges reaction forces. ....	25
Figure 25. Door latches reaction force.....	26
Figure 26. Maximum combined Bowden cable deployment tension.....	27
Figure 27. Maximum allowable latch spring stiffness calculation setup.....	28
Figure 28. Chute support 5052.15 N verification test mesh and factor of safety.....	37
Figure 29. 2,500 N hatch verification test factor of safety fringe plot.....	38
Figure 30. 5000 N hatch verification test mesh and factor of safety fringe plot.....	39
Figure 31. 5,400 N housing verification test mesh and factor of safety fringe plot.....	40
Figure 32. 5,500 N housing verification test mesh and factor of safety fringe plot.....	41
Figure 33. 147.15 N bottom door verification test mesh and safety factor fringe plot.....	42
Figure 34. 5,130.63 N chute frame verification test mesh and safety factor fringe plot.....	43
Figure 35. Sheet metal frame 1 drawing. ....	45
Figure 36. Sheet metal frame 2 drawing. ....	46
Figure 37. Housing drawing. ....	47
Figure 38. Hatch drawing. ....	48

Figure 39. Chute support drawing.....	49
Figure 40. Bottom door drawing.....	50
Figure 41. Chute support bracket drawing.....	51
Figure 42. Barrel adjuster bracket drawing.....	52
Figure 43. Left side door latch bracket drawing. ....	53
Figure 44. Emergency egress lever drawing.....	54
Figure 45. Emergency egress lever housing. ....	55
Figure 46. First generation release mechanism.....	56
Figure 47. Second generation release mechanism. ....	57
Figure 48. Second generation unit closed and open positions. ....	57
Figure 49. Third generation model. ....	58
Figure 50. Third generation chute ring. ....	59
Figure 51. Third generation bottom door latch. ....	59
Figure 52. Third generation steel hatch exploded view. ....	60
Figure 53. Third generation steel hatch deformation and stress due to 2500 N of force. ....	61
Figure 54. Third generation E-glass fiber hatch deformation and stress due to 2500N of force. ....	62
Figure 55. Third generation steel hatch deformation and stress due to a 5000N force.....	63
Figure 56. Third generation E-glass fiber hatch deformation and stress due to a 5000 N force.....	64
Figure 57. Force required to open the third generation hatches.....	65
Figure 58. Third generation housing stress and deformation due to 5000 N of force.....	65
Figure 59. Third generation housing stress and deformation results due to having ten people inside the chute.....	66
Figure 60. Third generation unit overall dimension.....	67
Figure 61. Third generation hatch drawing.....	68
Figure 62. Third generation housing dimensions.....	69
Figure 63. Axel Thoms' standard escape chute drawing. ....	71
Figure 64. Axel Thom's certificate. ....	72
Figure 65. Axel Thoms DIN explanation.....	73

## 1.0 INTRODUCTION

The growth of population has had many impacts on the world such as traffic congestion, global warming, and carbon footprint. Many companies and organizations have been working toward reducing these effects. One way of having a positive impact on these outcomes is by creating environmentally friendly public transportation networks. Metro systems are usually very costly and require tunneling and relocation or destruction of existing infrastructure or culturally valuable structures (Timan, 2015). Thus, metro systems are not an option for all places. Elevated transit systems bypass these obstacles since they are mostly built on existing roadways and are elevated above the ground. Personal rapid transit (PRT) networks and urban gondolas are two types of driverless transit vehicles that are attracting a lot of attention. These systems do not interact with ground traffic and have their right of way, which gives them high reliability in travel time (Tahmasseby & Kattan, 2015). They are also environmentally friendly and result in low emission, noise pollution, and energy use (Tahmasseby & Kattan, 2015).

Currently, multiple companies are working on automated transit network (ATN) vehicles with a goal of eliminating the need for using cars to get to the destination in urban environments. A variety of ATN vehicles can be seen in Figure 1. Spartan Superway is an interdisciplinary project from San José State University with the goal of designing a solar-powered personal rapid transportation system. The Spartan Superway system consists of mini-van sized vehicles that move along guideways that are elevated about nine meters above ground. The vehicle cabins, which can hold four to six people are suspended from the guideways using bogies (a sub-assembly of wheels and means of propulsion to move the vehicle). Each vehicle has its motor, route selection element, power supply, and brakes. Suspending the vehicles below the guideway frees the area above the guideway for mounting solar photovoltaic (PV) panels, which results in a slimmer guideway structure compared to the approach where a vehicle moves above the guideway (like an automobile on an overpass). Suspending vehicles reduce the possibility of accidents caused by people jumping from the guideway or putting themselves in front of a moving vehicle. Most of the noise from ATN vehicles is caused by the movements of the bogies over the guideway; covering the guideways with solar panels reduces sound pollution drastically. Suspending the vehicles below the guideway also allows the bogies to be protected from snow, ice, and debris, resulting in less maintenance. The goal is to cover most areas in cities and have multiple stations in most neighborhoods. A mobile app is being developed, which would give users the ability to request podcars at their desired station 24/7. The podcar will then take passengers from origin to destination with no stops in between. The goal is to revolutionize the transportation industry in urban environments while reducing carbon footprint and having a positive impact on global warming. However, there are many challenges that The Spartan Superway is facing, including the need to have an emergency egress system.

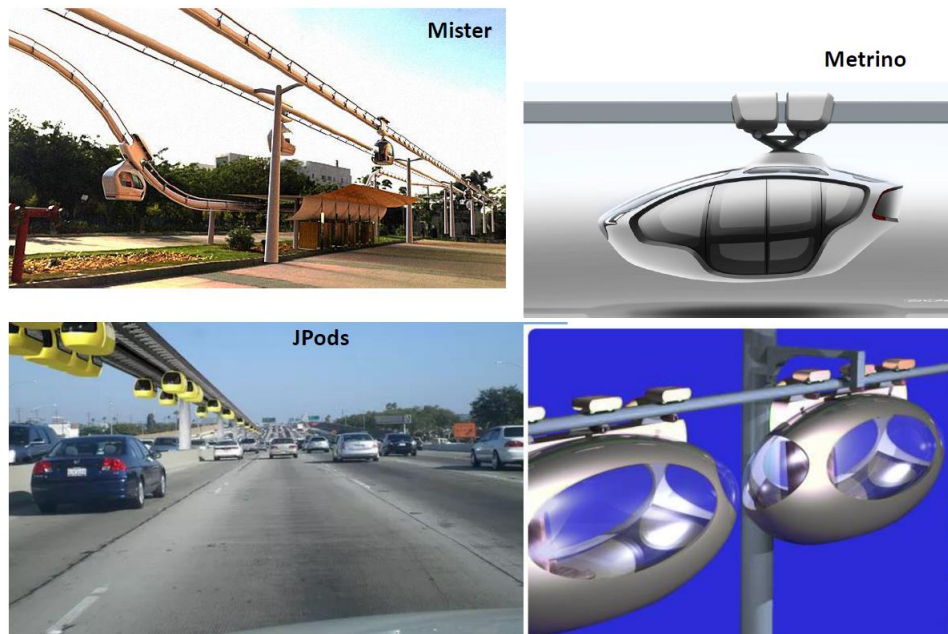


Figure 1. Different ATN vehicle designs (Louw, 2016). Suspended transit network vehicles don't interact with ground traffic and can mostly be constructed without significant changes to the current infrastructure of cities.

## 1.1 LITERATURE REVIEW

Based on the American Society of Civil Engineers (ASCE) (2013), all automated people movers are required to have elevated emergency walkways or an acceptable “other suitable means” to using an elevated walkway. Such a system will be useful in case of a fire, smoke, hazardous gas, toxins, vehicle collision, or act of terror which could have catastrophic and life-threatening outcomes.

Based on a study done on aircraft evacuation, it was found that the most critical factor that leads to successful and efficient evacuation are crew assistance and passenger safety education (Chang & Yang, 2011). Since ATN vehicles have no crew to educate or assist the passengers with evacuation, the emergency egress system has to be extremely easy to operate. The most common method to evacuate passengers from passenger rail systems is to send an evacuation team to the vehicles and evacuate passengers using walkways (American Society of Civil Engineers, 2013). This may be a relatively easy task for trains where all the passengers are in connected wagons, but it is going to be much more laborious and time-consuming to evacuate PRT vehicles this way since cabins are separated and distant from one another.

To design an evacuation system for ATN vehicles, many similar systems were studied such as fire escapes and public transportation egress systems. The initial plan to evacuate vehicles was to separate cabins from bogies and lower cabins to the ground using pulleys, gears,

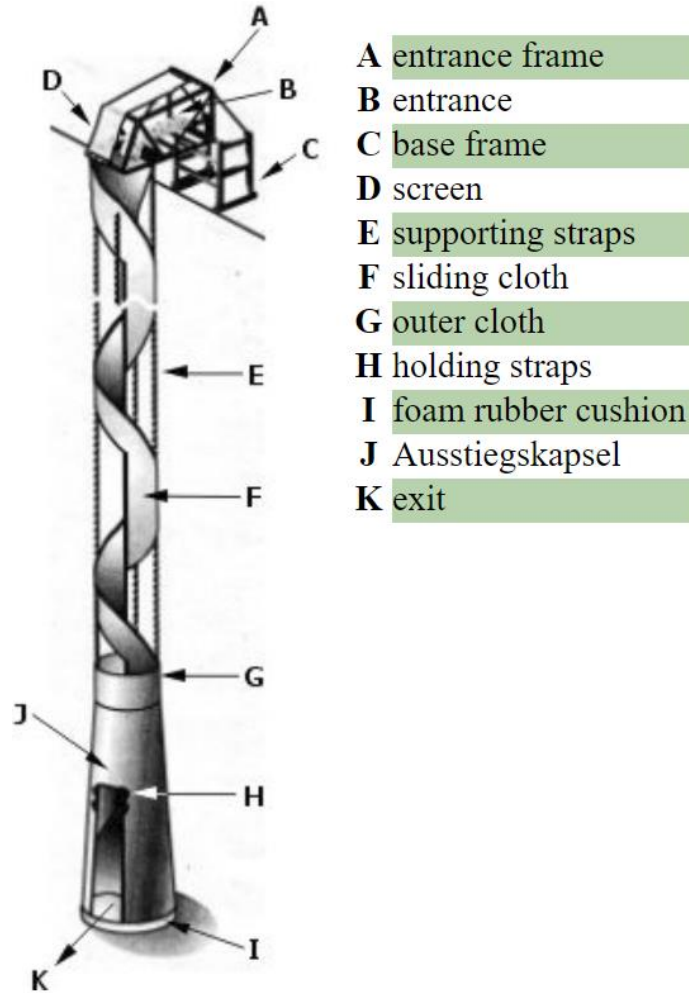
and cables. However, designing such a system would be very expensive and would not be practical for this project. An evacuation system that is used in gondola lifts and ski lifts is to send an evacuation team to climb up the supports, approach gondolas or lifts using climbing/rescue gears, and lower people to the ground one by one using harnesses and ropes. The ASCE requires passengers to be evacuated from automated people movers within no more than 15 minutes (American Society of Civil Engineers, 2013). Many times it takes hours to evacuate passengers in ski resorts when ski lifts or gondola lifts become disabled; thus, this method cannot be used for this project. Another evacuation method that was considered for this project is using emergency escape ladders. These ladders usually require a vertical surface along the length of the ladder against which they can rest. Otherwise, they would swing and would be hard to climb down from. More rigid escape ladders that don't require a vertical surface to lean against are available in the market, but they are heavy and require large storage spaces. Also, escape ladders are not very safe, especially for the elderly, children, and people with disabilities. Due to these reasons, it was decided not to use escape ladders for this project. Most subways use walkways to evacuate passengers. Since the Spartan Superway's podcars are suspended from the guideways, walkways need to be leveled with the cabins, or secondary pathways need to be designed to provide access to the walkways. In case of an emergency, after reaching the walkways, passengers need to walk to the nearest station to get to the point of safety. Walkways require stronger and larger supporting structures, take a lot of space, use a lot of material, and are not aesthetically pleasing. Due to these reasons, it was decided not to use walkways for vehicle evacuation. Another evacuation method that was studied is using SkySavers, which are used to evacuate buildings in case of an emergency. To use a SkySaver, the user must first attach the carabiner provided in the kit to a preassembled steel hanger over the window. The carabiner is connected to a cable, which is stored inside the backpack. The user should then put on the backpack, secure its straps, and jump out the window. The mechanism inside the backpack provides the user with a controlled descend and lowers the user to the ground safely. This method was also crossed out since it can cause death or serious injuries if not used properly and is not a suitable solution for people who have a fear of height.

An emergency evacuation system that has been attracting a lot of attention lately is escape chute. Escape chutes are fabric tubes used for vertical escape in a variety of places such as buildings and elevated public transportation systems. As shown in Figure 2, Hitachi, a Japanese company, is currently using spiral escape chute as a means of emergency egress in their Daegu monorail system in South Korea (Kimijima, Kim, Furuta, & Sakatsume, 2017). Portable spiral escape chutes are used by firefighters to lower people to the ground from a variety of places at different heights. The chutes are typically stored in custom designed units and can be deployed if needed. After deployment, users can enter the chute, and the chute gradually lowers them to the ground. Axel Thoms is a German manufacturer that custom designs spiral chutes based on customer's needs. Their escape chutes consist of an outer e-glass textile fire-proof layer, which protects users from fire and smoke. The inner layer of their chutes comprises of a spiral fabric, which allows users to slide down the chute with a speed of less than 2.5 meters per

second in a counterclockwise manner (Thoms, 2018). These chutes prevent users from a vertical collision and provide multiple exit points at two-meter intervals using multi-zipper exits (Hay, 2018). This makes them suitable for ATN vehicles since the descent elevation varies depending on the location of the vehicle. Axel Thoms chutes vary in length from two meters to 150 meters, have a mass of 1.25kg per meter, and have been load tested with a mass of up to 10,000 kilograms (Hay, 2018). A typical evacuation rate of Axel Thoms chute is eight to ten people per minute and can be used by children, pregnant women, disabled people, and most obese individuals (Thoms, 2018). Depending on customer requirements, these chute units typically cost anywhere between 6,000 to 11,080 dollars. However, if ordered in large quantities, a discount of 40 to 50 percent can be applied to the order (Thoms, 2018). The chutes can be packaged in small spaces and packaging is flexible (Thoms, 2018). Refer to Figure 3 to get a better understanding of Axel Thoms chute design. It was decided to use spiral escape chutes for emergency evacuation of ATN vehicles due to their advantages over the other candidates.



Figure 2. Hitachi Monorail emergency egress system (Kimijima, Kim, Furuta, & Sakatsume, 2017). Hitachi, a Japanese company, is using escape chutes for the emergency egress system of its monorails in South Korea.



- A entrance frame
- B entrance
- C base frame
- D screen
- E supporting straps
- F sliding cloth
- G outer cloth
- H holding straps
- I foam rubber cushion
- J Ausstiegskapsel
- K exit

Figure 3. Axel Thoms escape chute (**Axel Thoms**). Axel Thoms is a German manufacturer of ISO 9001 certified spiral chutes. These chutes are packable and can be deployed in case of an emergency. They allow people to descend to the ground smoothly through their inner part if needed. They protect users from Smoke and fire and have a thick padded bottom to reduce the final impact.

## 1.2 OBJECTIVES

The objective of this project was to design an emergency egress system to safely evacuate passengers from an ATN vehicle to the ground in case of an emergency. A unit consisting of the housing of the chute and its release mechanism was designed based on the requirements and standards set by the associated organizations and the author. The major components were analyzed to assess whether they could tolerate the operating conditions without any failure. Lastly, an animated movie was made to demonstrate the functionality of the unit.

## **2.0 METHODOLOGY**

During the first phase of the project, a state-of-the-art review of the literatures regarding egress systems was conducted. Then, standards and requirement related to suspended automated transit network vehicles were investigated to ensure the designed system would satisfy all the corresponding regulations and criteria. Also, a set of requirements were created based on the author's professional opinion. Throughout this comprehensive review, the most practical solution for emergency evacuation of the Spartan Superway's podcars was chosen. During the research phase, a variety of emergency egress systems such as building evacuation, public transit evacuation, and airplane evacuation systems were studied. Emails were sent to multiple escape chute manufacturers to obtain information about their products and to establish whether or not escape chute would be a practical evacuation system for automated transit network vehicles. After deciding on the evacuation method, release mechanisms, hatches, doors, locks, basic mechanisms, and materials were studied to develop a design. Based on the requirements, various hand sketches and simplified CAD models were generated and discussed with the committee members. After obtaining committee members' approvals, more detailed designs were generated using SolidWorks 2017. Throughout the design process, FEA analysis was performed using this software to check for failures and to make sure all the requirements were satisfied. Based on the FEA results, the design was improved and tested until all the design criteria were met. Hand calculations were used to calculate the maximum stiffness of the latch springs based on the maximum allowable lever pull force. The moments about the pivot point of the hatch were also hand calculated to assess whether the gas springs were capable of lifting the hatch after deployment. After obtaining a final design, an animated movie was produced to present the functionality of the unit.

## **3.0 DESIGN REQUIREMENTS AND SPECIFICATIONS**

As required by the ASCE, emergency egress systems for automated people movers must provide an evacuation method to evacuate vehicles within 15 minutes (American Society of Civil Engineers, 2013). Passengers should be able to open the emergency exit without powered assistance from the inside of the cabin with a force of no more than 130N (29lb) (American Society of Civil Engineers, 2013). The egress hatch should be operable with no more than one operation, and a hold-open device must be integrated into the hatch to automatically latch the door in the open position to prevent accidental closure (National Fire Protection Association, 2007). Passengers should be able to operate the emergency egress hatch manually without special tools from the interior and exterior of the vehicle (National Fire Protection Association, 2007).

The following requirements were chosen based on the professional opinion of the author. The system should be capable of being used by adults, children, pregnant women, disabled passengers, and obese people. Fast descent can cause distress, pressure change, and ear discomfort, thus the vertical egress travel speed should not exceed 10 m/s (Fortune). The emergency exit hatch should be able to withstand 2500 N of force applied to the center of the hatch on an area covered by a circle with a 30 cm diameter. The maximum deflection from this load should be less than one millimeter. The hatch should also be able to withstand 5000 N of force distributed over its top surface. The chute support should withstand the weight of the chute and five 100 kg passengers inside the chute. All models should pass the criteria with a safety factor of 1.5. Refer to

Table 1 for the overall list of the requirements.

Table 1. List of requirements. The specified requirements in this table were either chosen based on the conducted research or by the author’s professional opinion. The design of the emergency egress unit was based on these criteria.

<b>Requirements</b>	<b>Based On</b>
Vehicles must be able to be evacuated within 15 minutes.	ASCE
The egress system should be operable with a force of less than 130N (29lb).	ASCE
Accidental closure of the hatch must be prevented using a hold-open mechanism.	NFPA 130
Emergency egress hatch must be operable without the use of special tools.	NFPA 130
The egress hatch should be operable with no more than one operation.	NFPA 130
The system should be able to be used by adults, children, pregnant women, disabled passengers, and obese people.	Author
The egress travel speed should not exceed 10 m/s.	Author
The hatch should be able to withstand 2,5000 N of force applied to its center on a 30 cm diameter circle with a deflection of no more than one millimeter.	Author
The hatch should be able to withstand 5,000 N of force distributed over its top surface.	Author
The chute support should be able to withstand having five 100 kg people inside the chute.	Author
All models should pass the criteria with a safety factor of more than 1.5.	Author

The designed emergency egress unit has a flange on each side of its housing, which can be secured to the floor of the vehicles using adhesives. However, using adhesives will permanently bond the housing to the base of the cabin. It is also possible to machine the housing and add screw clearance holes on the flanges to mount the housing on the cabin using bolts. In order to install this egress system on a podcar, a stepped hole must be made in the floor of the cabin in the exact size of the housing. The unit consists of off-the-shelf items, machined parts, sheet metal parts, and sandwich-structure composites. Refer to Table 7 to see the Bill Of Material (BOM) of the top assembly. The estimated mass of the components can also be seen in Table 4.

#### **4.0 DESIGN DESCRIPTION**

A series of models were designed before reaching the final design. Refer to appendix to see some of the initially designed models. The following design procedures and descriptions apply to the final model only.

The first step in the design of the unit was the chute frame design, which encompasses the chute support, the chute, and some parts of the release mechanism. As shown in Figure 4, the main body of this subassembly consists of two sheet metal panels, which can be laser cut and bent to produce their final shape. The panels have a jog at one of their ends; these jogs would come in contact with the face of the other part after installation. To secure the panels in place, four spot welds need to be applied to each side of the frame. The maximum recommended thickness of each member to be spot welded is three millimeters (Make It Metal). Based on this recommendation, gauge 12 carbon steel was used for the panels, which has a thickness of 2.656 mm (Metal Supermarkets, 2018). The maximum common diameter of spot welds is 12.5 mm, and the spacing between them, from center to center should be a minimum of 10 material thickness (ideally 20 times the material thickness to reduce shunting effects with a minimum spacing of half an inch) (Make It Metal). The center of the weld should also be located one to two diameters away from the edge of the part or other features in the part (Make It Metal). Based on these recommendations, 12.5 mm diameter spot welds, 70 mm of space between the centers of the spot welds, and 26.5mm of space between the spot welds and the edge of the part were used in this design. The flanges on top of the frame are meant to be used to mount the frame to the housing.

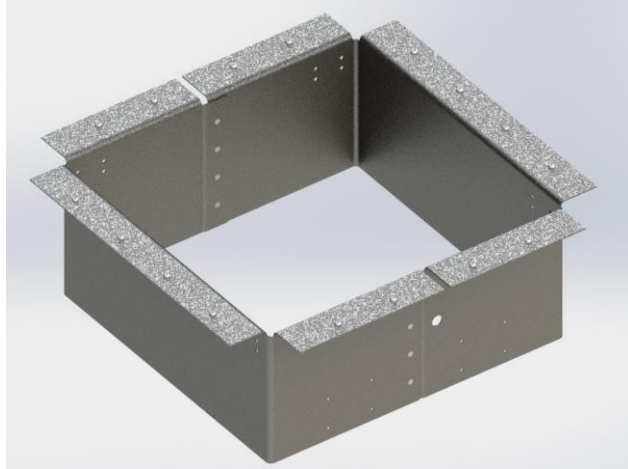


Figure 4. Chute frame. This frame encompasses the chute support, the chute, and parts of the release mechanism. It is mainly made out of two sheet metal panels which are bonded to each other using spot welds. Four metal brackets are connected to this frame using bolts to hold the chute support.

The chute support shown in Figure 5 is designed based on one of the standard model drawings obtained from Axel Thoms. Refer to Figure 63 in the appendix to see the drawing of this standard unit. However, the width of the support was increased by around 100 mm to take into consideration the size of obese people. Four 1023 carbon steel brackets are mounted on this frame to hold the chute support in place. These brackets can be machined using a CNC milling machine and can each be installed on the frame using four M8 bolts and nuts.

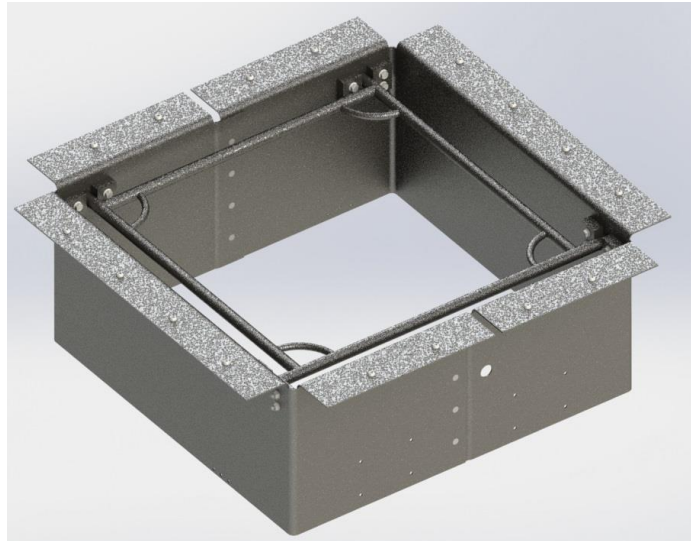


Figure 5. Chute Support. The chute support used in this model is the scaled-up model of Axel Thoms chute frame and can be installed on the frame using four machined brackets and 16 M8 nuts and bolts.

After installing the chute brackets, the bottom door needs to be installed on the chute frame. The bottom door is secured to one side of the chute frame using two hinges and nuts and bolts as shown in Figure 6. The purpose of this door is to hold the escape chute enclosed inside the frame after installation and release it as it's needed.

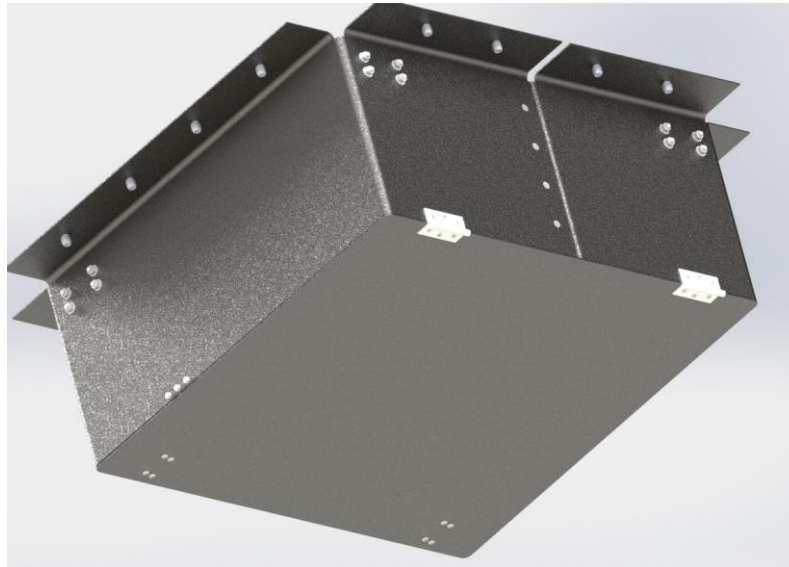


Figure 6. Bottom door. Two hinges secure the bottom door to the frame. The door is used to hold the chute enclosed inside the unit and deploy it as required.

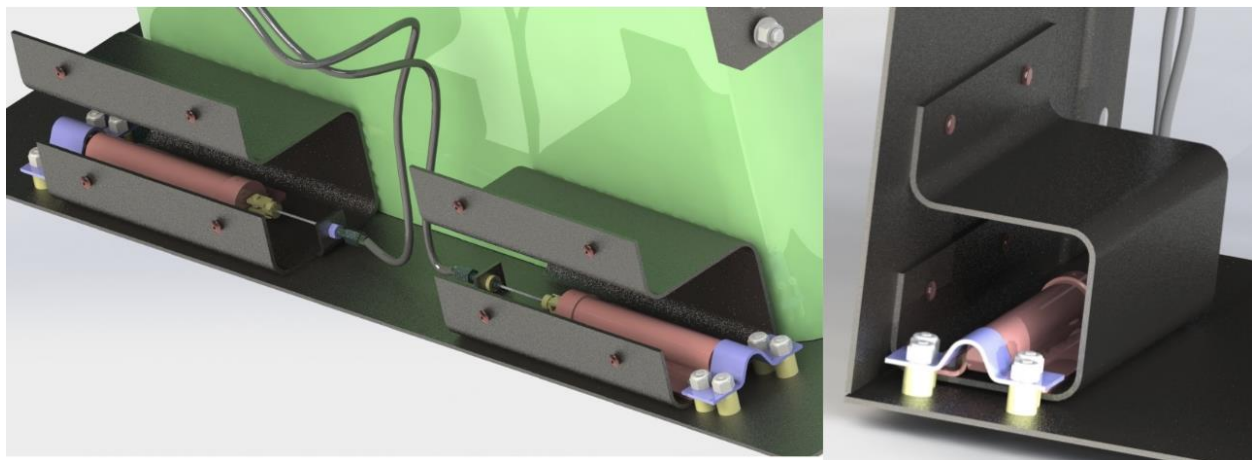


Figure 7. Bottom door latches. Two spring-loaded latches are secured on the chute frame using brackets. These latches and two hinges on the other side of the frame hold the door in the closed position. A cross-sectional view of the assembly is shown in the right figure. The chute frame is hidden in the left figure to present a better visual understanding of the position of these subassemblies.

The next installation procedure is the installation of two ball stud mounting bracket on each side of the chute frame using nuts and bolts. Then ball socket end fittings need to be installed at each end of the gas springs. These end fittings can then be pressed into the ball stud mounting brackets and can be secured in place using ball socket safety clips. The purpose of these gas springs is to push open the hatch as it is unlatched.



Figure 8. Gas spring setup. Two gas springs are mounted on the chute frame using ball socket end fittings and ball stud mounting brackets. These gas springs are used to force open the hatch as it is unlatched.

One of the most important and time-consuming parts of this unit was the design of the housing. The housing needs to be strong enough to support the chute and people inside of it. It should also be able to withstand the weight of the passengers standing on it. One crucial factor that was taken into consideration during this step was to design a lightweight and at the same time a robust housing. In order to achieve these goals, sandwich-structure composites were used for the housing. Sandwich composites are a special type of laminated composites where a relatively thick, soft, light-weight, and weaker core is sandwiched between two thin and stiff fiber reinforced skins (Kumar, Milwich, Deopura, & Plank, 2011). This structure creates a body with high bending stiffness and high strength to weight ratio compared to monolithic structures (Kumar, Milwich, Deopura, & Plank, 2011). The core of these structures carries the through-the-thickness shear load, while the laminated skins resist in-plane and bending loads (Daniel, Gdoutos, Wang, & Abot, 2002). The common types of failure for these types of structures subject to bending and shear loads include shear failure of the core, tension or compression failure of the faces, debonding of the core and face, local indentation, and global buckling (Daniel, Gdoutos, Wang, & Abot, 2002). Closed-cell Foams are common materials for the core

of these structures. Fiberglass is stronger than many metals by weight; it has a low cost, high production rate, high strength, high stiffness, relatively low density, it is non-flammable, and has a high heat resistance (E-Glass Fibre). Due to these advantages, it was decided to use E-glass fiber as the skin layer of the housing and the hatch.

During a series of experiments performed at Montana State University, test coupons were made from E-LT 5500 unidirectional E-Glass fiber and Epikote MGS RIMR 135/Epicure MGS RIMH 1366 epoxy resin. Static tensile, compressive, and shear stress-strain tests were then performed in the three primary material directions, which resulted in the determination of their strengths, elastic constants, and best fits to stress-strain curves (Samborsky, Mandell, & Agastra, 2017). Refer to Figure 9 for the material directions and coupon orientations for the test coupons. The material and mechanical properties of these specimens were used to run simulations on the models. These properties can be seen in Table 2.

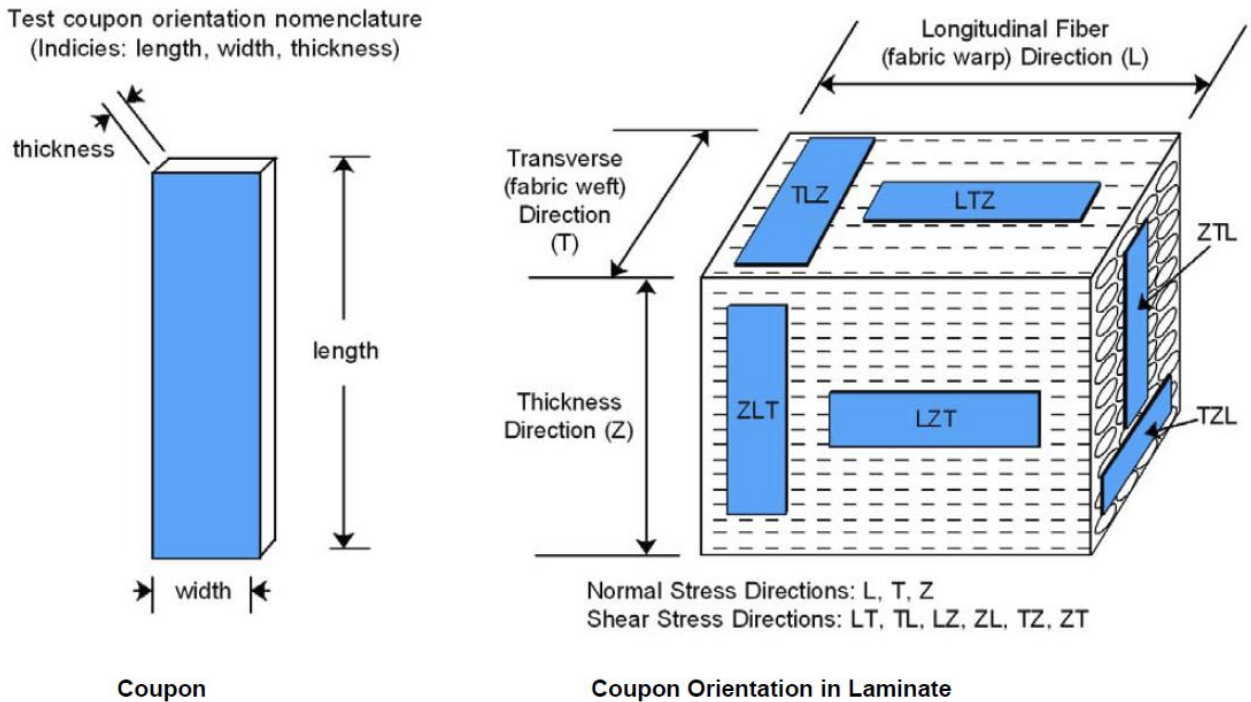


Figure 9. Coupon orientation indices and location in thick E-glass fiber/epoxy laminate (Samborsky, Mandell, & Agastra, 2017). The material and mechanical properties of the E-Glass fiber/epoxy specimens were found by mechanically testing the specimens with the orientation shown in this figure.

Table 2. Material properties of E-glass fiber/epoxy unidirectional laminate (**Samborsky, Mandell, & Agastra, 2017**) The following material properties were used for the fiberglass/epoxy laminate layer during the FEA analysis.

<b>Property</b>	<b>Value</b>	<b>Units</b>
Elastic Modulus EL	44600	MPa
Elastic Modulus in ET	17000	MPa
Elastic Modulus in EZ	16700	MPa
Poisson's Ratio $\nu_{LT}$	0.262	N/A
Poisson's Ratio $\nu_{TZ}$	0.35	N/A
Poisson's Ratio $\nu_{LZ}$	0.264	N/A
Shear Modulus GLT	3.49 e-6	MPa
Shear Modulus GTZ	3.46 e-6	MPa
Shear Modulus GLZ	3.77 e-6	MPa
Mass Density	1854.42	Kg/m <sup>3</sup>
Tensile Strength L	1240	MPa
Tensile Strength T	43.9	MPa
Compressive Strength L	774	MPa
Compressive Strength T	179	MPa
Shear Strength LT	55.8	MPa
Yield Strength	44	MPa

After doing some research, it was decided to use AIREX C70.200 PVC closed-cell, cross-linked polymer foam for the core of the sandwich-composite structures. This foam has excellent strength and stiffness to weight ratio; it has a good impact strength, high fatigue resistance, and self-extinguishing capability (3accorematerials, 2011). Machining operations such as sanding, milling, drilling, and sawing can be performed on this foam (3accorematerials, 2011). Closed cell foams have non-linear behavior, however, to simplify the analysis, AIREX C70.200 was assumed to be linear. Refer to Table 3 for the material properties of this foam.

Table 3. Material properties of AIREX C70.200 closed cell foam (**3accorematerials, 2011**). The following material properties were used during the FEA analysis of the housing and the hatch. Closed cell foams have non-linear behavior; however, to simplify the analysis the foam was assumed to be linear.

<b>Property</b>	<b>Value</b>	<b>Units</b>
Elastic Modulus	175	MPa
Poisson's Ratio	0.32	N/A
Shear Modulus	75	MPa
Mass Density	200	Kg/m <sup>3</sup>
Tensile Strength	6	MPa
Compressive Strength	5.2	MPa
Yield Strength	5.7	MPa
Thermal Conductivity	0.048	W/(m.K)

FEA analysis was performed on a variety of housings and hatches, and the models were refined and optimized to reach the final design. The final design of the housing and the hatch can be seen in Figure 10. The housing and the hatch are both sandwich-structural composites with AIREX C70.200 closed cell PVC foam core and fiberglass epoxy skin. The hatch is composed of a 40 mm thick layer of foam, which is covered with a 5 mm layer of fiberglass/epoxy laminate. The thickness of the foam layer in the housing varies due to its geometry; however, a uniform three-millimeter thick fiberglass/epoxy layer covers it completely. To fabricate the core, PVC foam blocks can be machined and bonded to each other using adhesives to generate the final shape. Since PVC foam is relatively soft, it is recommended to insert and bond wooden blocks to the foam in places where threaded inserts are to be installed. After fabricating the housing and the hatch and installing the threaded inserts, the hatch can be installed on the housing using two three-way adjustable concealed hinges. After that, the chute frame subassembly can be mounted onto the housing using 16 M8 bolts. The gas spring can then be connected to the hatch using ball socket end fittings and ball stud mounting bracket.

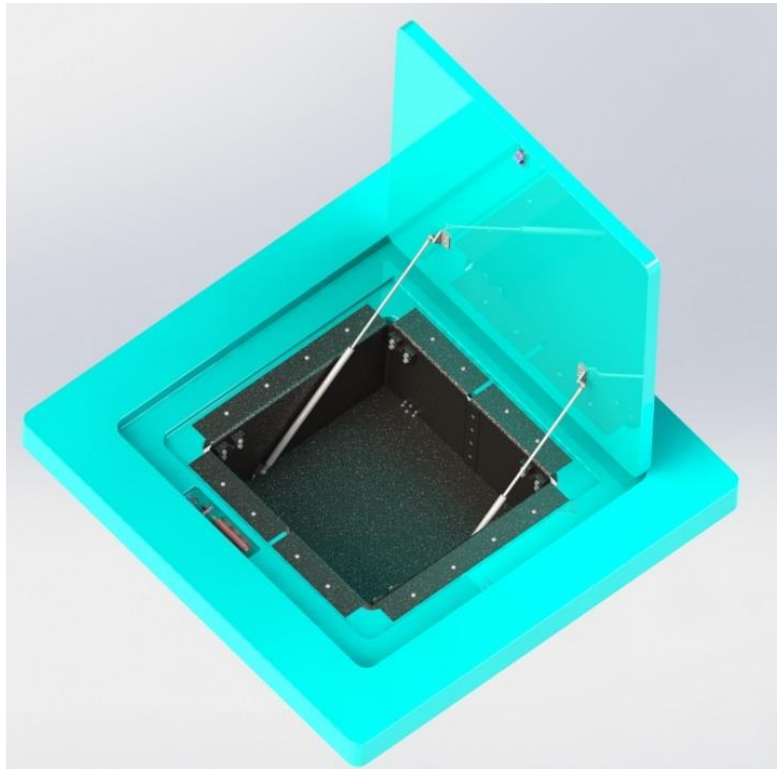


Figure 10. Housing and hatch design. The housing and the hatch are both sandwich-structural composites consisting of an AIREX C70.200 closed cell PVC foam core and a fiberglass epoxy skin.

The housing contains a pocket on its top surface where a spring-loaded latch has to be installed as shown in Figure 11. As the hatch is pressed down against this latch, it gets secured in the closed position. Similar to the bottom door latches, a Bowden cable is connected to the end

of the latch using a clevis connector. Increasing tension in the cable unlatches the hatch. A barrel adjuster is also mounted on a sheet metal bracket inside this pocket which allows assemblers to adjust the tension in the cable.

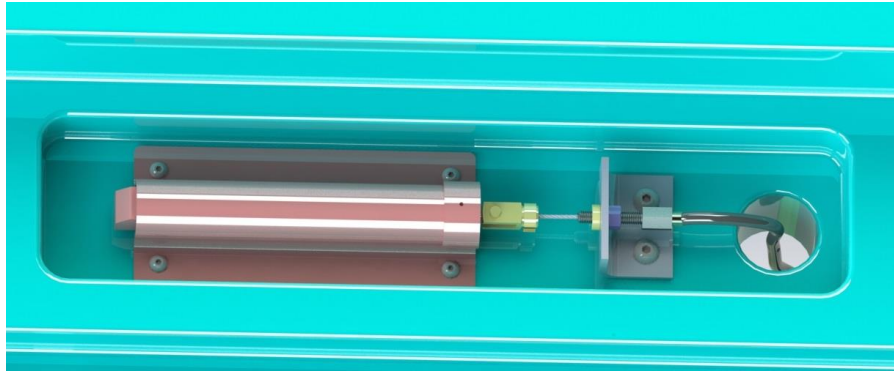


Figure 11. Hatch latch. The hatch latch has to be fastened in the pocket on the top surface of the housing. This spring-loaded latch secures the hatch in the closed position and releases it as tension in the Bowden cable attached to its end is increased.

After assembling all the components on the housing, the housing can be mounted on the floor of the vehicle using adhesives, which would permanently bond the housing in place. It is also possible to drill screw clearance holes on the flanges of the housing and use screws to mount the housing on the vehicle. As shown in Figure 12, a stepped hole has to be created on the floor of the vehicles in order to install the housing on the vehicle. After the assembly is completed, the top surface of the housing and the hatch would be flushed with the floor of the cabin.

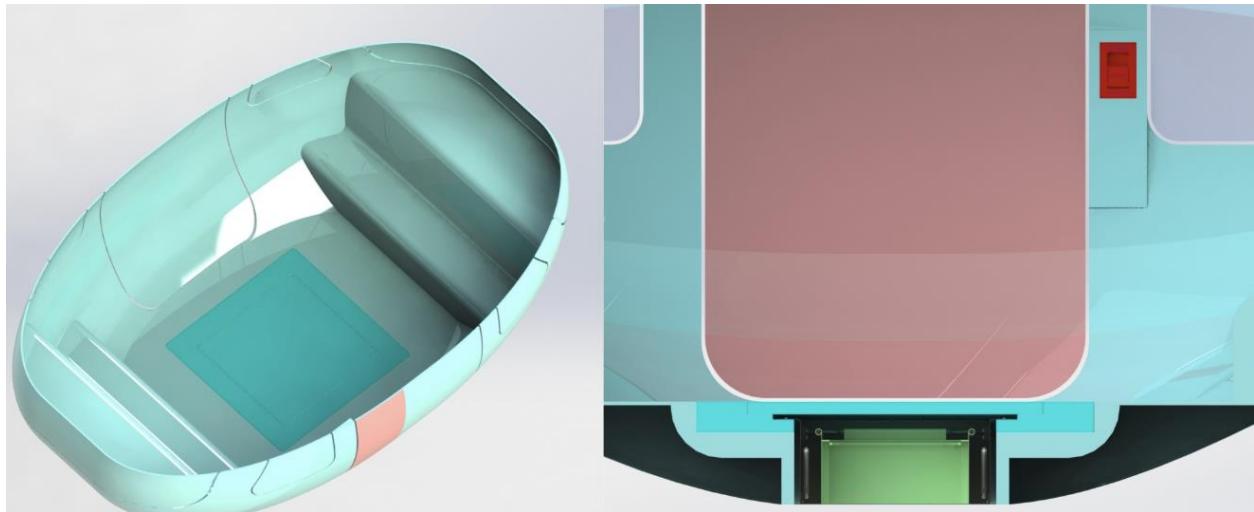


Figure 12. Housing installation on the vehicle. The housing can be installed on the pre-created stepped hole on the vehicle floor using adhesives. Both images show cross-sectional views of the vehicle.

Overall, three spring-loaded latches and three sets of Bowden cables and barrel adjusters exist in the system. Two latches secure the bottom door in place, and the other one secures the hatch. One side of the Bowden cables needs to be connected to the latches, and the other end to the emergency egress lever as shown in Figure 13. Pulling on the lever results in an increase of tension in the cables, thus the latches get retracted. It is recommended to install a tube or routing rings behind the wall of the cabin to guide the cables to the connecting points. It would be easier to first connect one end of the cables to the egress lever, guide them down through the routing rings or tubes toward the latches and then connect them to the latches. The emergency egress release unit needs to be placed on a panel on the wall of the vehicle as shown in Figure 12.

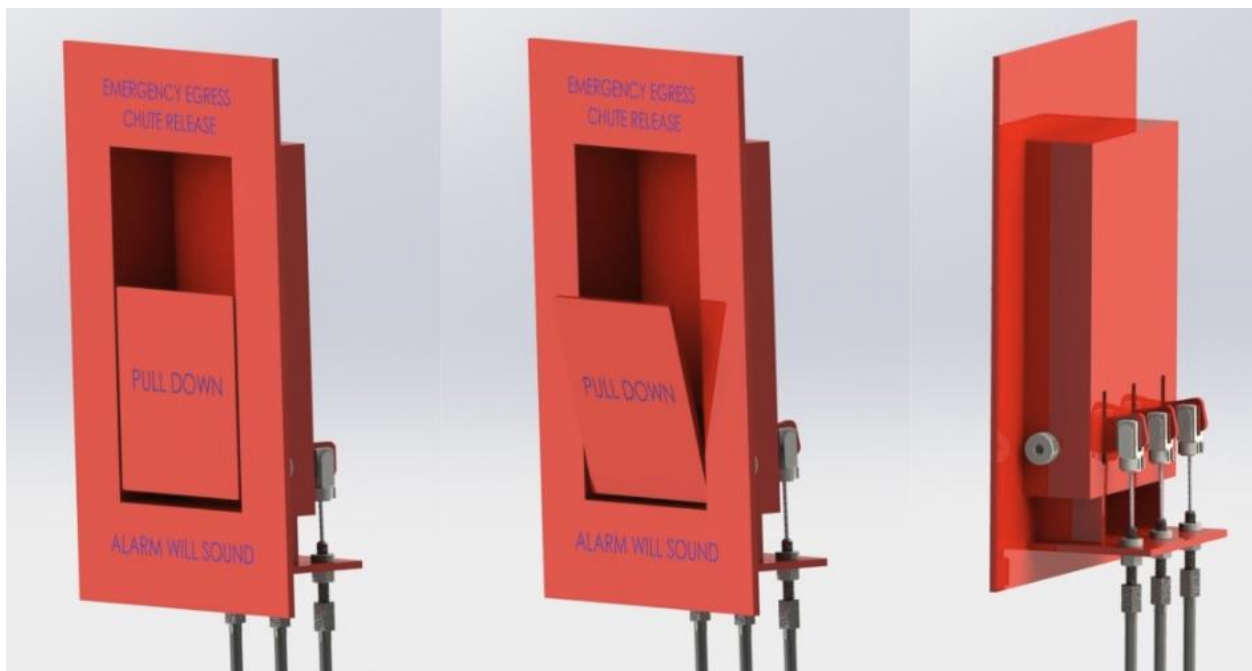


Figure 13. Emergency egress release lever. Three sets of Bowden cables are connected to the emergency egress release lever. The other ends of the cables are connected to the spring-loaded latches. Pulling on the lever pulls on the cables and unlatches the latches.

The Final step in the installation is the installation of the escape chute into the unit. The chute can be packed inside a bag or a cover and connected to the chute support before installation. This subassembly can then be installed inside the chute frame. The chute bag or cover needs to have a removable base that could be detached after installation to allow the chute to be deployed.



Figure 14. Packed escape chute. The escape chute can be packed inside a bag and connected to the chute support before installation. This subassembly can then be installed onto the frame.

After the unit is completely installed, the chute can be deployed as shown in Figure 15. Pulling down the emergency egress lever unlatches all three latches. The weight of the door and the chute would force open the bottom door, and the gas springs would push the hatch open, allowing passengers to use the chute to escape to safety.

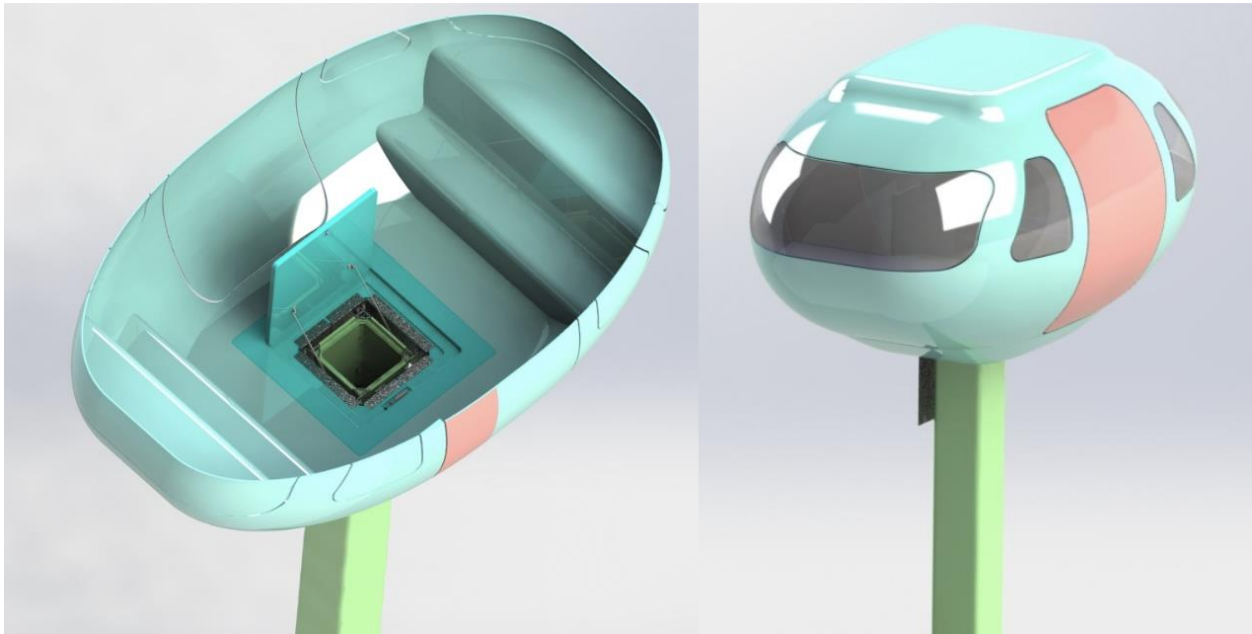


Figure 15. Deployed escape chute. The chute can be deployed by pulling down the emergency egress lever. The image on the left shows the cross-sectional view of the vehicle, and the image on the right shows the exterior of the vehicle when the chute is released. The bogies and the guideways are excluded from this figure.

## 5.0 DESIGN ANALYSIS

After doing some research and getting a better understanding of the system, a set of requirements were chosen. Some of these requirements were set based on the standards and regulations that are governed by the associated agencies and organizations, and some others were chosen by the author. To make sure the designed unit meets all the design criteria, FEA analysis and hand calculations were performed throughout the design process. All FEA analyses were performed using SolidWorks 2016.

As a requirement, the chute support must be able to withstand the weight of the chute and five 100 kg people inside the chute. In order to verify this, using SolidWorks simulation, roller fixtures were placed at each end of the support, on the same surfaces where contacts would be made with the chute support brackets. The chute weighs around 1.25 kg/m; thus, a ten-meter chute weighs about 12.5 kg. To take into consideration the weight of the chute bag and the chute connectors, the mass was rounded up to 15 kg. The mass of the chute, chute bag, and five 100 kg people inside the chute would result in a force of equal to 5,052.15 N. This force was then distributed vertically over the top surface of the support in the same locations where the chute supports would be secured. 1023 carbon steel was defined as the material of the support; the material property was chosen from the SolidWorks database as shown in **Table 8**. A fine standard mesh was applied to the part and a simulation was performed. The initial model failed the analysis due to high stress concentrations in its body. The model was then refined, and the diameter of the rods was increased until the support passed the simulation with a safety factor of 1.55. Refer to Figure 28 in the appendix to see the factor of safety plot and the meshed part. As shown in Figure 16, the maximum displacement in the chute support was found to be equal to 0.87 mm, and the maximum Von Mises was found to be equal to 182.2 MPa.

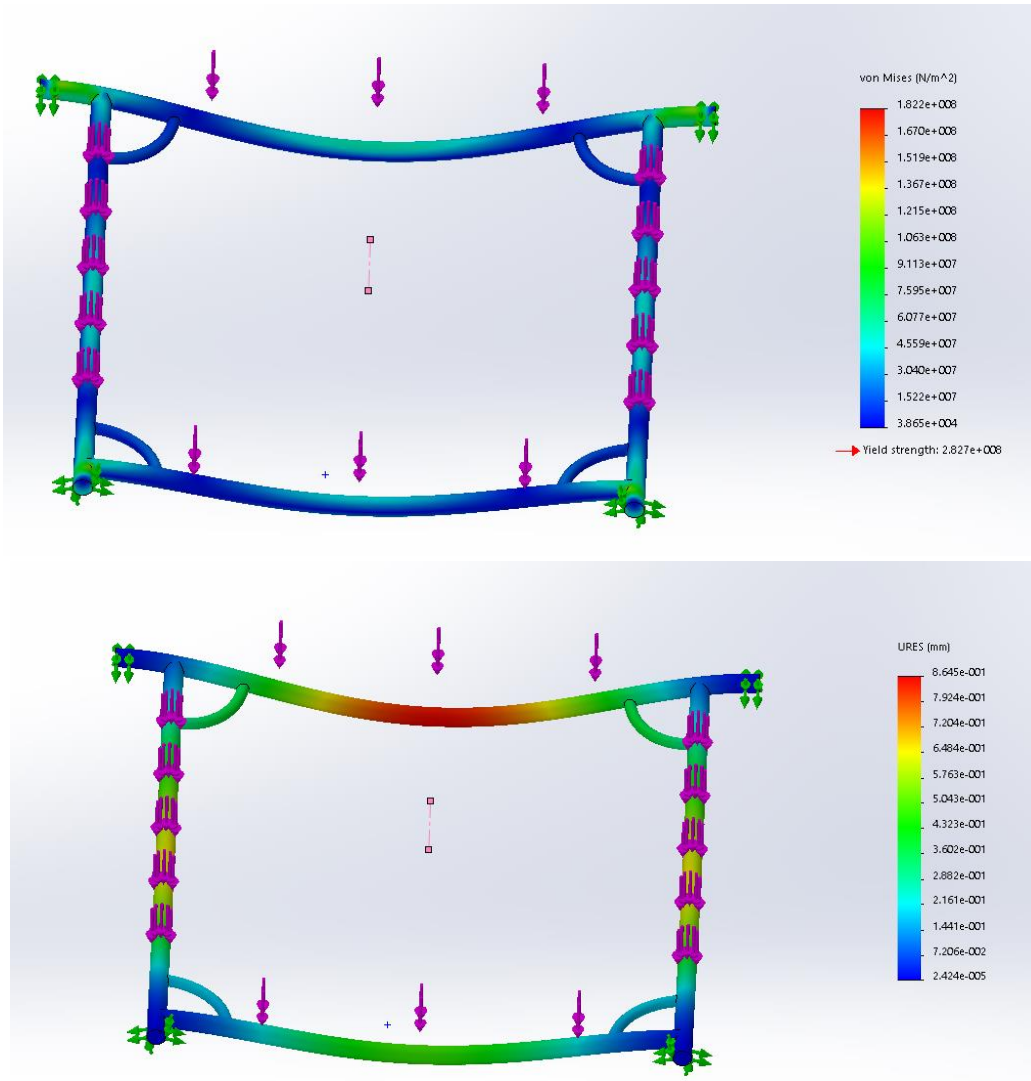


Figure 16. Chute support 5052.15 N verification test Von Mises stress and displacement fringe plots. FEA analysis was performed by adding rollers to the ends of the rods shown with green arrows and applying a force of 5052.15 N to the top surface of the support shown with purple arrows. As shown in the top image, the maximum Von Mises stress is equal to 182 MPa, and as seen in the bottom picture, the maximum displacement was found to be equal to 0.87 mm.

As a requirement, the hatch must be able to withstand a force of equal to 2,500 N at the center of its top surface in a circle with a diameter of 30 mm without failing or having a displacement of more than 1 mm. In order to simplify the analysis, the threaded insert, pockets, holes and all the external parts were removed from the model. The PVC foam core and the fiberglass/epoxy layer were modeled separately and mated to each other. The material properties of the core were defined as shown in Table 3, and the material properties of the fiberglass/epoxy skin were set as shown in Table 2. The direction of the fibers was defined to be parallel to the top

surface and the longer side of the hatch. A bonded contact was specified between the two bodies, and a standard fine mesh was applied to the subassembly as shown in Figure 30 in the appendix. The same surface of the hatch that would come in contact with the housing at its closed position was fixed, and 2,500 N of force was distributed on its top surface as previously described. The initial models failed to meet the requirements. Based on the simulation results, the overall thickness of the part was increased, and the thickness of the fiberglass/epoxy layer was changed to reach an optimum design with a high strength to weight ratio. As shown in Figure 17, the maximum displacement was found to be equal to 1 mm at the center of the hatch, and the maximum Von Mises stress was simulated to be equal to 6.62 MPa in the fiberglass/epoxy layer. As shown in Figure 29 in the appendix, hatch passed the simulation with a safety factor of 3.34.

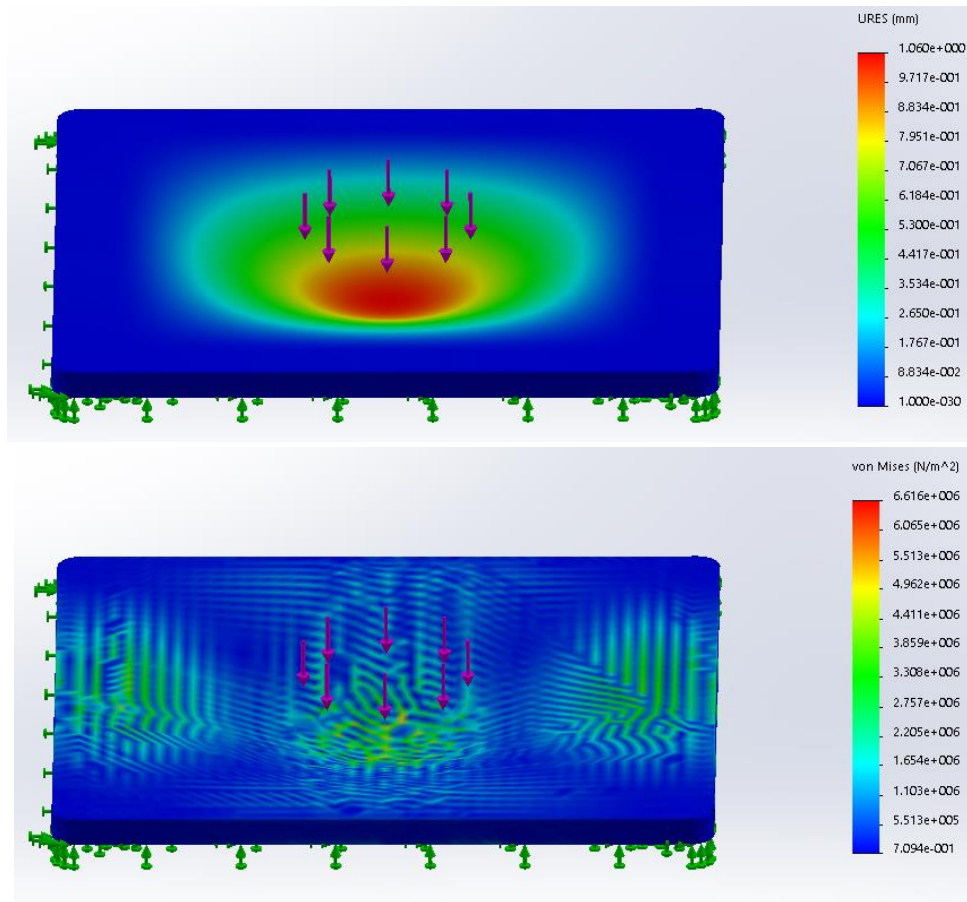


Figure 17. 2,500 N hatch verification test displacement and Von Mises stress fringe plots. The green arrows in the images represent the areas which were fixed during this analysis, and the purple arrows represent the direction of the force and the location at which they were applied. As shown in the top image the maximum displacement was found to be equal to 1 mm at the center of the hatch, and as presented in the bottom image, the maximum Von Mises stress was found to be equal to 6.62 MPa located in the fiberglass/epoxy layer.

As a requirement, the hatch must be able to withstand 5,000 N of force distributed over its top surface without any failure, using a safety factor of 1.5. The same model and fixture as the previous analysis were used to run this simulation. However, instead of 2,500 N of force, 5,000 N of force was distributed over the top surface of the hatch. As shown in Figure 18, the maximum displacement was found to be equal to 2.45 mm at the center of the hatch, and the maximum Von Mises stress was found to be equal to 15.8 MPa in the fiberglass/epoxy layer. As presented in Figure 30, the hatch passed the simulation with a safety factor of 1.52.

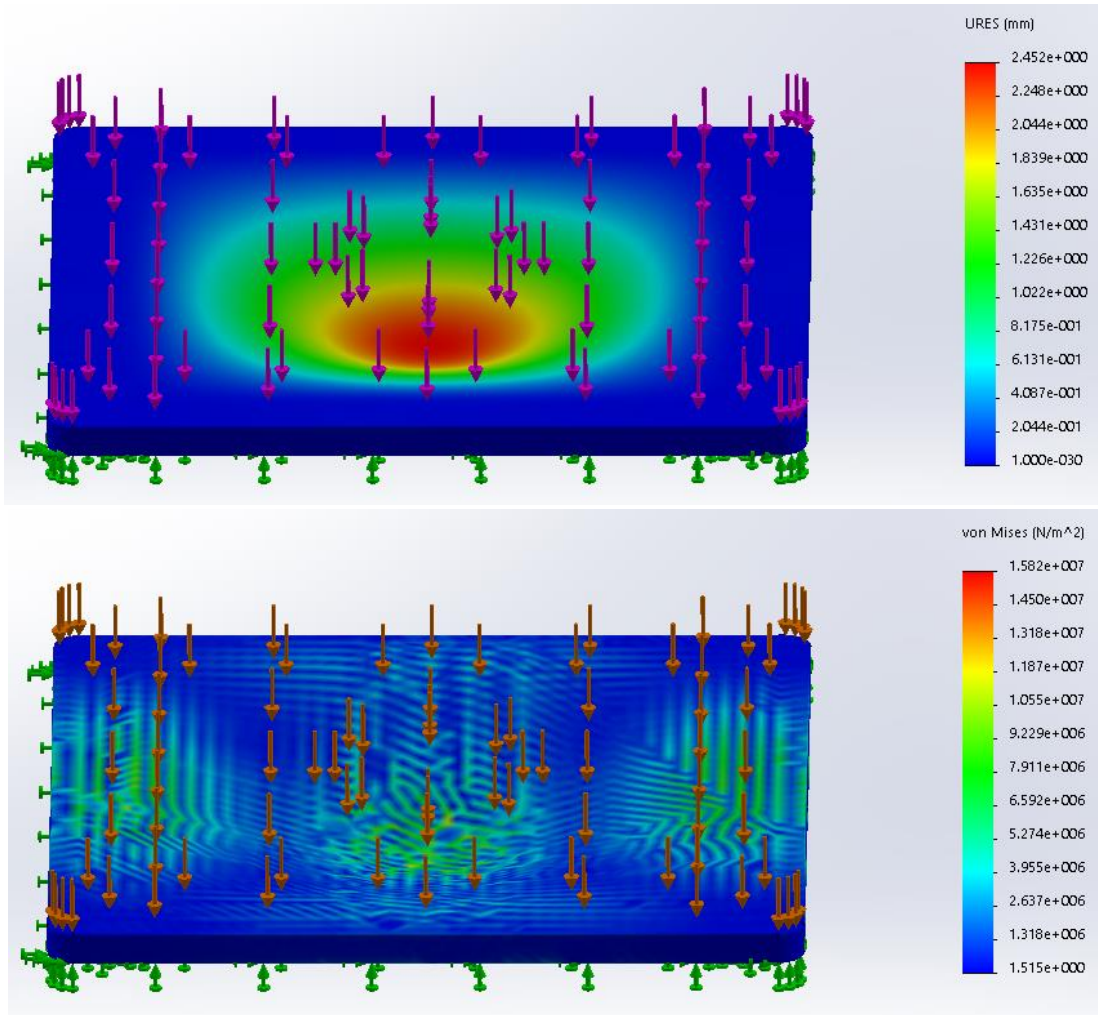


Figure 18. 5,000 N hatch verification test displacement and Von Mises stress fringe plots. The green arrows in the images represent the areas which were fixed during this analysis, and the purple arrows represent the direction of the force and the location at which they were applied. As shown in the top image, the maximum displacement was found to be equal to 2.45 mm at the center of the hatch, and as presented in the bottom image, the maximum Von Mises stress was found to be equal to 15.8 MPa in the fiberglass/epoxy layer.

As a requirement, the housing must be able to withstand the weight of the hatch and five 100 kg people standing on it. To test the housing, the PVC foam core and the fiberglass/epoxy layer were modeled separately and mated to each other. The material properties of the core were defined as shown in Table 3, and the material properties of the fiberglass/epoxy skin were specified as shown in Table 2. The direction of the fibers was defined to be parallel to the top surface and the longer side of the hatch. A bonded contact was defined between the two bodies, and a standard fine mesh was applied to the subassembly as shown in Figure 31 in the appendix. The same surface of the housing that would be bonded to the vehicle floor was fixed; this fixed area consists of a 140 mm wide area all around the bottom surface of the hatch toward its side faces. After that, 5400 N of force which is approximately equal to the weight of the hatch and five 100 kg people was applied normal to the surface where the hatch would be mounted on. The initial models passed the test. However, it was decided to reduce the thickness of the fiberglass/epoxy layer to reduce the weight of the hatch. After a series of designs and simulations, it was decided to use a 3mm thick fiberglass/epoxy layer. As shown in Figure 19, the maximum displacement was found to be equal to 0.19 mm, and the maximum Von Mises stress was established to be equal to 4.2 MPa in the fiberglass/epoxy layer. As presented in Figure 31 in the appendix, the housing passed the simulation with a safety factor of 10.

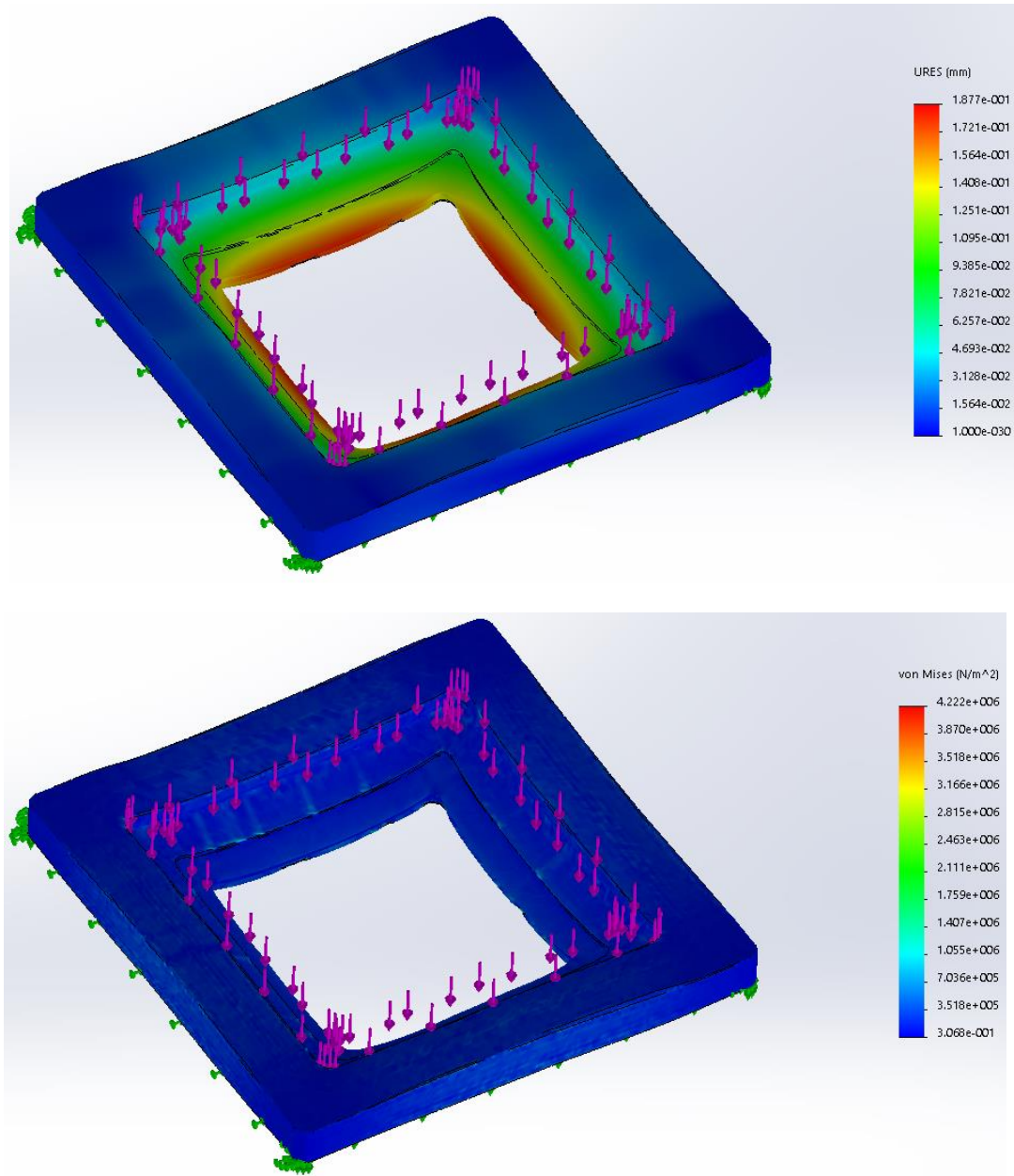


Figure 19. 5,400 N housing verification test displacement and Von Mises stress fringe plots. The green arrows in the images represent the areas which were fixed during this analysis, and the purple arrows represent the direction of the force and the location at which they were applied. As shown in the top image, the maximum displacement was found to be equal to 0.19 mm, and as seen in the bottom image, the maximum Von Mises stress was established to be equal to 4.2 MPa in the fiberglass/epoxy layer.

As a requirement, the housing must be able to withstand the weight of the chute frame, all its enclosed parts, and the five 100 kg people inside the chute with a safety factor of 1.5. The resulting force was approximated to be equal to 5,500 N. The same model and fixture as the

previous analysis was used to run this simulation. However, the magnitude of the force and the location where it was applied was changed. To run the simulation, 5,500 N of force was distributed normally on the surface where the chute frame would be mounted on. As shown in Figure 20, the maximum displacement was found to be equal to 0.56 mm, and the maximum Von Mises stress was established to be equal to 10 MPa in the fiberglass/epoxy layer. As presented in Figure 32, the housing passed the simulation with a safety factor of 4.35.

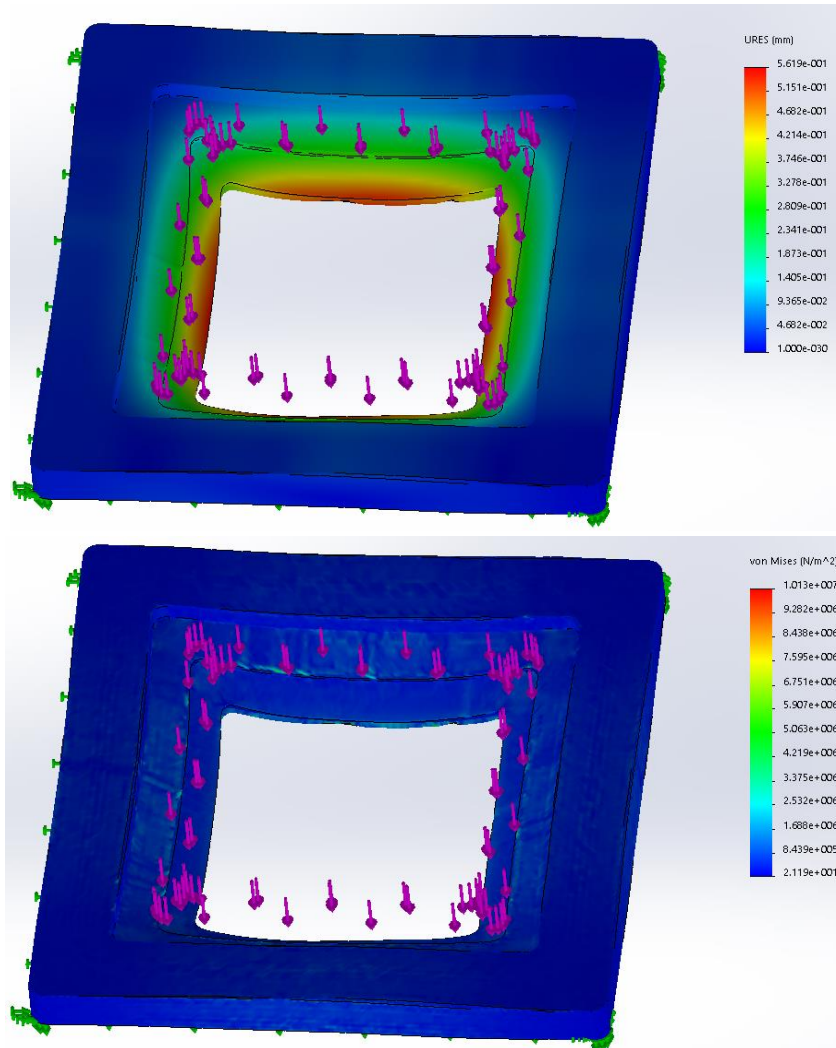


Figure 20. 5,500 N housing verification test displacement and Von Mises stress fringe plots. The green arrows in the images represent the areas which were fixed during this analysis, and the purple arrows represent the direction of the force and the location at which they were applied. As shown in the top image the maximum displacement was found to be equal to 0.56 mm, and as presented in the bottom picture, the maximum Von Mises stress was established to be equal to 10 MPa in the fiberglass/epoxy layer.

As a requirement, the bottom door must be able to withstand the weight of the chute and the chute bag; this results in approximately 15 kg of mass. The door is held in the closed position

using two hinges and two latches. Overall 14 clearance holes are used to fasten the door to the hinges and the latches. In order to run the simulation, all these holes were fixed, and a force of 147.15 N was applied to the same surface where the chute and its bag would be placed. As shown in Figure 33 the door was meshed using a fine standard mesh. Gauge 12 1023 carbon steel was used to design the door, and SolidWorks material property database was used to run the simulation. Refer to Table 8 in the appendix to see the material properties used throughout the analysis. As presented in Figure 21, the maximum Von Mises stress was found to be equal to 105.2 MPa, and the maximum deformation was established to be equal to 1.062 mm at the center of the door. As seen in Figure 33, the part passed the analysis with a safety factor of 2.

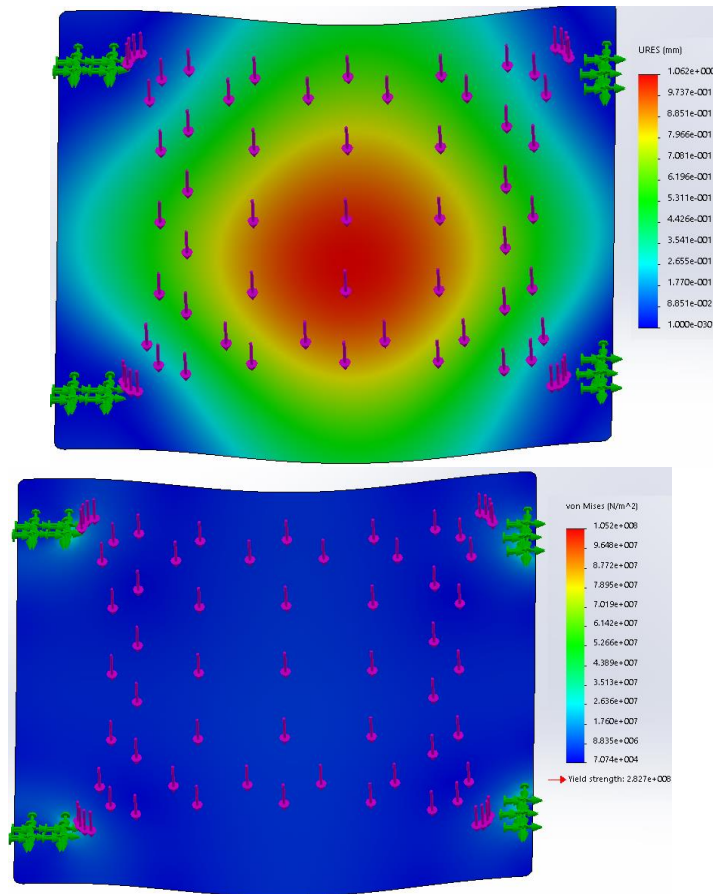


Figure 21. 147.15 N bottom door verification test displacement and Von Mises stress fringe plots. To run the simulation, the door was fixed at the clearance holes shown with green arrows. 147.15 N of force was then applied normal to its top surface, based on the weight of the chute and its cover. The force direction and the location over which it was distributed is shown with purple arrows. As presented in the top image, a maximum deformation of 1.062 mm was established at the center of the door and based on the bottom image, a maximum Von Mises Stress of 105.2 MPa was found in the part.

As a requirement, the chute frame must be able to withstand the weight of the chute, the chute bag, the chute support, and five 100kg people inside the chute. This results in approximately 523 kg of mass. The chute support transfers the load of all the mentioned masses to the chute frame. In order to simplify the analysis, all the parts except the sheet metal frame and the chute support brackets were excluded from the analysis. Pinned connections without rotation and translation were defined between all the clearance holes of the chute support brackets and the sheet metal frame. 1023 carbon steel was used for all the parts based on the SolidWorks material property database. Refer to Table 8 to see the material properties that were used during the simulation. As described in section 4.0, four 12.5 mm in diameter spot weld connections were defined at the contact points of the sheet metal parts, and the bottom surface of the chute frame flanges was fixed. Then a downward force of 5130.63 N was distributed between the four chute frame brackets on the same surfaces where the chute support would be mounted on. As shown in Figure 34, a fine standard mesh was applied to the subassembly, and the simulation was performed to check for failures. Due to multiple failed analyses, the thickness of the sheet metal parts and the clearance hole sizes were modified until a safety factor of greater than 1.5 was achieved. As shown in Figure 22, 0.22 mm of maximum deformation was found in the frame, and the maximum stress was established to be equal to 127.3 MPa located around the clearance hole of the sheet metal frame. Based on the safety factor fringe plot presented in Figure 34, the subassembly passed the simulation with a safety factor of 2.22.

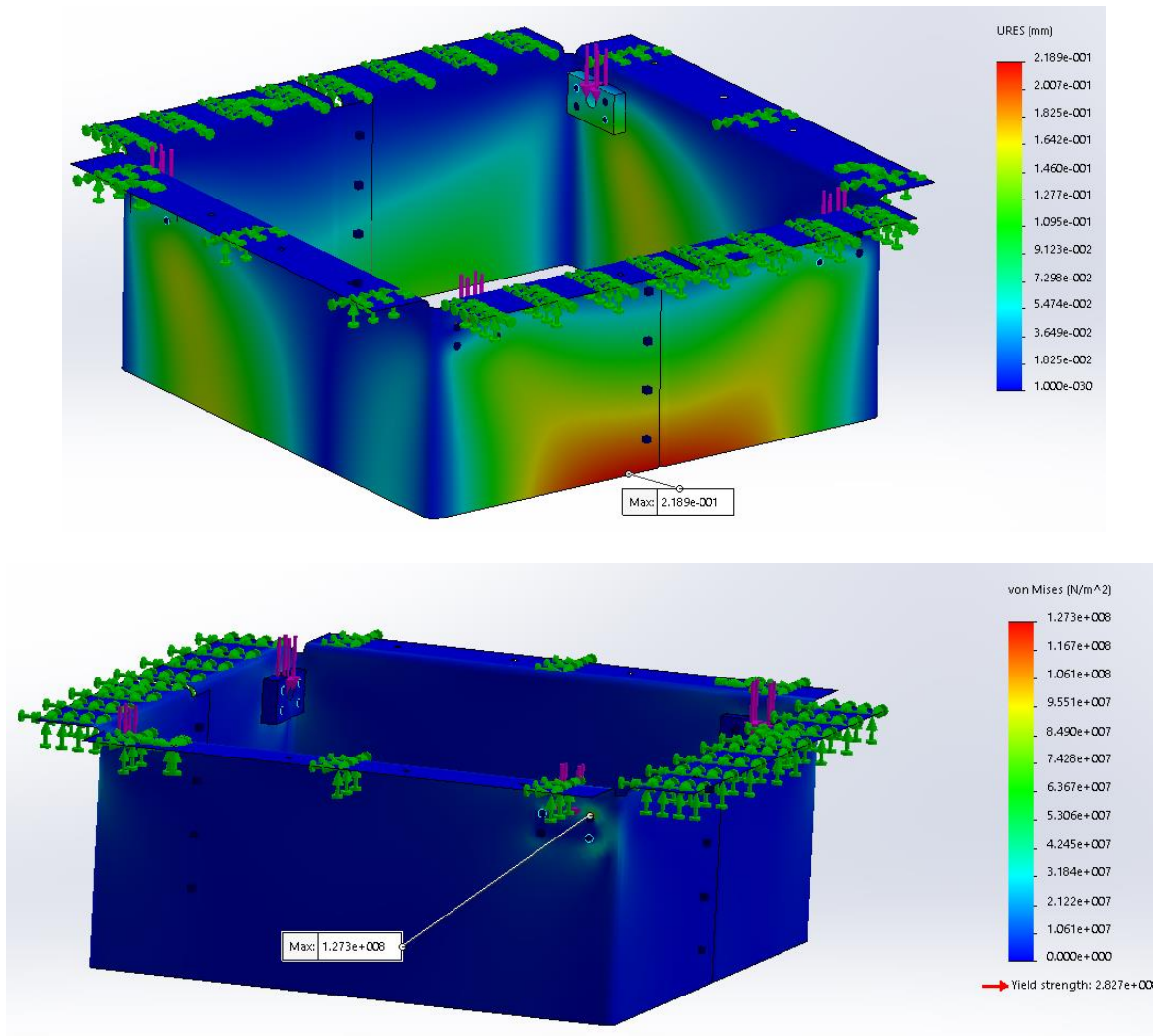


Figure 22. 5,130.63 N chute frame verification test deformation and Von Mises stress fringe plots. To run the simulation, the bottom surfaces of flanges was fixed, and eight spot weld connections were defined between the two sheet metal parts. Pinned connections were specified through the clearance holes of the brackets and the frame, and a downward force of 5,130.63 N, shown with purple arrows was distributed on the brackets. As shown in the top image, 0.22 mm of maximum deformation was found in the chute frame, and a maximum Von Mises stress of 127.3 MPa was established around the clearance hole of the sheet metal frame.

In order to choose gas springs, hand calculations were performed to estimate the minimum force required to lift the hatch. The setup shown in Figure 23 was used to estimate this unknown.

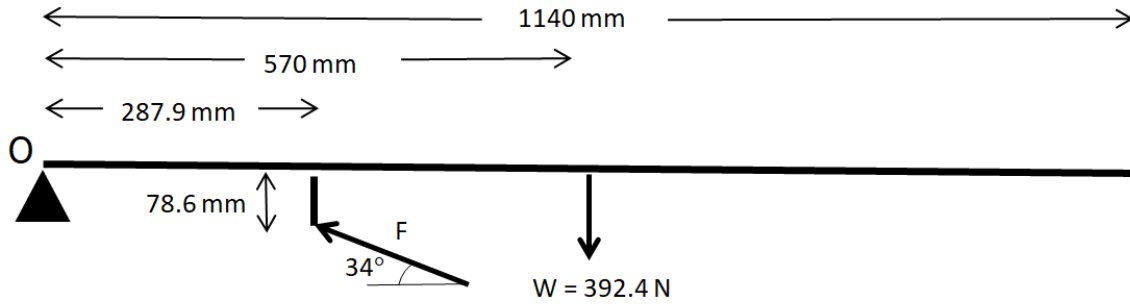


Figure 23. Gas spring force calculation setup. The setup shown in this figure was used to calculate the minimum force required to lift open the hatch. The horizontal line represents the hatch.  $W$  is the force due to the mass of the hatch at its center of gravity. The triangle in this image represents the hinges and is a pinned connection, and  $F$  represents the minimum required force to open the hatch.

$$\begin{matrix} \curvearrowright \\ + \end{matrix} \sum M_O = 0 \quad \longrightarrow \quad \sum M_O = 287.9 \times F \sin(34^\circ) - 78.6 \times F \cos(34^\circ) - 570(392.4) = 0 \quad (1)$$

$$F = 2,330.12 \text{ N} < 2(F_{gs}) \quad (2)$$

$$F_{gs} > 1,165.06 \text{ N} \quad (3)$$

$$F_{gs} = 1,468 \text{ N} \quad (4)$$

Based on the above calculations, each gas spring needs to exert a minimum force of 1,165.06 N when fully compressed. Each of the gas springs that were chosen for the model exert a force of 1,468 N when fully compressed.

It is required by the ASCE for the emergency egress system to be operable with a force of no more than 130N. To ensure this criterion is met, the reaction forces at the latches in the undeployed position of the unit had to be calculated. To calculate the hatch latch reaction force, the setup shown in Figure 24 was created and the following calculations were executed.

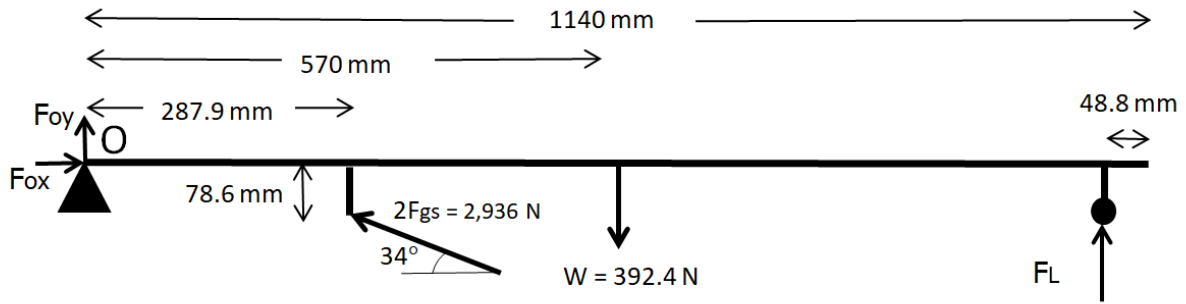


Figure 24. Hatch latch and hatch hinges reaction forces. The setup shown in this figure was used to calculate the reaction forces at the hatch latch and hatch hinges. The horizontal line represents the hatch.  $W$  is the force due to the mass of the hatch at its center of gravity. The triangle in this image represents the hinge (pinned connection), and the roller on the right side represents the latch.  $F_{gs}$  is the gas spring compressed force,  $F_L$  is the latch reaction force, and  $F_{ox}$  and  $F_{oy}$  are the hinge reaction forces.

$$\begin{aligned} \sum M_O = 0 \quad \longrightarrow \quad \sum M_O = 287.9 \times 2,936 \sin(34^\circ) - 78.6 \times 2,936 \cos(34^\circ) - 570(392.4) + (1,140 - 48.8)F_L = 0 \end{aligned} \quad (5)$$

$$F_L = -52.87 \text{ N} \quad (6)$$

$$\sum F_x = 0 \quad \longrightarrow \quad \sum F_x = F_{ox} - 2,936 \cos(34^\circ) = 0 \quad \longrightarrow \quad F_{ox} = 2,434 \text{ N} \quad (7)$$

$$\sum F_y = 0 \quad \longrightarrow \quad \sum F_y = F_{oy} + 2,936 \sin(34^\circ) - 392.4 + F_L = 0 \quad \longrightarrow \quad F_{oy} = -F_L - 1,249.4 \quad (8)$$

$$F_{oy} = -1,196.53 \text{ N} \quad (9)$$

Based on the above calculations, the hatch latch reaction force was found to be equal to 57.87 N. After that the bottom door latch reaction forces had to be calculated. In order to calculate these reaction forces, the setup shown in Figure 25 was created, and the following calculations were executed.

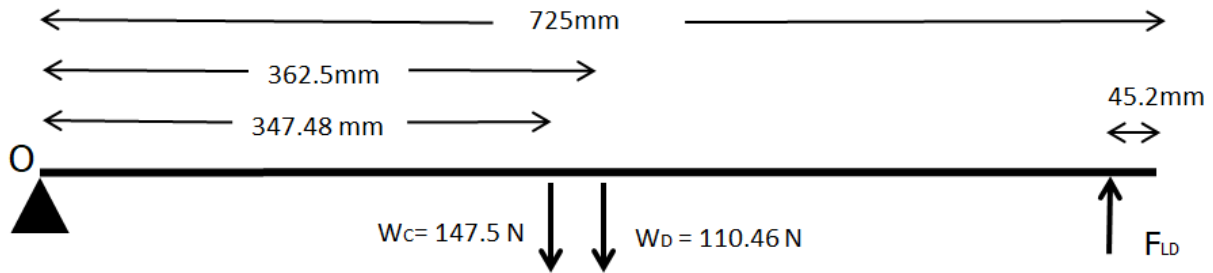


Figure 25. Door latches reaction force. The setup shown in this figure was used to calculate the reaction forces at the door latches. The horizontal line represents the door.  $W_D$  is the force due to the mass of the door at its center of gravity.  $W_C$  is the force due to the mass of the chute/chute bag at its center of gravity, and  $F_{LD}$  is the total latch reaction force. The triangle in this image represents the hinges and is a pinned connection.

$$\curvearrowleft \quad \sum M_O = 0 \quad \longrightarrow \quad \sum M_O = 147.5(347.48) + 110.46(362.5) - (725 - 45.2)F_{LD} = 0 \quad (10)$$

$$F_{LD} = 134.3 \text{ N} \quad (11)$$

$$F_{L2} = F_{L3} = \frac{F_{LD}}{2} = 67.15 \text{ N} \quad (12)$$

Based on the above calculations 67.15 N of force is exerted on each of the door latches in the undeployed position of the unit. Since the latch spring constants were not provided by the manufacturers, it was decided to calculate the maximum allowable latch spring stiffness based on the maximum allowable egress lever pull force. To calculate this unknown, first, the tension in the Bowden cables at the pulled position had to be calculated. To calculate the maximum allowable egress lever pull force, the setup shown in Figure 26 was created. The following calculations were executed to calculate the maximum tension in the Bowden cables.

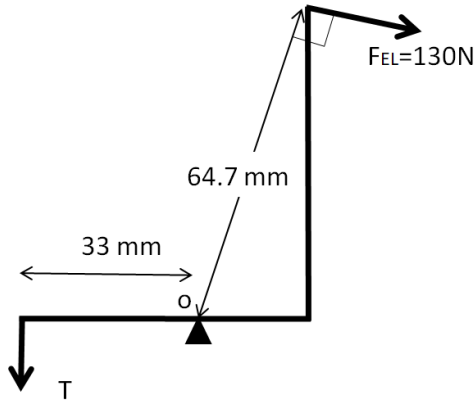


Figure 26. Maximum combined Bowden cable deployment tension. The setup shown in this figure represents the emergency egress lever at its inactivated position. This setup was used to calculate the maximum combined tension in the Bowden cables. FEL represents the maximum allowable pull force, T is the maximum combined tension of the cables and O is the pivot point.

$$\curvearrowright \sum M_o = 0 \quad \longrightarrow \quad \sum M_o = 64.7(130) - 33T = 0 \quad (13)$$

$$T = 254.88 \text{ N} \quad (14)$$

Based on these calculations, the maximum overall tension in the cables was found to be equal to 254.88 N. In order to calculate the maximum allowable latch spring stiffness, the setup shown in Figure 27 was created. The latch friction coefficient was assumed to be 0.2, and using the 3D model, the latch displacement due to deployment was measured to be equal to 7.62 mm. The previously calculated latch reaction forces and the maximum allowable combined cable tension were added to this model, and the maximum allowable latch spring stiffness was calculated as shown below.

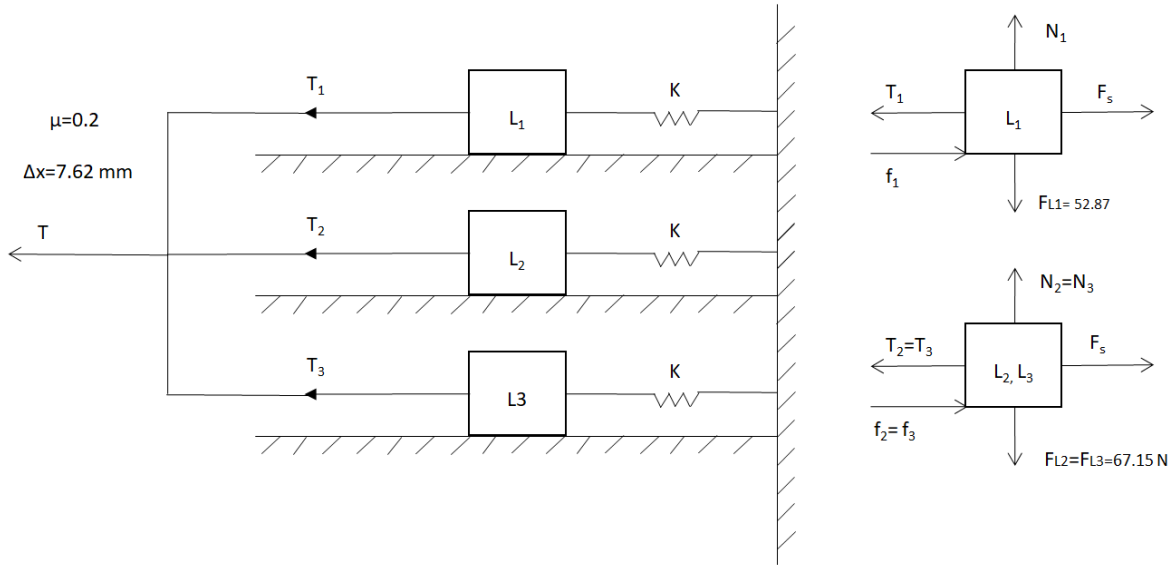


Figure 27. Maximum allowable latch spring stiffness calculation setup. The setup shown on the left side of this figure was used to calculate the maximum allowable latch spring stiffness represented with  $K$ . On the right side of this figure, the free body diagrams of the latches are shown.  $L_1$  represents the hatch latch, and  $L_2$  and  $L_3$  represent the door latches. The latch friction coefficient was assumed to be 0.2, and the latch displacement due to deployment was measured to be equal to 7.62 mm.  $FL_1$ ,  $FL_2$ , and  $FL_3$  represent the latch reaction forces, which were previously calculated.  $f_1$ ,  $f_2$ , and  $f_3$  are the forces due to friction.  $T$  is the maximum combined Bowden cable tension, and  $T_1$ ,  $T_2$ , and  $T_3$  are the cable tensions for each of the latches.

$$f = \mu N \quad (15)$$

$$f_1 = \mu N_1 = 0.2(52.87) = 10.57 \text{ N} \quad (16)$$

$$f_2 = f_3 = \mu N_2 = \mu N_3 = 0.2(67.15) = 13.43 \text{ N} \quad (17)$$

$$F_s = K\Delta x = 7.62K \quad (18)$$

$$T > f_1 + 2f_2 + 3F_s \quad \longrightarrow \quad 254.88 \text{ N} > 10.57 + 2(13.43) + 3(7.62)K \quad (19)$$

$$K < 9.5 \text{ N/mm} \quad (20)$$

Based on the above calculations, the maximum allowable latch spring stiffness is equal to 9.5 N/mm, which is relatively very high spring stiffness. Thus, the egress system can be easily deployed with a force of much smaller than 130 N.

## 6.0 RESULTS AND DISCUSSION

As a requirement, the overall mass of the unit has to be less than 2000 kg. Using the SolidWorks mass property table, the mass of the major components in the model was recorded. Based on these values, the total mass of the unit was estimated to be equal to 183.56 kg. Refer to Table 4 to see the estimated mass of the major components composing the unit. Even though the total mass of the unit is less than the maximum allowable mass, it's still relatively heavy. The hatch and the housing have the largest masses between all the components inside the assembly. By reducing the weight of these parts, the overall mass of the unit can be reduced. One way of doing this is by reducing the size of the chute opening. This results in the decreased size of almost all the other components. By using smaller off-the-shelf or custom designed latches, the latch brackets can be made much smaller, which provides the capability of using a smaller chute frame and housing. Since fiberglass/epoxy has a much larger density compared to closed-cell PVC foam, by reducing the thickness of the skin, the overall mass can be reduced.

However, this may cause failure in the hatch or the housing. Housings and hatches with a variety of overall thicknesses and skin thickness can be made and analyzed to assess how far the thickness of the skin can be reduced. The overall weight and size of the unit can also be reduced drastically if instead of designing a housing, the floor of the cabins provides mounting points for the hatch and the chute frame. This would reduce the fabrication cost, simplify the assembly process and would reduce the overall weight of the unit. Also, the housing in the model is mounted on the center point of the floor of the cabin. By moving the housing closed to the wall of the cabin, more room would become available in front of the entry point of the unit, allowing passengers to enter the chute with more ease.

Table 4. The estimated overall mass of the unit and the major component. The mass of the component shown in this figure was retrieved from the SolidWorks mass property table.

<b>Part</b>	<b>Estimated Mass (Kg)</b>
Escape chute	12.5
Escape chute bag	2.5
Bottom Door	11.26
Chute support	8.1
Chute frame and brackets	32.5
Hatch	36.5
Latch bracket (each)	1.2
Housing	57.8
Estimated mass of the remaining components	20
<b>Total</b>	<b>183.56</b>

Based on the requirements, some of the significant parts of the assembly were analyzed, and their performance and strength were verified. Table 5 represents all the important results that were obtained from the FEA analysis verification test. Initially, most of the parts failed the simulations; due to these results, the parts were then modified, and simulations were performed until all the parts passed the requirements with a safety factor of greater than 1.5. Most of the simulation results have a safety factor of close to 1.5. However, the factor of safety of the housing is much greater than 1.5, which means that it can be modified even more to reduce its weight and possibly its cost. It is recommended to build samples of the models and mechanically test them based on the same boundary conditions and forces to see how accurate the simulated results are.

Table 5. FEA tabulated results. The maximum Von Mises stress, the maximum deformation, and the factor of safety of the finite element analysis of the parts are represented in this table.

<b>Analyzed Part</b>	<b>Description of the Applied Force</b>	<b>Maximum Von Mises Stress (MPa)</b>	<b>Maximum Deformation (mm)</b>	<b>Factor of Safety</b>
Chute support	5052.15 N of force applied to top surface of the support where the chute would be mounted on.	182.2	0.87	1.55
Hatch	2500 N of force distributed normally over a circle with 30 cm diameter at the center of the hatch.	6.62	1	3.34
Hatch	5000 N of force distributed normally over the top surface of the hatch.	15.8	2.45	1.52
Housing	5400 N of force distributed normally over the top surface of the housing where the hatch would be place on.	4.2	0.19	10
Housing	5500 N of force distributed normally over the top surface of the housing where the chute frame would be placed on.	10	0.56	4.35
Door	147.15 N of force distributed over the top surface of the door where the chute would be place on.	105.2	1.062	2
Chute Frame/Chute Support Bracket	5130.63 N of force distributed normally on the top surfaces of the chute support brackets were the chute support would be mounted on.	127.3	0.22	2.22

Table 6, represents the essential values that were used for or obtained from the hand calculations. Based on these results, each of the gas springs has to exert a force of at least 1,165.06 N at their fully compressed position. Based on this calculated result, it was decided to use gas springs with a compressed force of 1,468 N. These gas springs have a stroke length of 400 mm and have a damper that prevents them from opening the hatch at a high rate, which could lead to injuries. As required by the ASCE, the egress release mechanism should be operable with a force of no more than 130 N. Based on a series of calculation and using a friction coefficient of 0.2 within the latch components, the maximum allowable latch spring stiffness was calculated to be equal to 9.5 N/mm, which is relatively high spring stiffness. Thus, the chute release mechanism can be easily deployed with most small size spring-loaded latches.

Table 6. Hand calculated results. All the essential values of the unknowns that were calculated are presented in this table.

Minimum required total gas spring force to open the hatch (F)	2,330.12 N
Total actual gas spring compressed force ( $2F_{gs}$ )	2,936 N
Top latch reaction force ( $F_L$ )	-57.87 N
Total hatch hinges horizontal reaction force ( $F_{ox}$ )	2,434 N
Total hatch hinges vertical reaction force ( $F_{oy}$ )	-1,196.53 N
Door latch hatch reaction force ( $F_{L2}=F_{L3}$ )	67.15 N
Maximum allowable egress lever pull force ( $F_{EL}$ )	130 N
Combined Bowden cable tension (T)	254.88 N
Maximum allowable latch spring stiffness	9.5 N/mm

Since the fiberglass/epoxy skin is brittle, it needs to be protected with floor covers such as carpets and resilient matting; many times cabin floors are covered with a layer of rubber.

The emergency egress unit can be deployed by pulling down the emergency egress lever. This will force open the hatch, will unlatch the bottom door and will release the escape chute. Passengers can then enter into the top opening of the chute, which would lower them to the ground with a speed of less than 2.5 m/s. After deployment, to remove the chute from the vehicle, the chute support which contains the escape chute can either be lifted up entirely or dropped to the ground. In order to install a new chute into the frame, the bottom door needs to be pushed to get latched in place. Then, a pre-packed chute connected to the chute support can be installed inside the frame from the top. After detaching the bottom face of the chute bag, the hatch needs to be pressed down to be latched in place. After this final step, the chute is ready to be deployed.

## 7.0 CONCLUSIONS AND RECOMMENDATIONS FOR FUTURE WORK

The primary purpose of this project was to design an emergency egress system for the Spartan Superway's elevated ATN vehicles to evacuate passengers in case of an emergency. Spiral escape chutes were found to be the most practical solution for the rapid evacuation of the vehicles. In order to utilize escape chutes into the cabins, the housing, the hatch, and the release mechanism of the chutes were designed. The designed unit can be preassembled and installed on the floor of chute compatible cabins. An emergency egress release lever needs to be mounted on the interior wall of the cabin. Pulling down on the egress lever unlatches the spring-loaded latches, which keep the hatch and the bottom door fastened. As the bottom door is unlatched, the weight of the door and the chute force open the door, and the chute gets deployed. At the same time, as the top hatch is unlatched, gas springs force open the door, allowing passengers to enter the chute to be lowered to the ground. After the chute is deployed, it needs to be removed to allow installation of the new chute. In order to reach the final design, some of the critical parts of the unit such as the housing, the hatch, the chute frame, the chute support, and the door were analyzed using finite element analysis. The models were optimized based on the simulations until all the criteria were met. All the analyzed parts passed the simulations with a safety factor of greater than 1.5. The minimum overall compressed gas spring force required to open the hatch was calculated to be equal to 2,330.12 N. Based on this requirement, two gas spring with a combined compressed force of 2,936 N were used in the model. As required by the ASCE, the egress system should be operable with a force of no more than 130 N. Based on this requirement, the maximum allowable latch-spring stiffness was calculated to be equal to 9.5 N/mm, which is a very high stiffness. Thus, most small sized latches can be used in this unit. The overall mass of the unit was estimated to be 183.56 Kg, which is relatively high. Since the housing passed the simulation with a large safety factor, it is possible to reduce its weight by modifying its overall size and the thickness of the fiberglass/epoxy layer. By custom designing the latches or using smaller ones, the overall size of the chute frame can be reduced, which results in a smaller hatch, housing, and a smaller overall mass. Since fiberglass/epoxy is brittle, it is recommended to cover its top surface with carpets and resilient matting. It is also recommended to mount the unit closer to the wall of the cabin; this clears more room at the entry point of the chute, allowing passengers to enter the chute with more ease. It is highly recommended to integrate the stepped hole feature of the housing into the floor of the vehicle. This eliminated the need of a housings, and the chute frame and the hatch can be mounted directly on the floor of the cabin, resulting in a lower overall cost, and simpler assembly process. It is also recommended to fabricate the simulated parts, test them mechanically based on the simulation setups, and compare the actual results with the computer generated results.

## REFERENCES

- 3accorematerials. (2011, July). *AIREX C70*. Retrieved 2018, from [https://www.3accorematerials.com/uploads/documents/TDS-AIREX-C70-E\\_1106.pdf](https://www.3accorematerials.com/uploads/documents/TDS-AIREX-C70-E_1106.pdf)
- American Society of Civil Engineers. (2013). *Automated People Mover Standards*. Reston, Virginia: ASCE.
- Axel Thoms. (n.d.). *Description of the Personal Safety Escape Chute*. Retrieved 2018, from escape-chute: [http://www.escape-chute.net/neu/uk/pe\\_safety\\_equipment\\_2\\_pop.php](http://www.escape-chute.net/neu/uk/pe_safety_equipment_2_pop.php)
- Chang, Y.-H., & Yang, H.-H. (2011). Cabin safety and emergency evacuation: Passenger experience of flight CI-120 accident. *Accident Analysis and Prevention*, 43(3), 1049-1055.
- Daniel, M., Gdoutos, E., Wang, K., & Abot, L. (2002, October 1). Failure Modes of Composite Sandwich Beams. *International Journal of Damage Mechanics*, 11(4). Retrieved 2018
- E-Glass Fibre*. (n.d.). Retrieved May 2018, from AZO Materials: <https://www.azom.com/properties.aspx?ArticleID=764>
- Fortune, J. (n.d.). *How Fast Should Tall Building Elevators Go?* Retrieved from <http://www.ctbuh.org>: <http://www.ctbuh.org/LinkClick.aspx?fileticket=k8a6x1dFxxw%3D&tabid=6497&language=en-GB>
- Hay, D. (2018, April). Axel Thoms Escape Chute Systems . (R. B. Khosroshahi, Interviewer)
- Kimijima, N., Kim, S.-J., Furuta, K., & Sakatsume, T. (2017). *Daegu Urban Railway Line 3 Monorail System in South Korea*. Retrieved 2018, from Hitachi: [https://www.hitachi.com/rev/archive/2017/r2017\\_02/04/index.html?WT.mc\\_id=ksearch\\_113](https://www.hitachi.com/rev/archive/2017/r2017_02/04/index.html?WT.mc_id=ksearch_113)
- Kumar, S., Milwich, M., Deopura, B. L., & Plank, H. (2011). Finite element analysis of Carbon composite sandwich material with agglomerated Cork core. *Procedia Engineering*, 10, 478-483. Retrieved 2018
- Louw, A. (2016). The Futran Public Transportation System.
- Make It Metal. (n.d.). *Chapter 13 - Design Consideration for Spot Welding*. Retrieved 2018, from [http://www.makeitmetal.com/resources/ch13\\_spweld.htm](http://www.makeitmetal.com/resources/ch13_spweld.htm)
- Markos, S. H. (2013). *Passenger train emergency systems: review of egress variables and egress simulation models*. Washinfnton, DC: U.S. Department of Transportation, Federal Railroad Administration, Office of Research and Development.
- Metal Supermarkets. (2018, February 1). *Sheet Metal Gauge Chart*. Retrieved 2018, from <https://www.metalsupermarkets.com/sheet-metal-gauge-chart/>

- National Fire Protection Association. (2007). *NFPA 130: Standard for Fixed Guideway Transit and Passenger Rail Systems*. NFPA.
- Samborsky, D. D., Mandell, J. F., & Agastra, P. (2017). *3-D Static Elastic Constants and Strength Properties of a Glass/Epoxy Unidirectional Laminate*. Montana State University, Department of Chemical and Biological Engineering, Bozeman. Retrieved 2018
- Tahmasseby, S., & Kattan, L. (2015). *Preliminary economic appraisal of personal rapid transit (PRT) and urban gondola feeder systems serving a university campus and its surrounding major attractions*. NRC Research Press.
- Thoms, S. (2018, April). Axel Thoms Escape Chute System. (R. B. Khosroshahi, Interviewer)
- Timan, P. (2015). Why Monorail Systems Provide a Great Solution for Metropolitan Areas. *Urban Rail Transit*, 1(1), 13-25.
- Watson, D. C. (1982). *Mechanical Properties of E293/1581 Fiberglass-Epoxy Composite and of Several Adhesive Systems*. Air Force Wright Aeronautical Laboratories, Materials Integrity Branch. Retrieved 2018

## APPENDICES

### APPENDIX A: FINAL MODEL RELEVANT DOCUMENTS

Table 7. Top assembly BOM. This BOM represents all the parts and subassemblies that were used in the final model.

ITEM NO.	PART NAME	VENDOR	VENDOR NO.	QTY.
1	SHEET METAL FRAME 1	N/A	N/A	1
2	SHEET METAL FRAME 2	N/A	N/A	1
3	CHUTE SUPPORT	N/A	N/A	1
4	CHUTE SUPPORT BRACKET	N/A	N/A	4
5	HOUSING	N/A	N/A	1
6	HATCH	N/A	N/A	1
7	BOTTOM DOOR	N/A	N/A	1
8	DOOR LATCH BRACKET, RIGHT	N/A	N/A	1
9	DOOR LATCH BRACKET, LEFT	N/A	N/A	1
10	ESCAPE CHUTE BAG	N/A	N/A	1
11	ESCAPE CHUTE	N/A	N/A	1
12	EMERGENCY EGRESS LEVER HOUSING	N/A	N/A	1
13	EGRESS LEVER	N/A	N/A	1
14	BARREL ADJUSTER BRACKET	N/A	N/A	1
15	BARREL ADJUSTER	N/A	N/A	6
16	BOWDEN CABLE	N/A	N/A	A/R
17	POD V3 concept	N/A	N/A	1
18	GAS SPRING 400	MCMASTER	9416K23	2
19	GAS SPRING END FITTING	MCMASTER	9416K75	2
20	BOTTOM DOOR HINGE	MCMASTER	1798A21	2
21	BALL STUD GAS SPRING MOUNTING BRACKET (FRAME)	MCMASTER	5992K31	2
22	CONCEALED HATCH HINGE	SUGATSUNE	HES3D-E190	2
23	M5-0.8X18 HEX DRIVE FLAT HEAD SCREW	MCMASTER	91294A213	4
24	M8-1.25X35 HEX HEAD SCREW	MCMASTER	98093A553	16
25	M8-1.25X8 SERRATED FLANGE LOCKNUT	MCMASTER	96595A102	16
26	BALL STUD GAS SPRING MOUNTING BRACKET (HATCH)	MCMASTER	5992K32	2
27	SPRING-LOADED LATCH (BOTTOM DOOR)	MCMASTER	1437A4	2
28	SPRING-LOADED LATCH STRIKE PLATE	MCMASTER	1437A4	3
29	13 MM OD, 12, MM LONG, M6 SPACER	MCMASTER	92871A347	8
30	SPRING-LOADED LATCH (HATCH)	MCMASTER	1437A400	1
31	13MM OD, 9MM LONG, M6 SPACER	MCMASTER	92871A345	4

<b>ITEM NO.</b>	<b>PART NAME</b>	<b>VENDOR</b>	<b>VENDOR NO.</b>	<b>QTY.</b>
32	PRESS-FIT M5-0.8 NUT	MCMaster	94100A140	3
33	M6-1X90 SHOULDER SCREW	MCMaster	92981A794	1
34	M6-1X6 FLANGE NUT	MCMaster	94777A101	1
35	SLEEVE WITH RUNNING BEARING (10 MM LONG, 8MM SHAFT)	MCMaster	6679K120	2
36	CLEVIS ROD END	MCMaster	2448K41	6
37	PRESS-FIT M5-0.8 NUT	MCMaster	94100A140	3
38	0.25-20 BUTTON HEAD HEX DRIVE SCREW	MCMaster	92949A542	6
39	12-28 BUTTON HEAD HEX DRIVE SCREW	MCMaster	92949A436	8
40	12-28 LOCKNUT	MCMaster	91831A124	8
41	8-32 FLAT HEAD SCREW	MCMaster	91253A192	12
42	8-32 HEX NUT	MCMaster	90387A326	12
43	M5X0.8 TAPPING INSERT	MCMaster	95631A100	8
44	0.25 INCH DIAMETER, 0.5 INCH LONG BLIND RIVET	MCMaster	97526A370	8
45	6-32 PRESS-FIT NUT	MCMaster	94674A510	8
46	6-32 SOCKET HEAD SCREW	MCMaster	91251A269	8
47	M6X1 TAPPING INSERT	MCMaster	95631A125	4
48	M5 X 0.8 TAPPING INSERT	MCMaster	95631A100	2
49	M5-0.8X14 HEX DRIVE SCREW	MCMaster	91239A230	2
50	6-32 TAPPING INSERT	MCMaster	90016A007	4
51	6-32 HEX DRIVE SCREW	MCMaster	91255A133	4
52	M6-1X25 HEX DRIVE SCREW	MCMaster	91239A327	4
53	M8-18X1.25 HEX DRIVE SCREW	MCMaster	91239A420	16
54	M8X1.25 TAPPING INSERT	MCMaster	95631A150	16
55	M6-1X14 HEX DRIVE SCREW	MCMaster	91239A319	6
56	M6X1 HEX NUT	MCMaster	94223A101	6

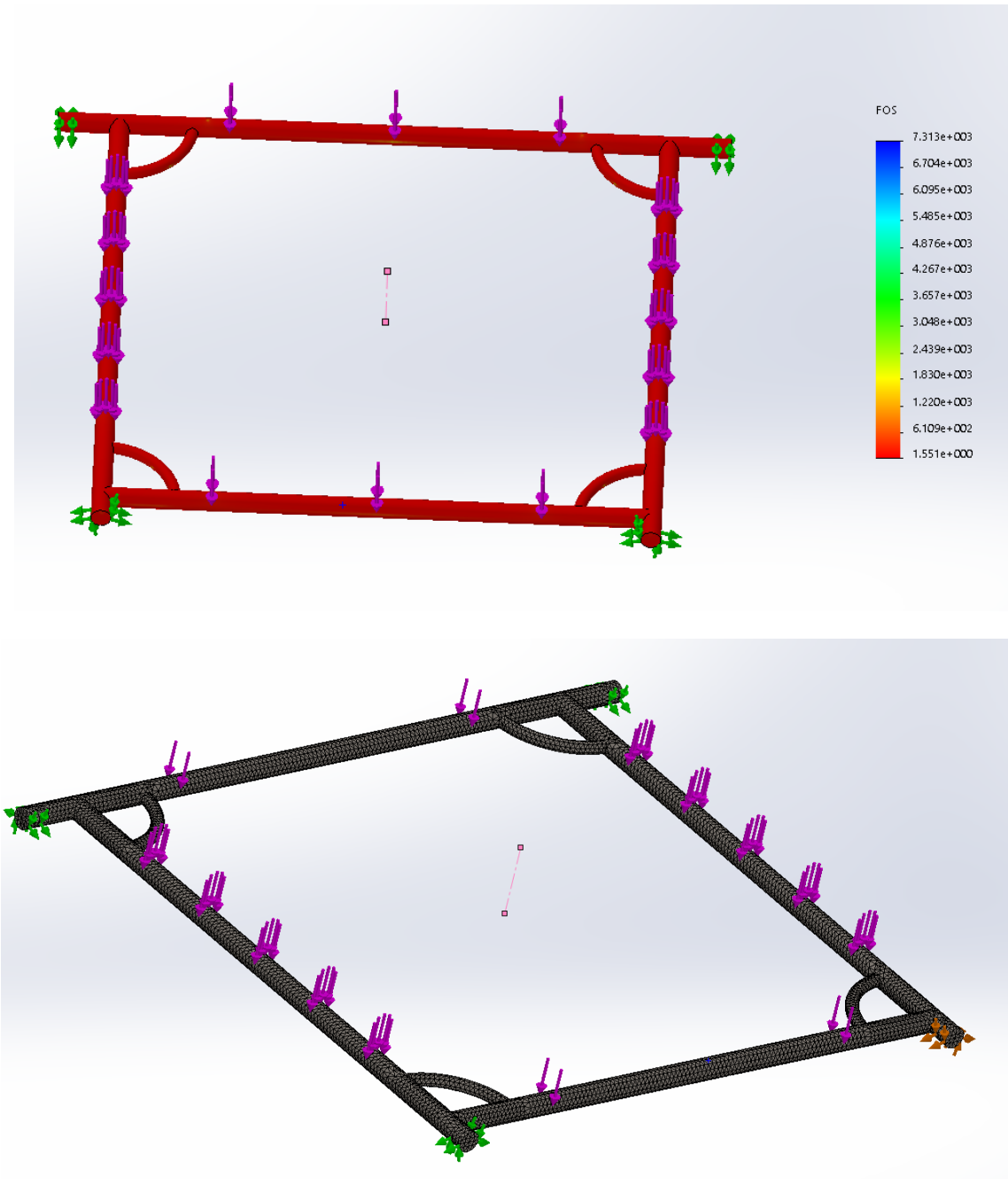


Figure 28. Chute support 5052.15 N verification test mesh and factor of safety. A fine standard mesh was used during this analysis as shown in the bottom image. The FEA analysis was performed by adding rollers to the ends of the rods shown with green arrows and applying a force of 5052.15 N to the top surface of the support demonstrated with purple arrows. The model passed the test with a safety factor of 1.55 as presented in the top image.

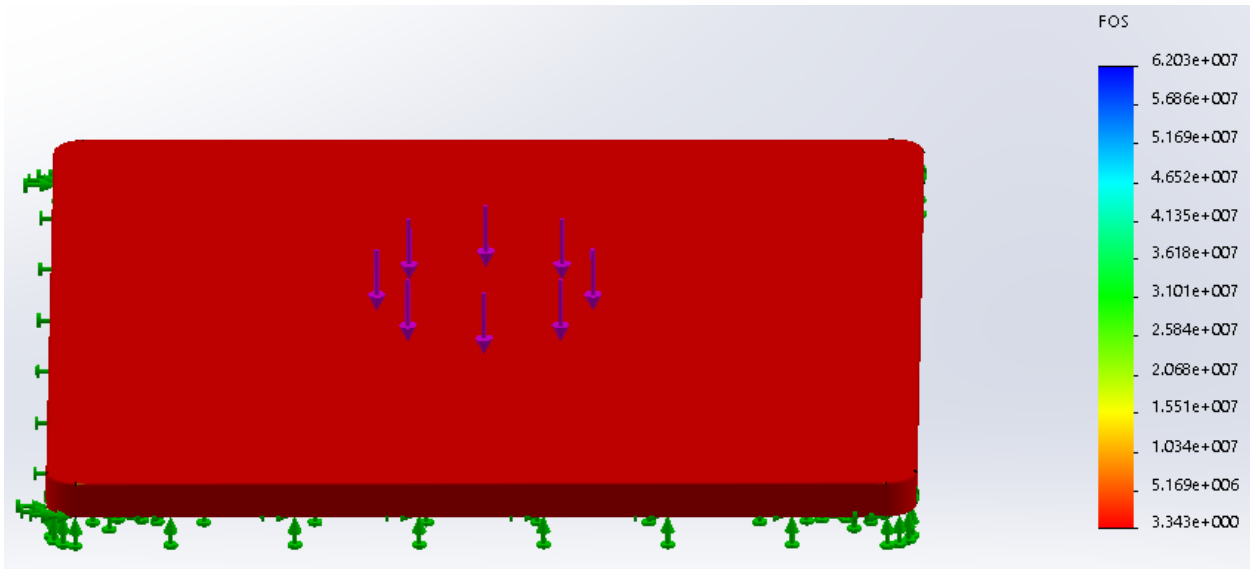


Figure 29. 2,500 N hatch verification test factor of safety fringe plot. The green arrows in this image represent the areas which were fixed during this analysis, and the purple arrows represent the direction of the force and the location at which they were applied. As shown in this image, the factor of safety was found to be equal to 3.34.

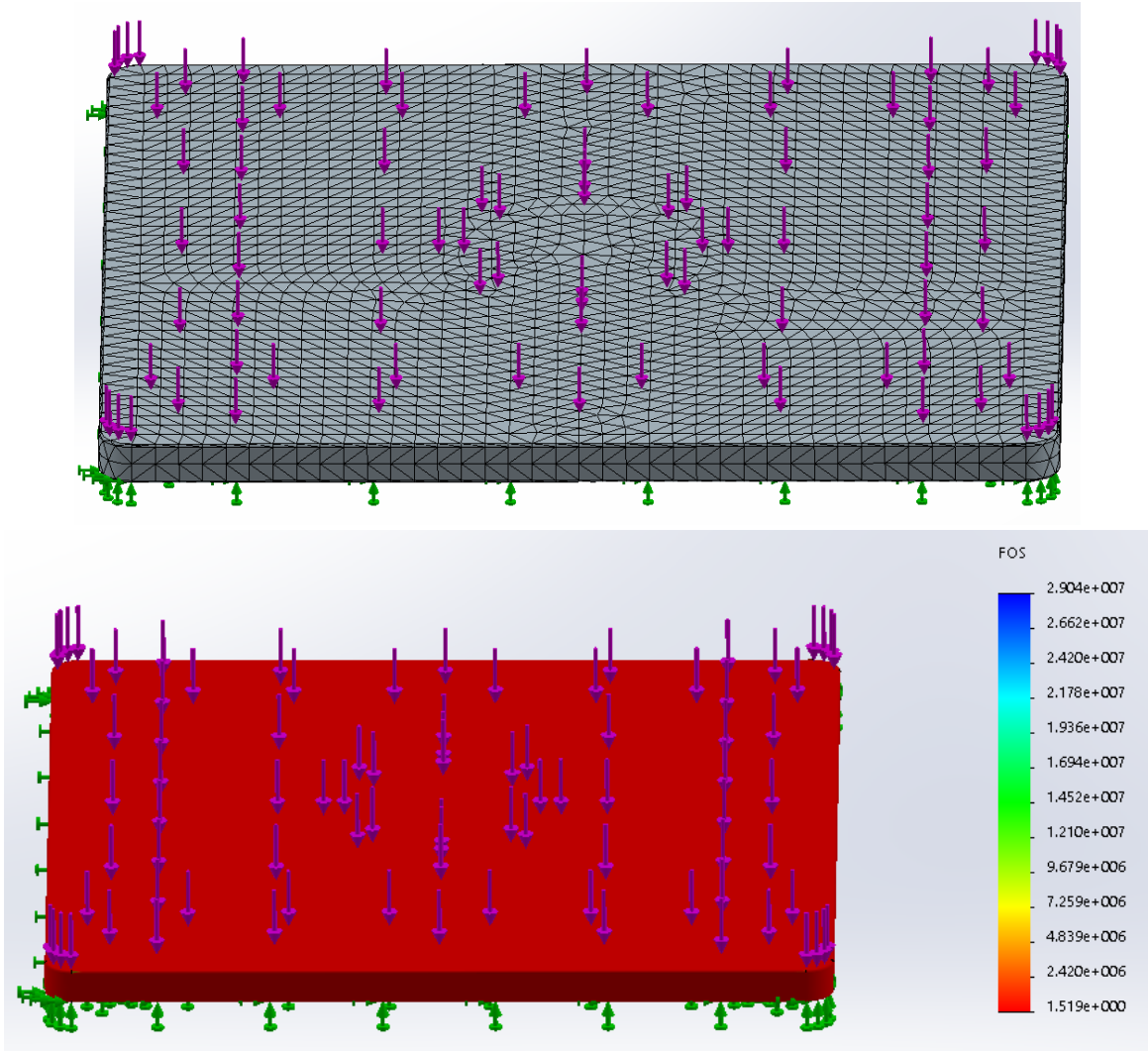


Figure 30. 5000 N hatch verification test mesh and factor of safety fringe plot. The green arrows in the images represent the areas which were fixed during this analysis, and the purple arrows represent the direction of the force and the location at which they were applied. The mesh can be seen in the top image. As shown in the bottom image, the factor of safety was found to be equal to 1.52.

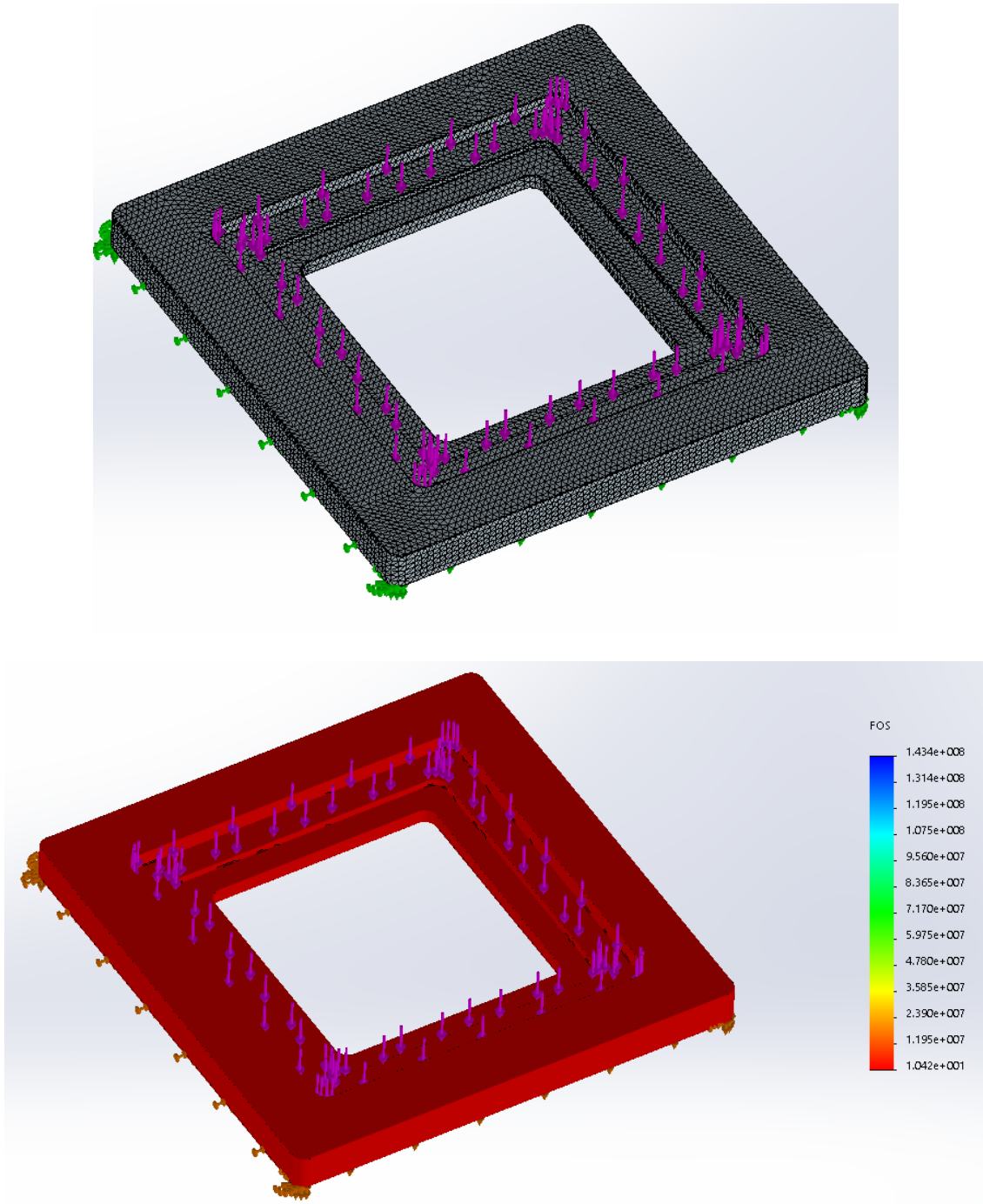


Figure 31. 5,400 N housing verification test mesh and factor of safety fringe plot. The green and brown arrows in these images represent the areas which were fixed during the analysis, and the purple arrows represent the direction of the force and the location at which they were applied. The mesh can be seen in the top image. As shown in the bottom image, the factor of safety was found to be equal to 10.

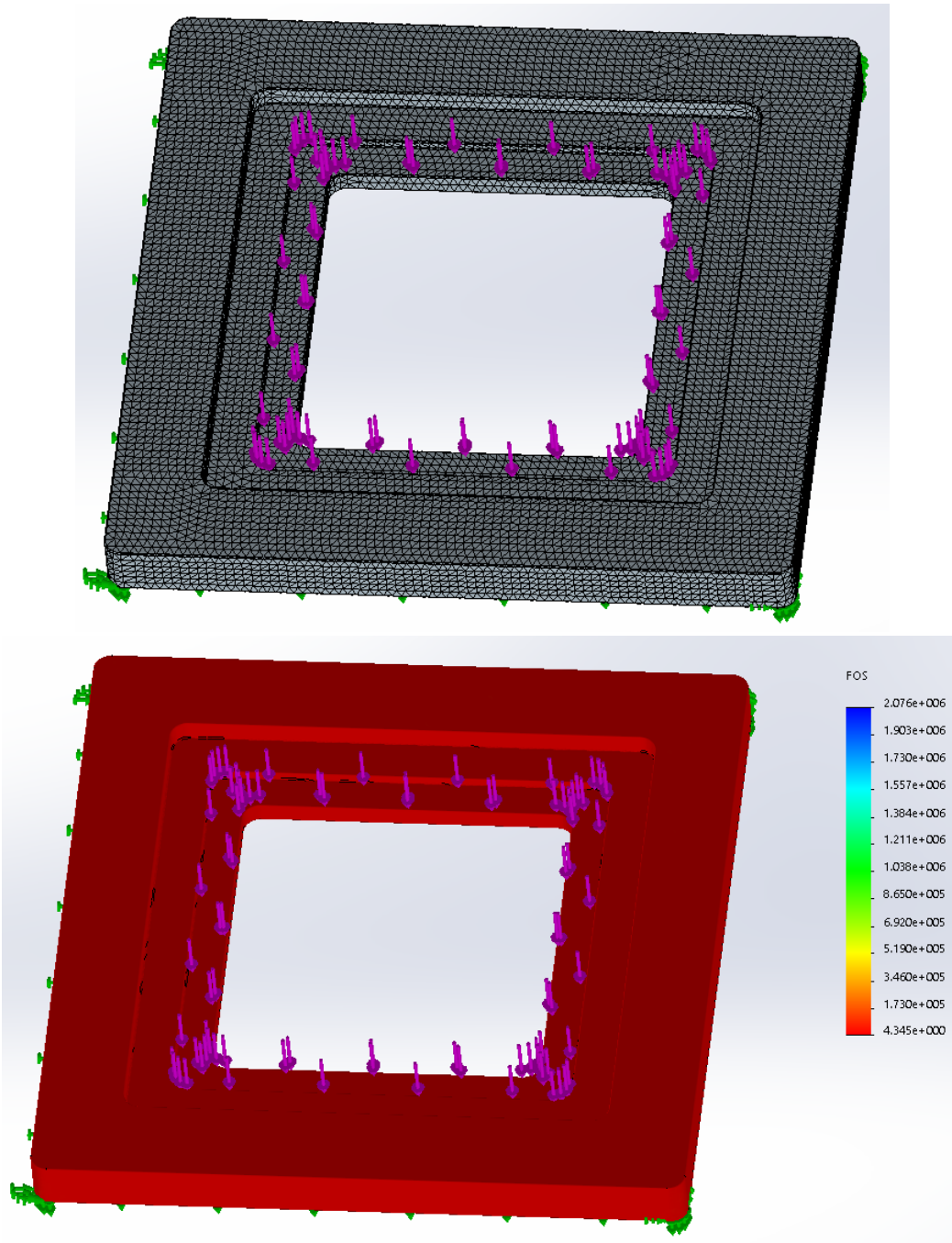


Figure 32. 5,500 N housing verification test mesh and factor of safety fringe plot. The green arrows in these images represent the areas which were fixed during this analysis, and the purple arrows represent the direction of the force and the location at which they were applied. The mesh can be seen in the top image. As shown in the bottom image, the factor of safety was found to be equal to 4.35.

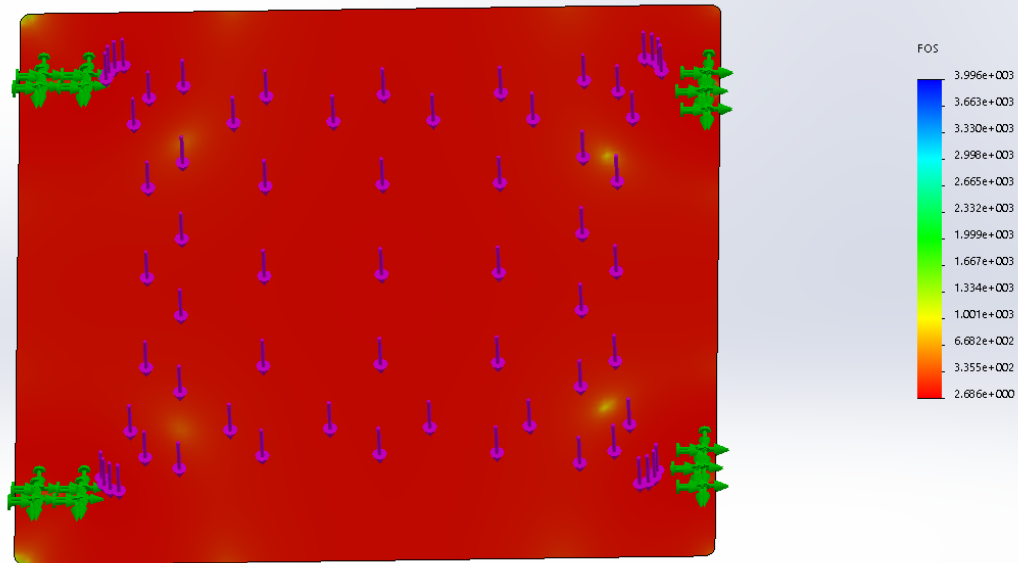
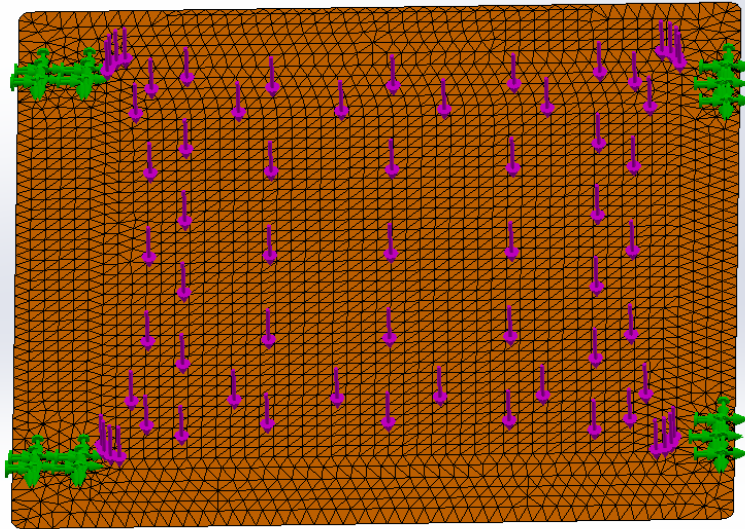


Figure 33. 147.15 N bottom door verification test mesh and safety factor fringe plot. To run the simulation, the door was fixed at the clearance holes shown with green arrows. 147.15 N of force was then applied normal to its top surface based on the weight of the chute and its cover. The force direction and the location over which it was distributed are presented with purple arrows. The mesh can be seen in the top figure. As shown in the bottom image, the analysis resulted in a safety factor of 2.69.

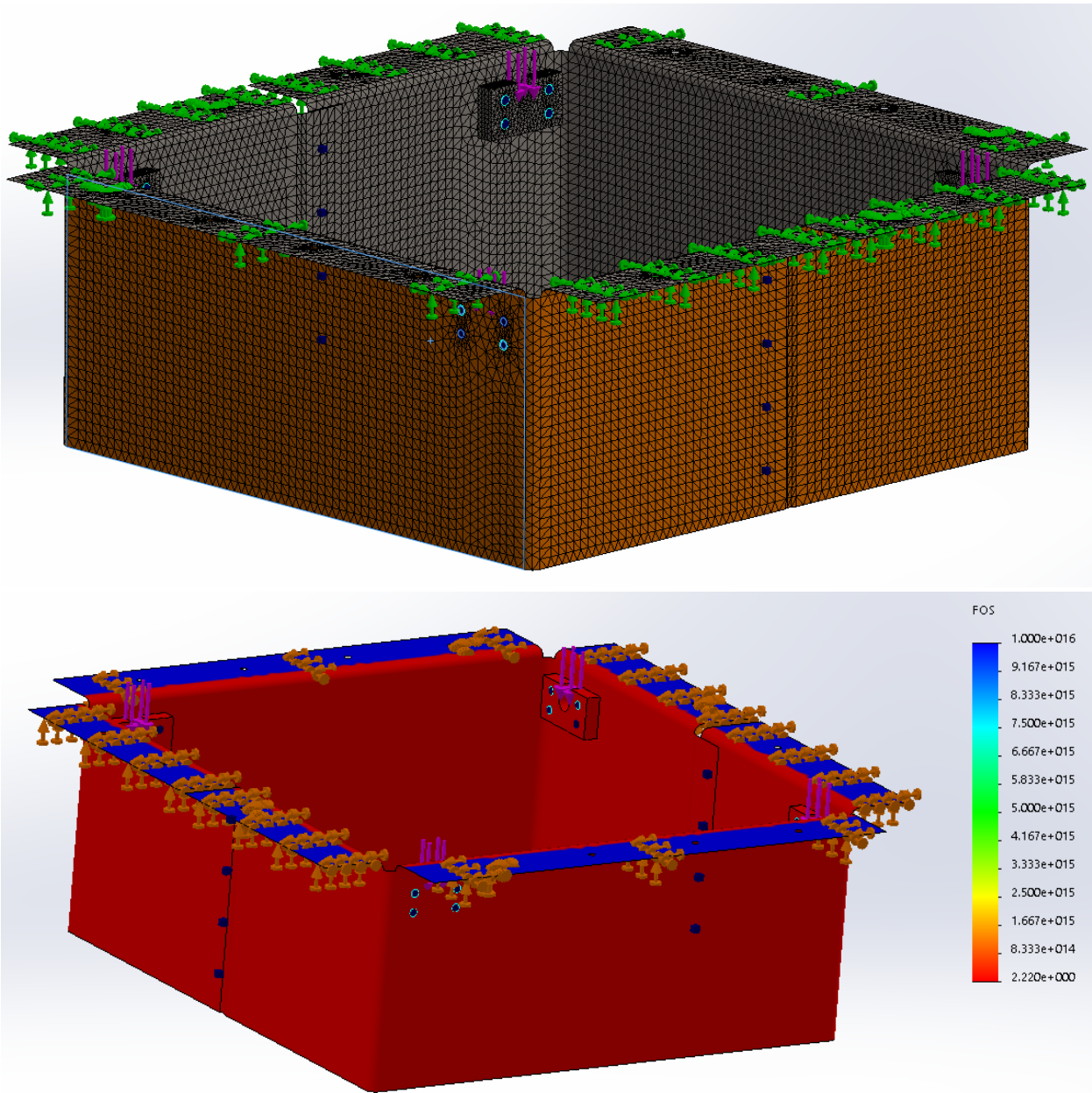


Figure 34. 5,130.63 N chute frame verification test mesh and safety factor fringe plot. As shown in the top image, a fine standard mesh was used to mesh the subassembly. The bottom surface of the flanges was fixed, and eight spot weld connections were assigned between the two sheet metal parts. Pinned connections were defined through the clearance holes of the brackets and the frame, and a downward force of 5,130.63 N, shown with purple arrows was distributed on the brackets. The subassembly passed the analysis with a safety factor of 2.22.

Table 8. 1023 carbon steel material properties. The following material properties were retrieved from the SolidWorks material property database. These properties were used to run simulations on parts made from 1023 carbon steel.

Property	Value	Units
Elastic Modulus	204999.9984	N/mm <sup>2</sup>
Poisson's Ratio	0.29	N/A
Tensile Strength	425.0000032	N/mm <sup>2</sup>
Yield Strength	282.685049	N/mm <sup>2</sup>
Tangent Modulus		N/mm <sup>2</sup>
Thermal Expansion Coefficient	1.2e-005	/K
Mass Density	7858.000032	kg/m <sup>3</sup>
Hardening Factor	0.85	N/A

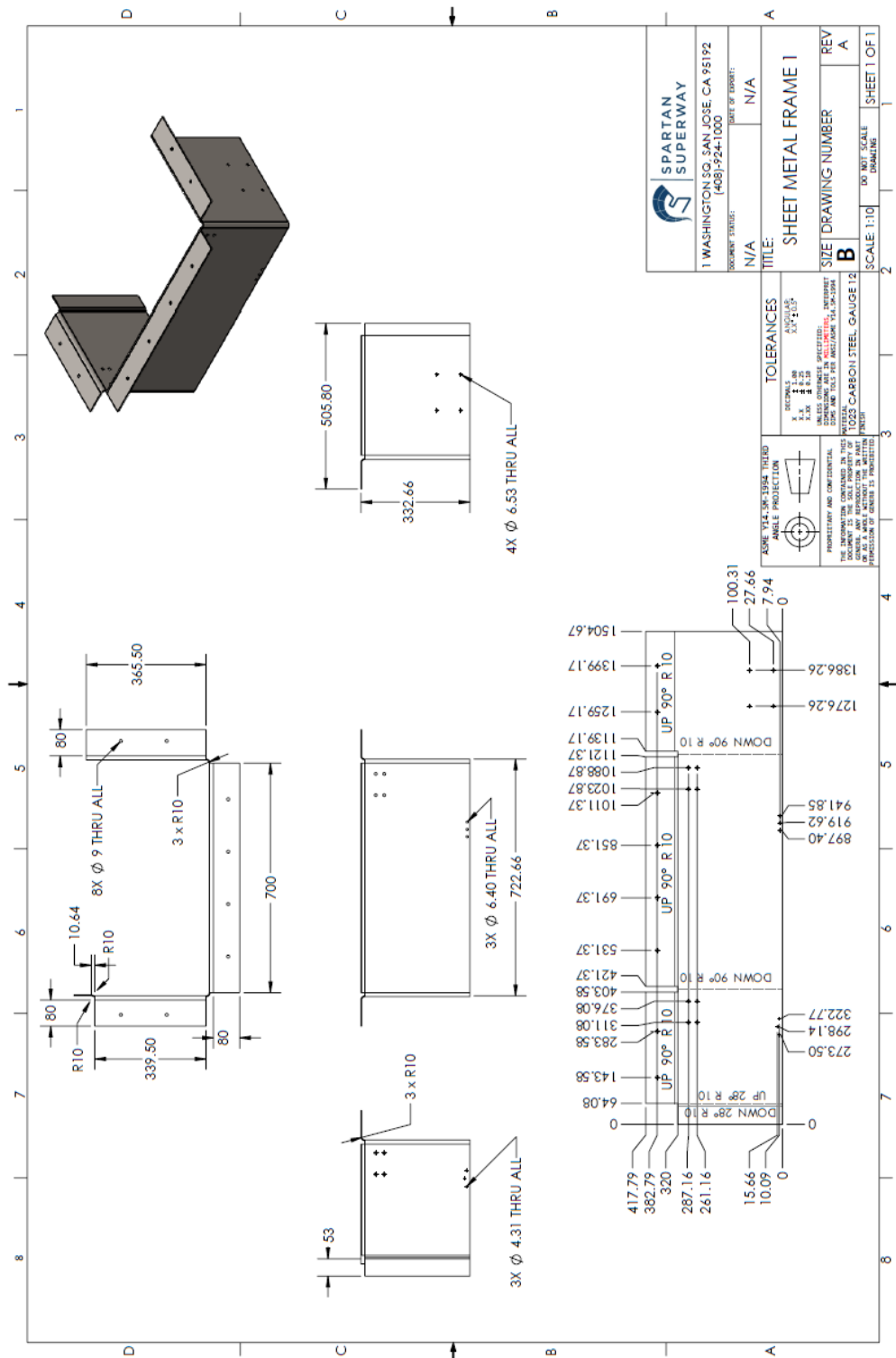


Figure 35. Sheet metal frame #1 drawing. The chute frame consists of two 12 gauge carbon steel sheet metal panels, which are connected to each other using eight spot welds. This figure shows panel number one.





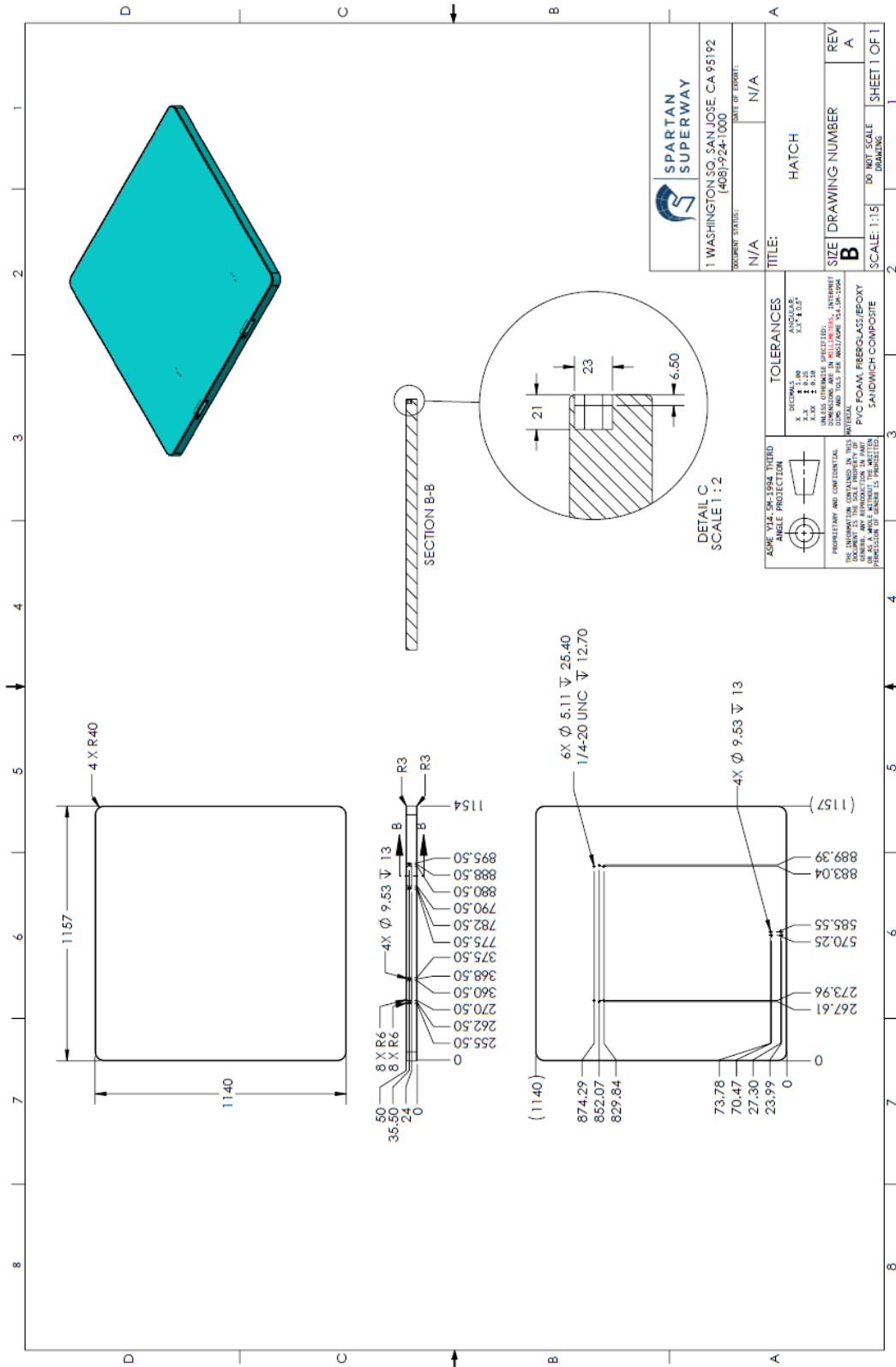


Figure 38. Hatch drawing. The hatch of the unit is made out of a PVC foam core and a fiberglass/epoxy skin. The drawing of the hatch is shown in this figure.

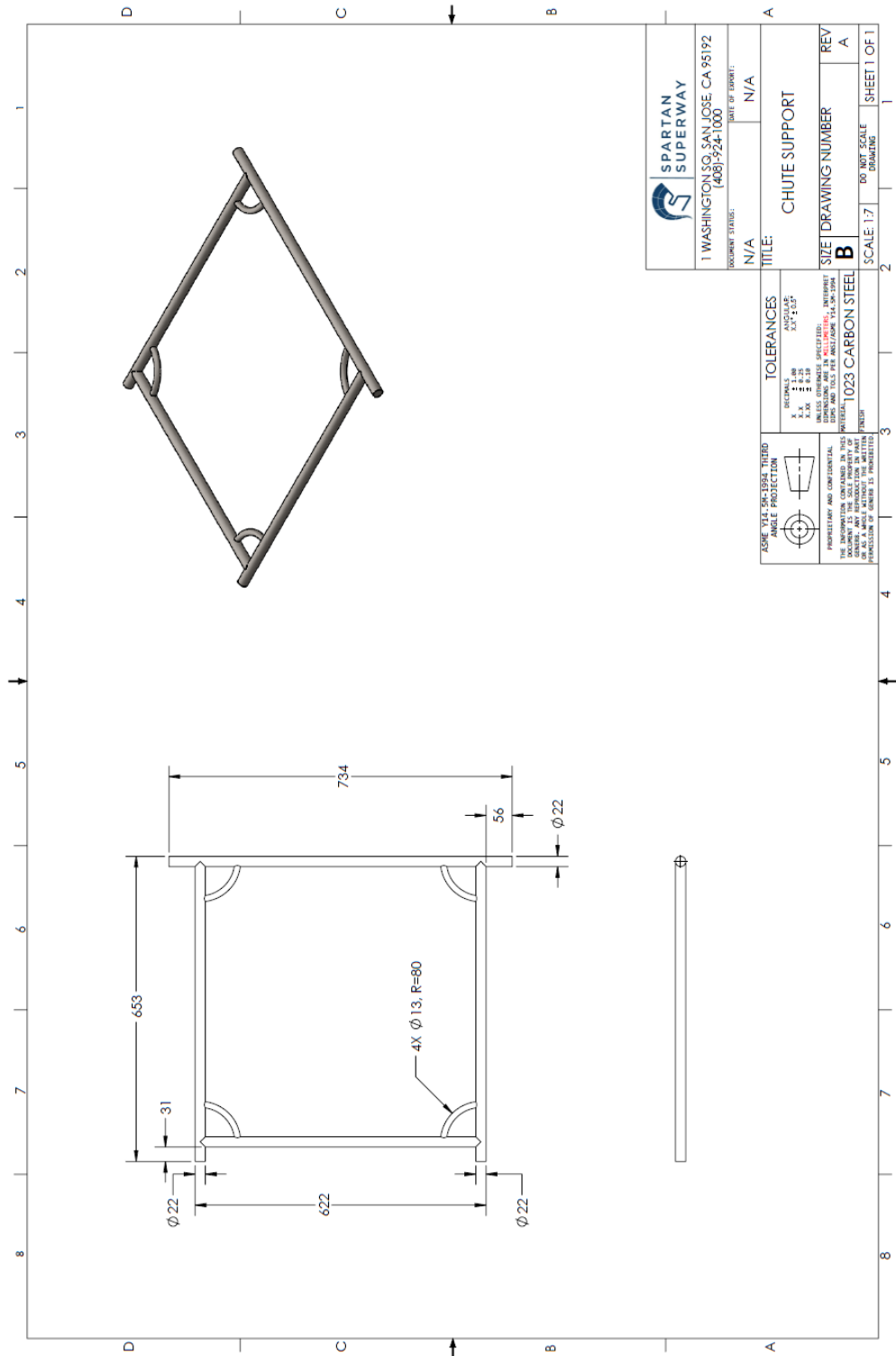


Figure 39. Chute support drawing. The chute support design is based on Axel Thoms' standard model shown in Figure 63. The escape chute gets connected to this steel support, which would be mounted on the chute frame. The drawing of the chute support is shown in this figure.

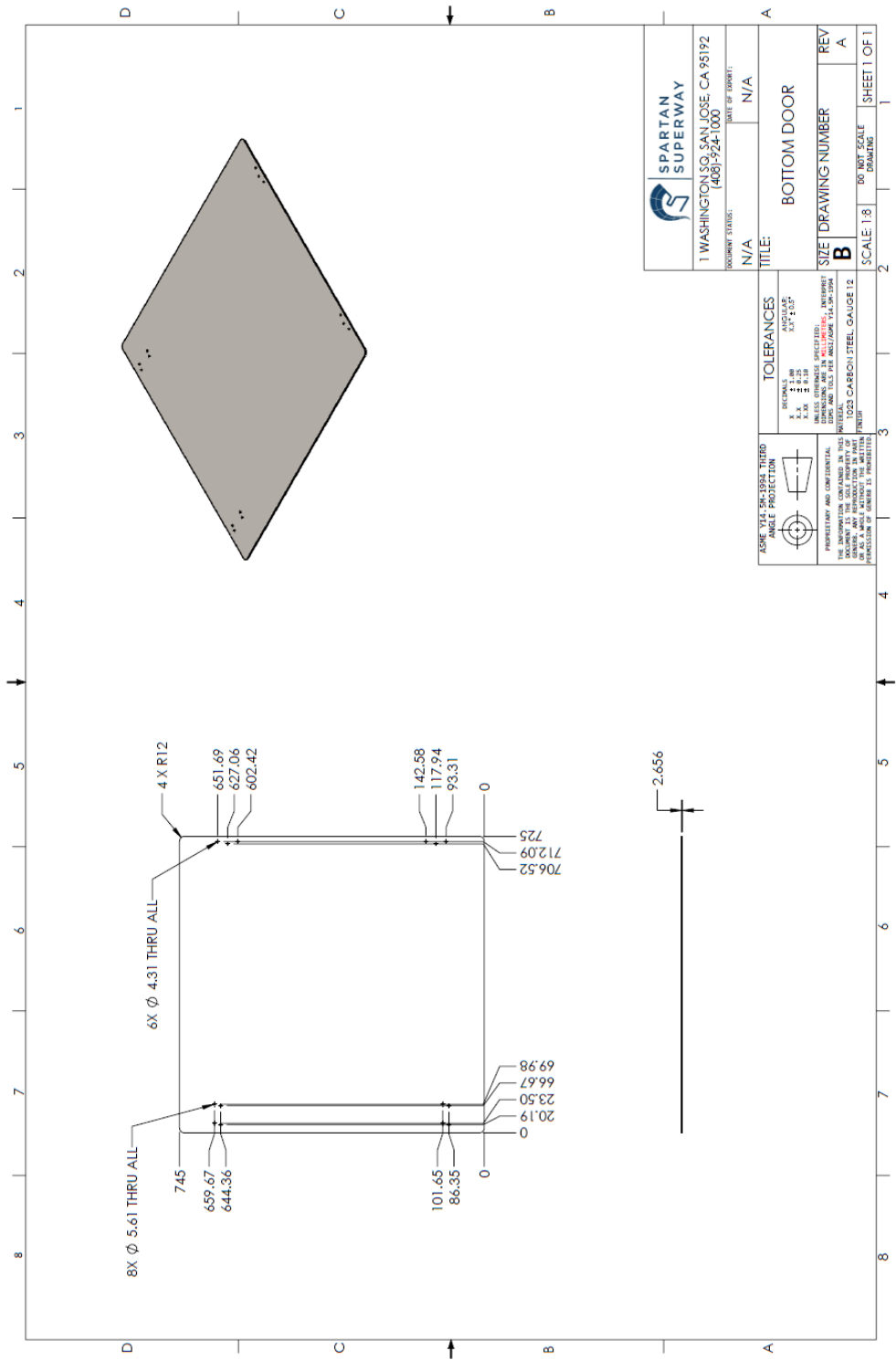


Figure 40. Bottom door drawing. The bottom door is made out of 12 gauge 1023 carbon steel and carries the weight of the chute, and releases the chute as the release mechanism is disengaged. This figure represents the drawing of the bottom door.

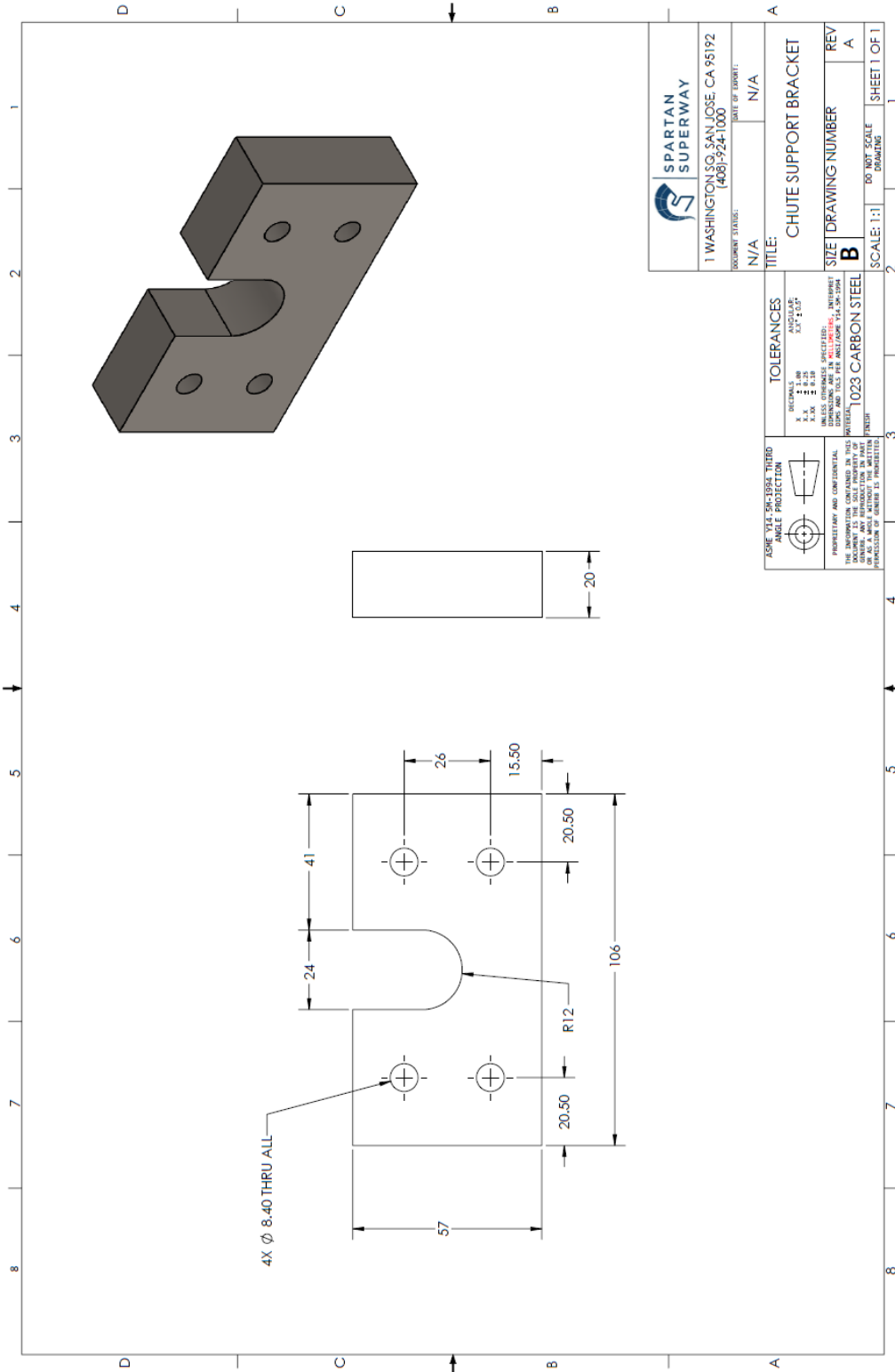
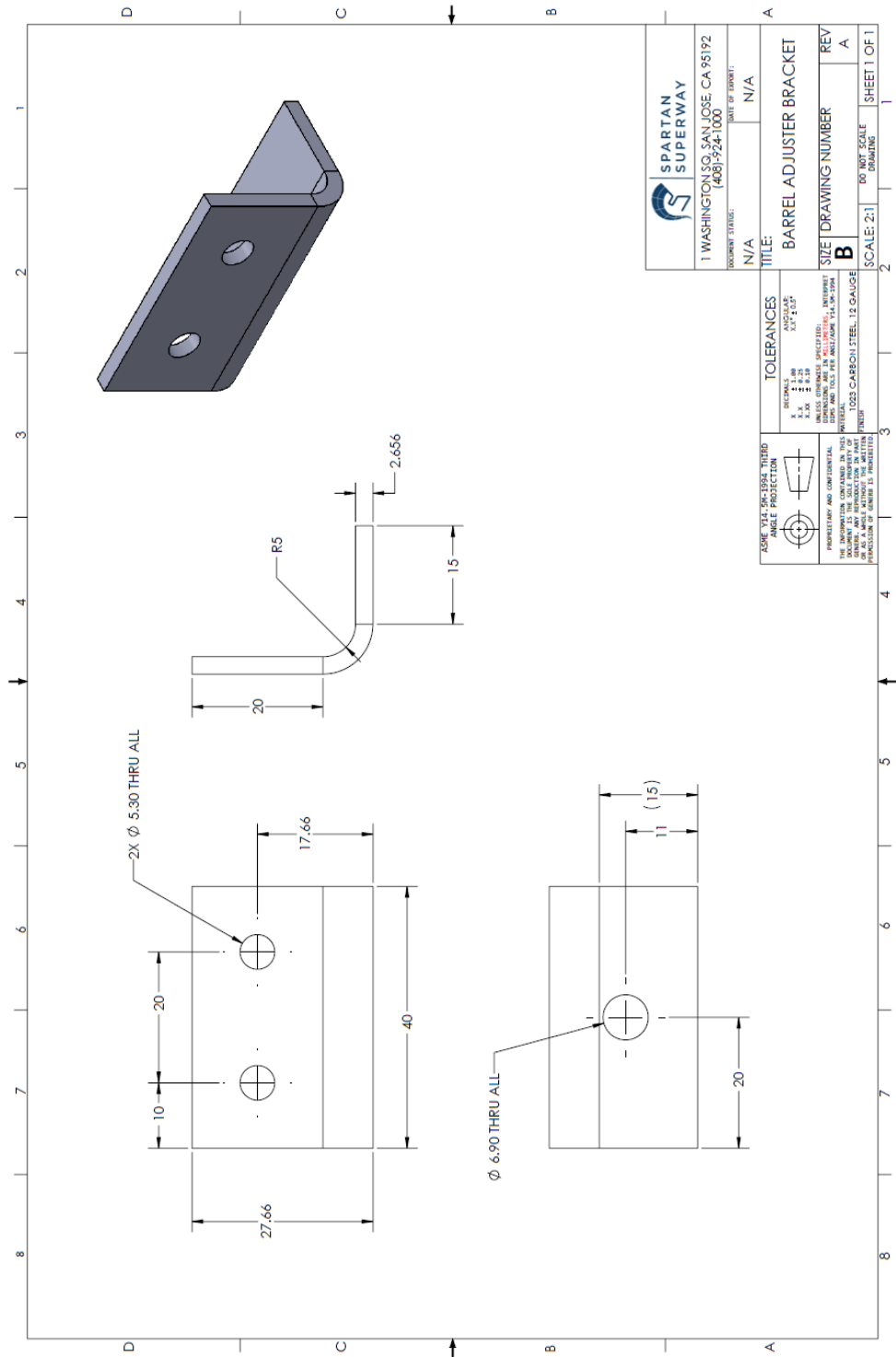


Figure 41. Chute support bracket drawing. Four chute support brackets get assembled on the chute frame. The chute support then gets mounted on these brackets. This figure represents the drawing of a chute support bracket.



1 WASHINGTON SQ. SAN JOSE, CA 95192 (408) 524-1000	
EQUIPMENT TYPE: N/A	PART OR PART NUMBER: N/A
TITLE: BARREL ADJUSTER BRACKET	
SIZE: B	DRAWING NUMBER: REV A
SCALE: 2:1	
SHEET 1 OF 1	

ASK FOR SPECIFIC TOLERANCES AND PROJECTIONS	TOLERANCES:
ANGULAR: ±0.1°	REGIONAL:
DIMENSIONAL: ±0.15	F. DIM.: ±0.15
FINISH:	H. DIM.: ±0.15
MATERIAL:	I. DIM.: ±0.15
FINISH:	J. DIM.: ±0.15
FINISH:	K. DIM.: ±0.15
FINISH:	L. DIM.: ±0.15
FINISH:	M. DIM.: ±0.15
FINISH:	N. DIM.: ±0.15
FINISH:	O. DIM.: ±0.15
FINISH:	P. DIM.: ±0.15
FINISH:	Q. DIM.: ±0.15
FINISH:	R. DIM.: ±0.15
FINISH:	S. DIM.: ±0.15
FINISH:	T. DIM.: ±0.15
FINISH:	U. DIM.: ±0.15
FINISH:	V. DIM.: ±0.15
FINISH:	W. DIM.: ±0.15
FINISH:	X. DIM.: ±0.15
FINISH:	Y. DIM.: ±0.15
FINISH:	Z. DIM.: ±0.15

Figure 42. Barrel adjuster bracket drawing. This bracket is mounted on the top surface of the housing, next to the hatch latch. The barrel adjuster gets fastened on a pressed-fit nut on this bracket, which is used to adjust the tension in the Bowden cable connected to the hatch latch. The drawing of this bracket is shown in the above image.

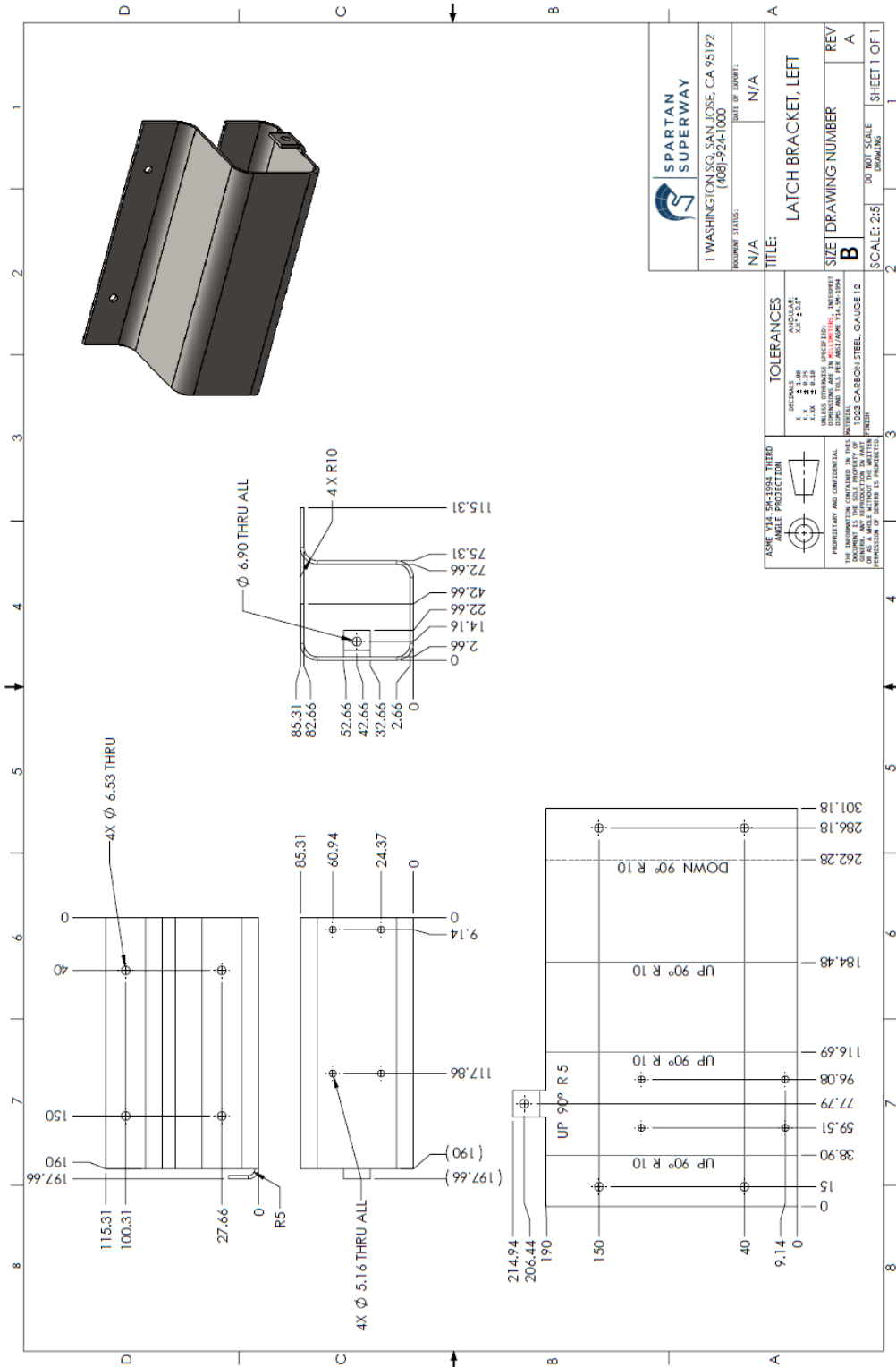


Figure 43. Left side door latch bracket drawing. This figure represents the drawing of the left side door latch bracket, which is symmetric to the right side door latch bracket. These brackets get secured to the chute frame using rivets and are designed to support the door latches and the barrel adjusters.

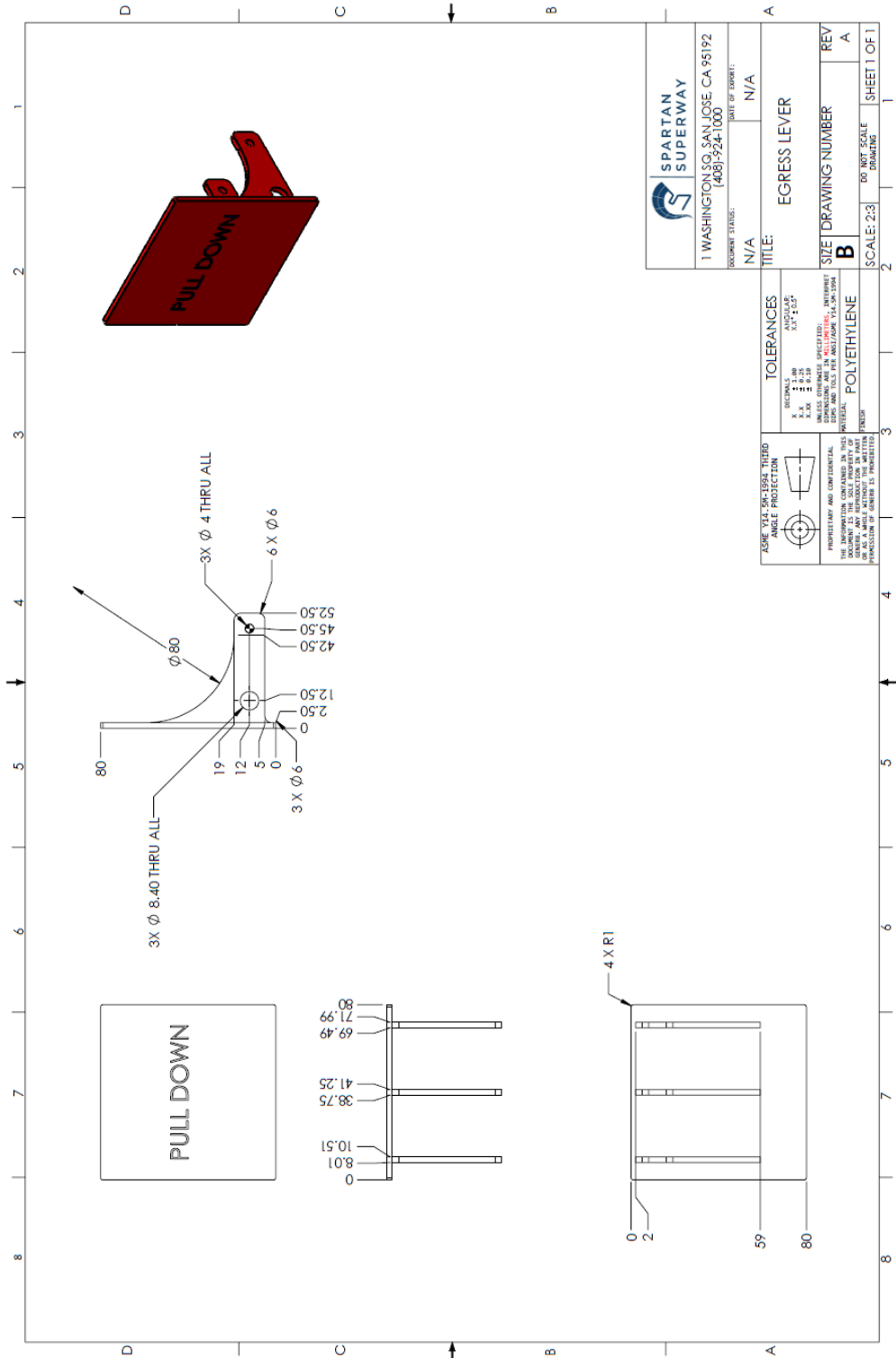
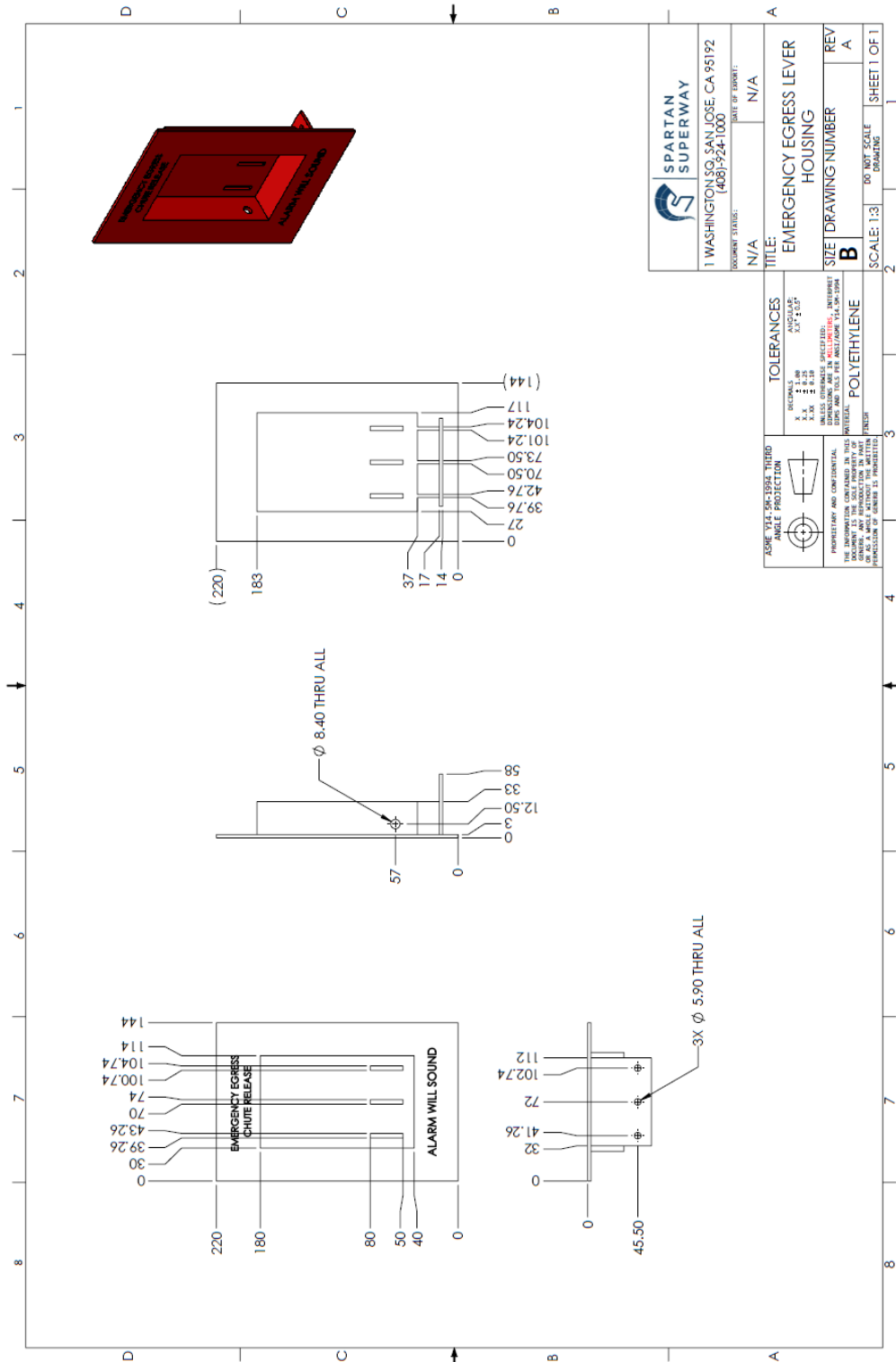


Figure 44. Emergency egress lever drawing. Pulling down on the emergency egress lever deploys the chute by increasing the tension in the Bowden cables attached to its end. The drawing of the emergency egress lever is shown above.



## APPENDIX B: PREVIOUS MODELS RELEVANT DOCUMENTS

### FIRST GENERATION UNIT



Figure 46. First generation release mechanism. These images represent the open and closed positions of one of the old release mechanisms. Twisting the handle unlatches the bottom door, and gravity forces the door open.

## SECOND GENERATION UNIT

The second generation of the unit was capable of being installed underneath the seats as shown in Figure 48 and Figure 47. To deploy the chute, the seats would have to be folded up to gain access to the entry point. Then, the release handle would have to be twisted to unlock the top hatch and the bottom doors. As soon as the bottom doors are unlocked, the weight of the doors and the chute force opens the doors, and the chute gets deployed. Then, passengers can enter the chute from the top opening. This design was based on Axel Thoms' standard unit drawing (Figure 63), which was obtained from the company employees. It is required by NFPA 130 for all hatches to be operable with no more than one operation; thus, this model was eliminated due to the excessive number of operations (National Fire Protection Association, 2007).



Figure 47. Second generation release mechanism. Twisting the handle of this unit releases the chute and unlocks the hatch. Passengers then have to open the hatch to gain access to the entry point.

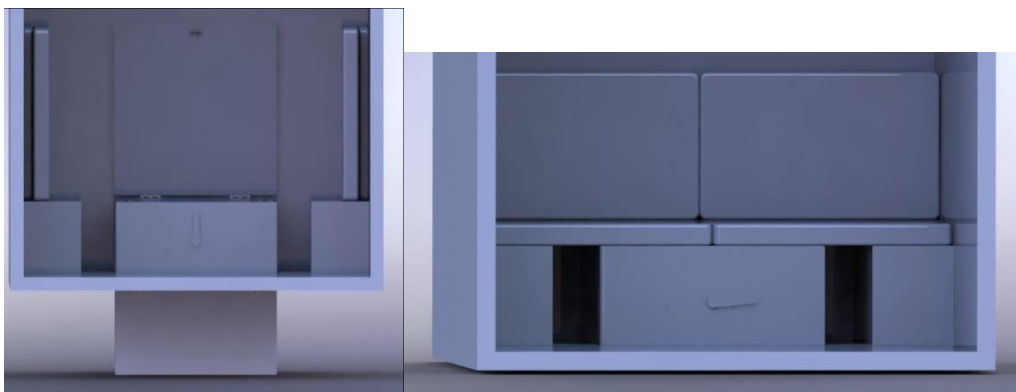


Figure 48. Second generation unit closed and open positions. This unit can be installed on the floor of the cabin underneath the seats. To gain access to the unit, the seats would have to be folded up, which increases the number of operations required to deploy and use the chute.

### THIRD GENERATION UNIT

The third generation emergency egress unit can be preassembled and installed on the floor of the cabin using eight bolts. The closed and open positions of this unit are shown in Figure 49. To deploy the chute, passengers first have to pull on the hatch handle, which unlatches the bottom door. As soon as the bottom door is unlatched, the weight of the door and the chute force open the door, and one end of the chute falls to the ground. Passengers then have to rotate the handle to unlock the hatch and manually open the hatch to gain access to the entry point. Lastly, passengers can enter the chute to be lowered to the ground. This model was eliminated due to its large mass. The housing and the hatch were made entirely out of E-glass fiber, which resulted in an overall mass of around 440kg.

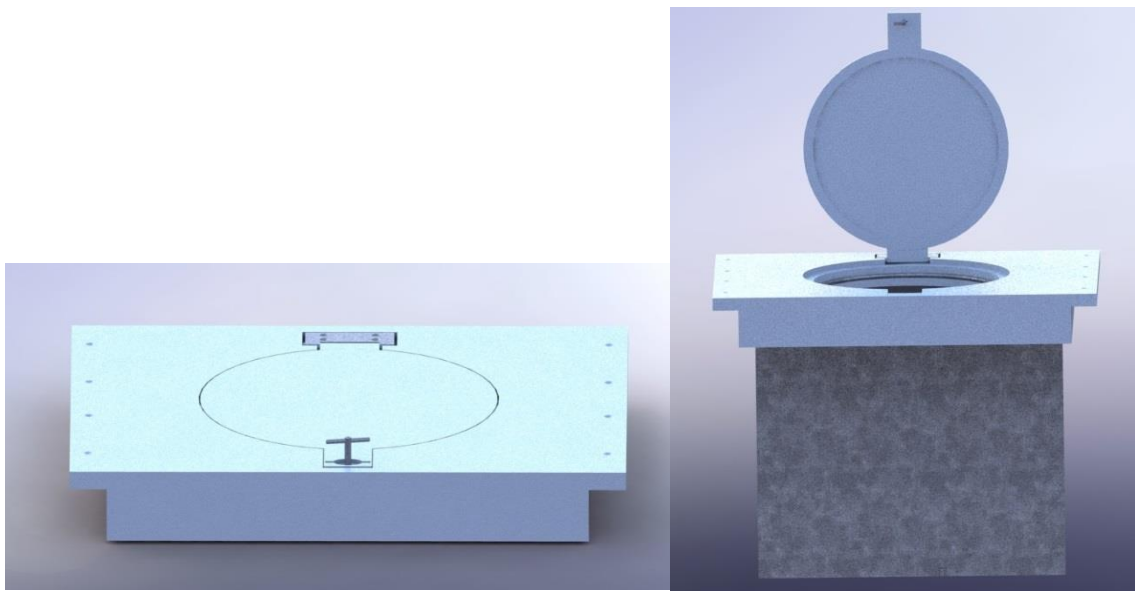


Figure 49. Third generation model. This unit is capable of being installed on the floor of the podcars using bolts. The housing and the hatch are made entirely out of E-glass fiber, which resulted in a major increase in the mass of the unit. Due to a large number of deployment operations and a large mass of the unit, this model was eliminated.

In order to install the chute on this unit, the bottom opening must be closed. The chute has to be mounted on the ring shown in Figure 50. After securing the chute on the ring, the chute can be packed inside the housing, and the ring can be placed on the stepped hole inside the housing as shown in this Figure 50; the ledge at the inner surface of the hole supports the ring and prevents it from moving passed the hole.

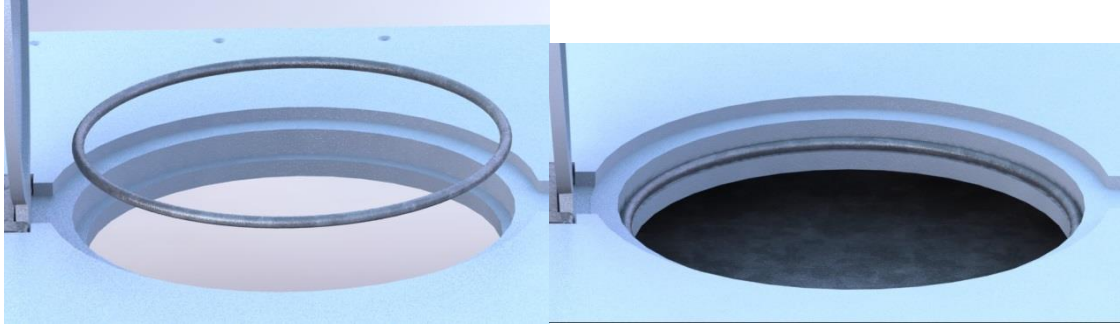


Figure 50. Third generation chute ring. The chute ring is used to support the escape chute. After attaching one end of the chute to the ring, the ring can be placed on the stepped hole inside the housing.

The bottom opening locking mechanism is based on Scott Russel straight-line generator mechanism. Pulling on the hatch handle moves the top link of the mechanism upward, which retracts the latch and unlocks the door. As soon as the hatch handle is rotated, a spring pushes the latch to its locked position. The curved surface of the latch and the spring inside of it allow installers to secure the bottom door in place by just pushing it upward against the latch. The latch will automatically secure the door in the closed position, which enables installers to install the chute inside the unit from the top.

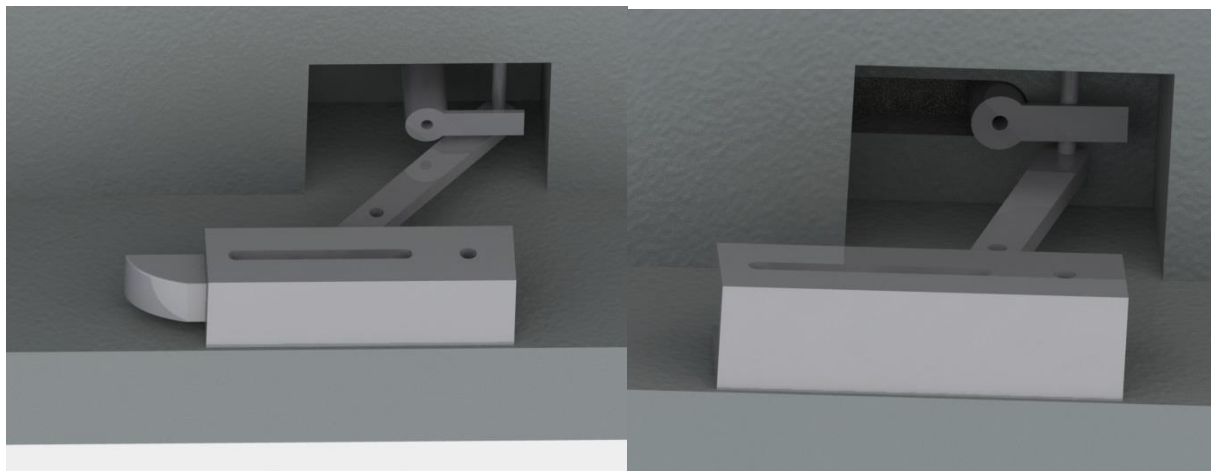


Figure 51. Third generation bottom door latch. This release mechanism is based on Scott Russel straight line generator. Pulling on the top link unlatches the door and releases the chute.

Since, the hatch is required to withstand high forces, have a small deflection, and need to be lifted with no more than 130 N of force, it has to be very stiff and light. After studying hatch and door designs, it was decided to design a model similar to military bunkers blast doors. Blast doors are designed with two main steel outer surfaces and an inner steel grid structure for added strength. The exploded view of the hatch can be seen in Figure 52. All of the parts seen in this

figure need be made out of sheet metal and welded on one another to form a rigid piece. Due to the high strength of the E-glass fiber, and its fast production rate, it was decided to design another hatch using fiberglass, and test its performance.

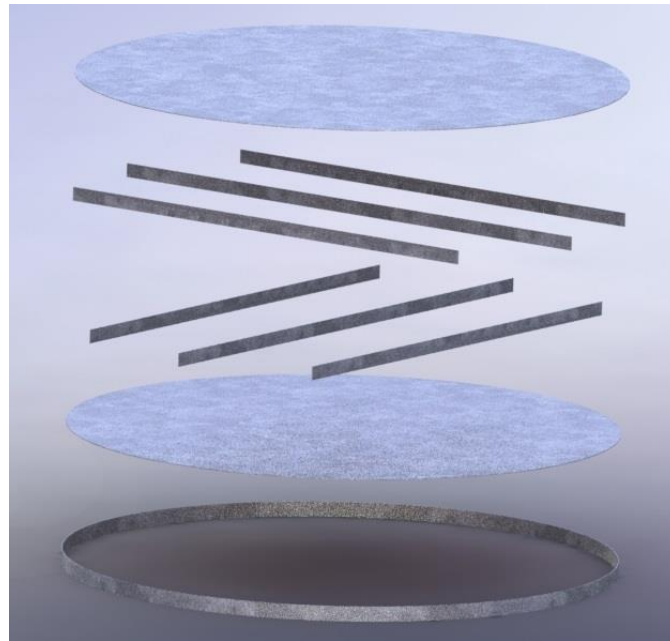


Figure 52. Third generation steel hatch exploded view. This hatch consists of an inner grid structure, an outer ring, and two plates of sheet metal which have to be welded to one another to form a rigid hatch.

Using SolidWorks, two emergency escape hatch models were designed and analyzed for the third generation unit. Based on the requirements, the hatch must have less than one millimeter of deflection with 2500 N of force applied on a 30 cm diameter circle at the center of the hatch. Before running the analysis, the same surface that rests on the housing was fixed, and a bonded contact was defined between all surfaces. Based on these requirements, the steel hatch was modified by reducing the number of core filling grids and lowering the thickness of the hatch until a deflection close to one millimeter was obtained. Steel hatch deformation and stress due to the 2500 N force can be seen in Figure 53 **Error! Reference source not found.** Maximum Von Mises stress was found to be 105 MPa and deformation was found to be 0.721 mm, which satisfy the requirements. The maximum stress in the steel hatch is almost half the yield strength of the material, which means that the hatch passes the requirement of having a safety factor of 1.5.

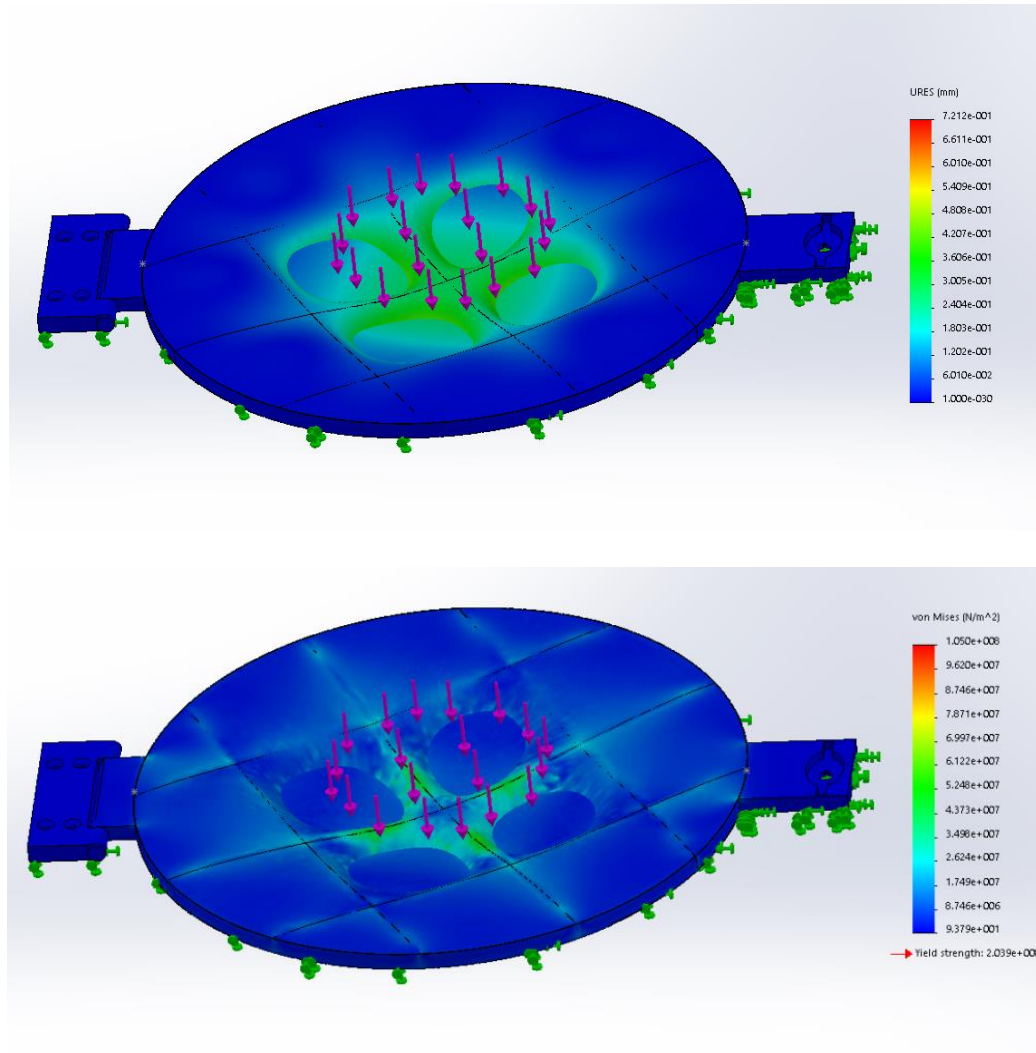


Figure 53. Third generation steel hatch deformation and stress due to 2500 N of force. In these images, the green arrows represent the surfaces that were fixed, and the purple arrows represent the direction of the force and the location at which they were applied. Based on the simulation results, the maximum deformation was found to be equal to 0.721 mm, and the maximum Von Mises stress was estimated to be equal to 105 MPa.

The same boundary conditions and forces were applied to the fiberglass hatch, and static analysis was performed to compare the results between the two hatches. The maximum deformation was found to be equal to 0.661 mm, which is smaller than the deformation of the steel hatch and satisfies the requirement of having a deflection of less than 1 mm. The maximum Von Mises stress in the hatch was found to be 13.97 Mpa. Having a yield strength of 2.875 Gpa, the fiberglass hatch passes the test with a safety factor of 205.8. Refer to Figure 54 for the fringe plot of this analysis.

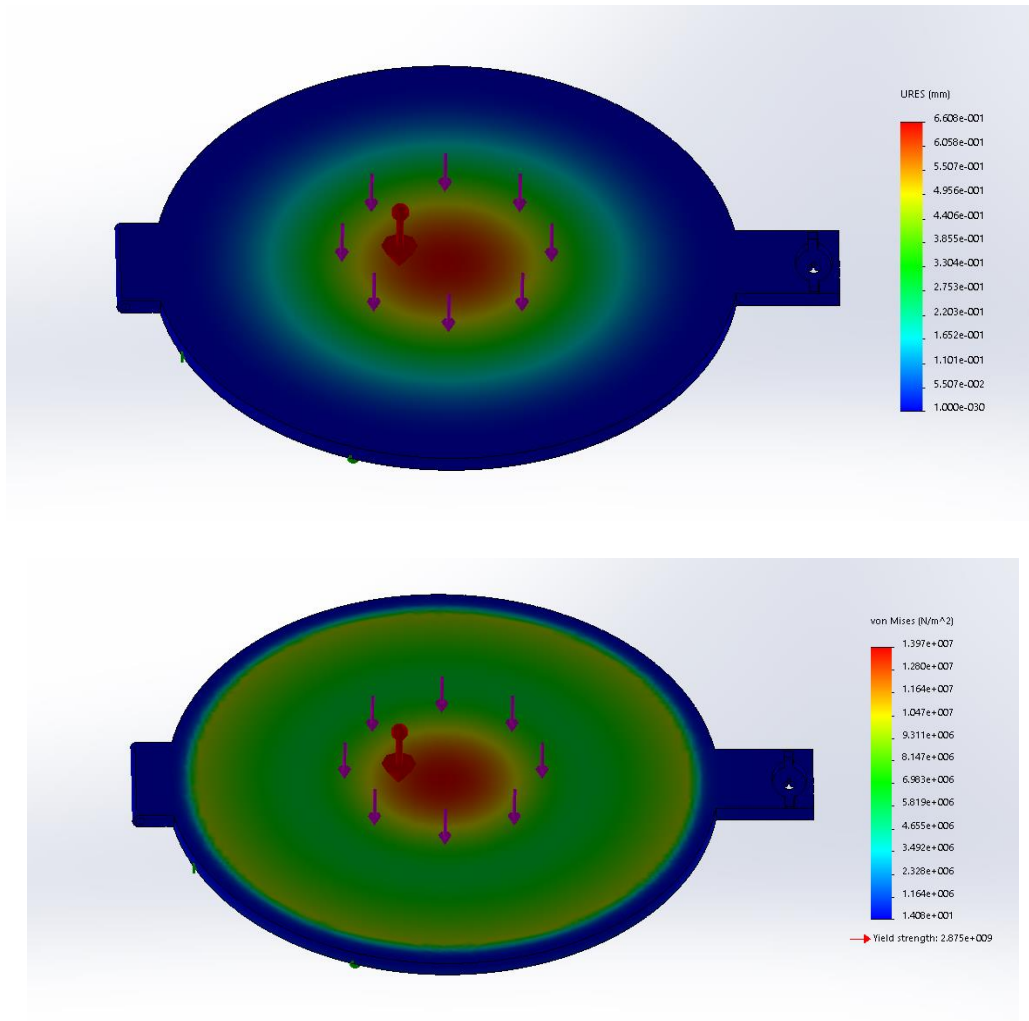


Figure 54. Third generation E-glass fiber hatch deformation and stress due to 2500N of force. In these images, the green arrows represent the surfaces that were fixed, and the purple arrows represent the direction of the force and the location at which they were applied. Based on the simulation results, the maximum deformation was found to be equal to 0.661 mm, and the maximum Von Mises stress was estimated to be equal to 13.97 MPa.

To test the strength of the hatches and makes sure they can withstand common operating conditions, 5000 N of force was applied to the top circular faces of the hatches, which is equivalent to having more than five 100kg people standing on it. Same boundary conditions as the previous analysis were applied to the models. The steel hatch was found to have a maximum deformation of 0.382mm and a maximum stress of 85.16Mpa, which means the model passed the analysis with a safety factor of 1.94.

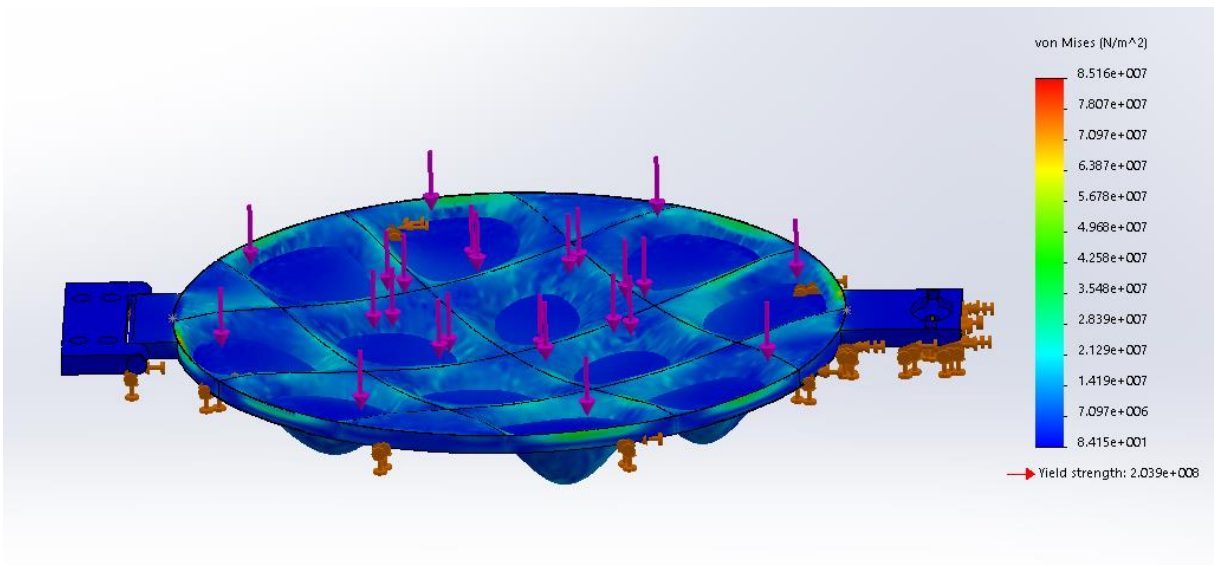
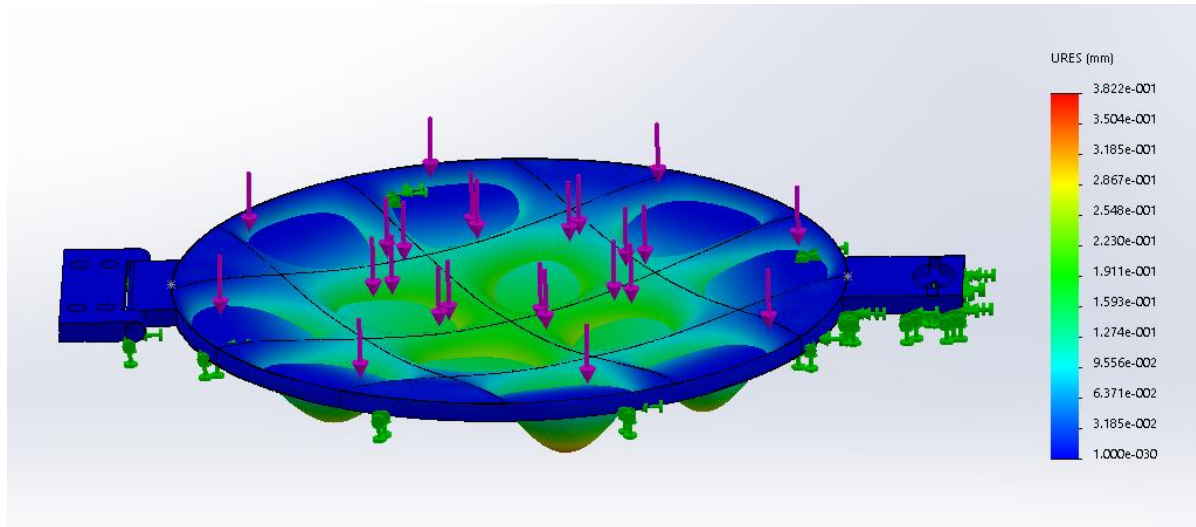


Figure 55. Third generation steel hatch deformation and stress due to a 5000N force. In this image, the brown arrows represent the surfaces that were fixed, and the purple arrows represent the direction of the force and the location at which they were applied. Based on the simulation results, the maximum deformation was found to be equal to 0.382 mm and the maximum Von Mises stress to be equal to 85.16 MPa.

The fiberglass hatch was analyzed using the same boundary conditions as the previous analysis using 5000N of force. Maximum deformation of 0.376 mm and a maximum stress of 8.915 MPa were found from the static analysis. The fiberglass hatch passed the analysis with a safety factor of 319.

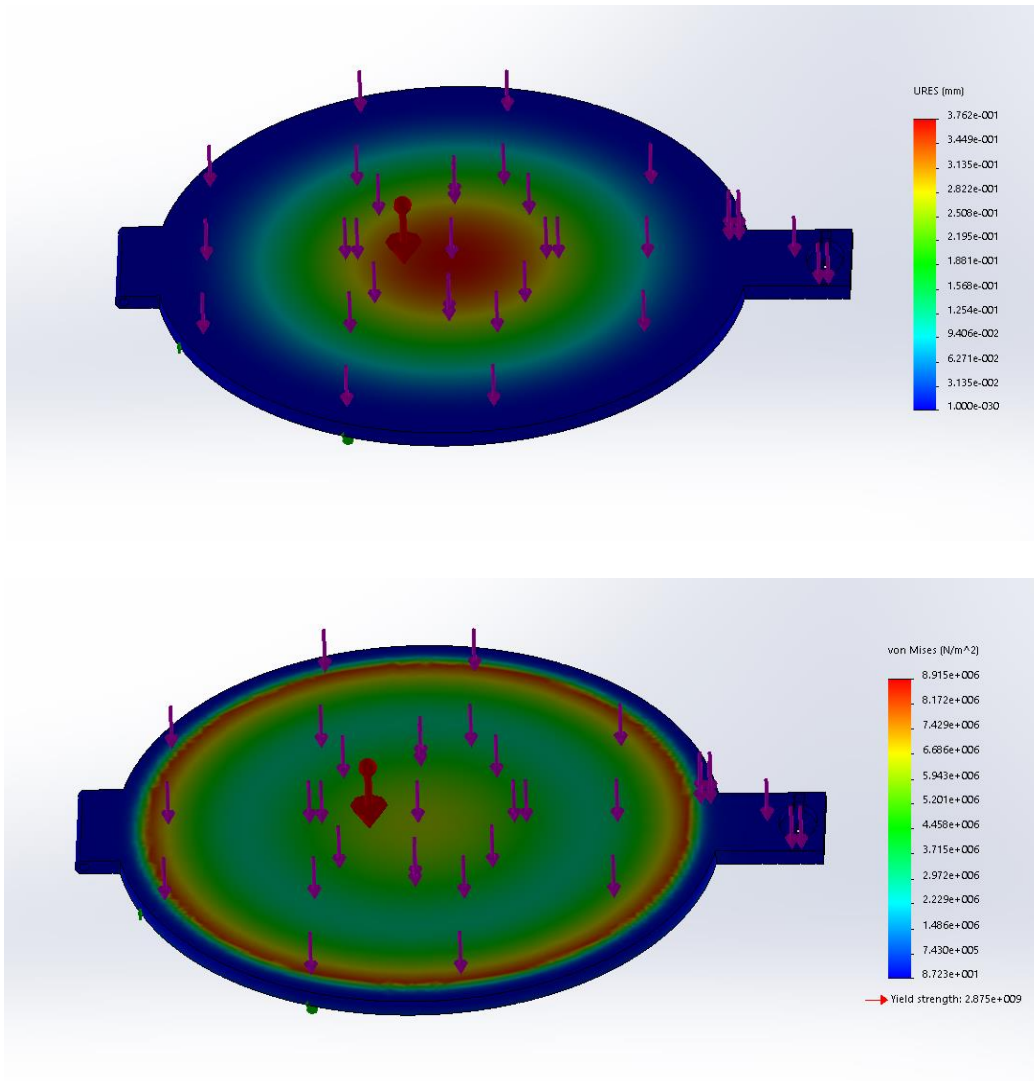


Figure 56. Third generation E-glass fiber hatch deformation and stress due to a 5000 N force. To run this simulation, the same surface of the hatch that would contact the housing was fixed, and 5000 N of force was distributed normally on its top surface. The maximum deformation was determined to be equal to 0.376 mm, and the maximum stress was found to be equal to 8.915 MPa.

Both hatches were tested to see how much force is required to lift them open them. Static analysis was performed by adding a pin connection to the hinge and fixing the hinge connecting piece. A downward gravitational force was added to the model, and the handle was fixed. After running the analysis, the force required to open the hatch was measured at the handle. National Fire Protection Association requires all hatches to be operable with a force of no more than 130 N. As shown in Figure 57, the steel hatch can be opened with a force of more than 68.3 N, and

the fiberglass hatch can be opened with a force of more than 98.2 N. Thus, both hatches pass the test.

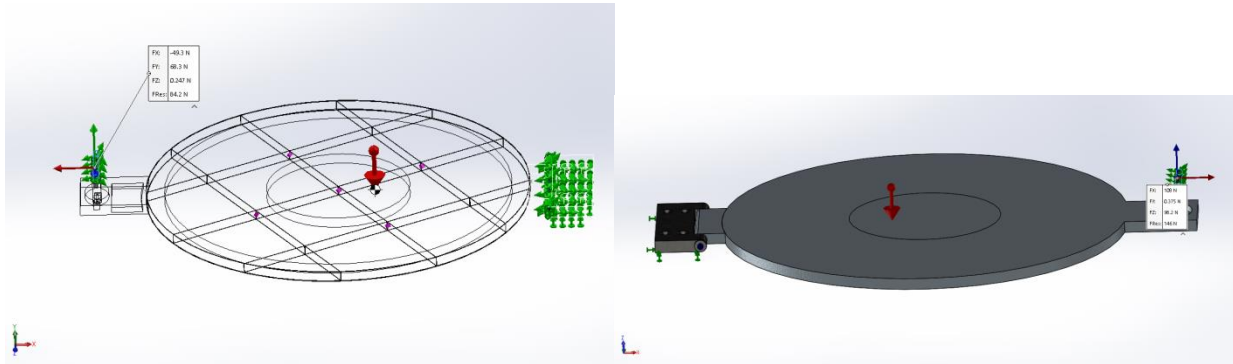


Figure 57. Force required to open the third generation hatches. The image on the left represents the steel hatch, and the image on the right represents the fiberglass hatch. Based on the simulation, the steel hatch can be opened with a force of more than 68.3 N, and the fiberglass hatch can be opened with a force of more than 98.2 N.

After analyzing the hatch, static analysis was performed on the housing to assess whether it could tolerate the operating conditions and satisfy the criteria. The bottom faces of the flanges which would be mounted on the floor of the cabin were fixed, and 5000 N of force was exerted on the surface where the hatch rests on. The maximum deformation was found to be equal to 0.01181mm, and the maximum Von Mises stress was determined to be equal to 912.4 KPa. Based on the yield strength of 2.875 GPa, the main body can withstand much higher forces.

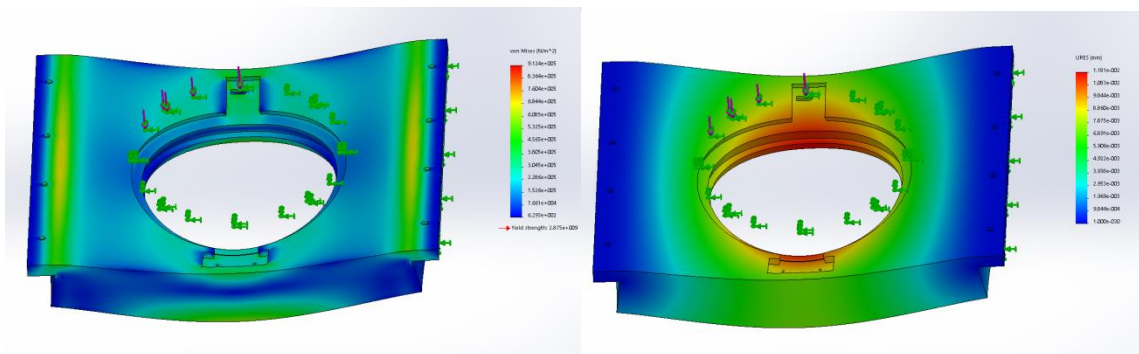


Figure 58. Third generation housing stress and deformation due to 5000 N of force. To run the simulation, the bottom surface of the flanges were fixed, and 5000 N of force was exerted on the same surface where the hatch would be mounted on. The maximum deformation was found to be equal to 0.01181, and the maximum Von Mises stress was determined to be equal to 912 KPa.

The housing was also tested to see if it could withstand having five 100 kg people inside the chute. The chute has a mass of 1.25 kg per meter; a ten-meter chute has a mass of 12.5 kg. To

run this analysis, the bottom surface of the flanges were fixed, and a force of 5027.625 N was exerted on the surface where the chute frame rests on; this force is equal to the weight of the chute and ten people inside of it. Maximum deformation was found to be equal to 0.01306 mm, and the maximum stress was determined to be equal to 989.8 KPa; thus, the model passed the analysis by a factor of 2904.62.

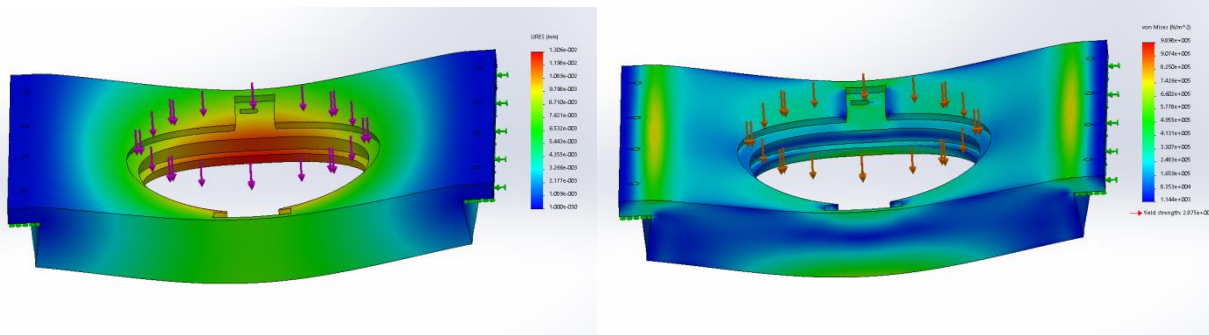


Figure 59. Third generation housing stress and deformation results due to having ten people inside the chute. To run this simulation, the bottom surface of the flanges were fixed, and 5027.625 N of force was exerted on the surface where the chute frame would be placed on. Based on the simulation results, the maximum deformation was found to be equal to 0.01306 mm, and the maximum stress was determined to be equal to 989.9 KPa.

Even though the housing and the hatch did not fail the FEA analysis, the third generation unit was disregarded due to its large mass. The complete assembly including the chute has a mass of 440.5kg, which is extremely high. The large mass is mainly due to the mass of the housing, which is 389 kg. The large mass of the unit reduces the efficiency of the system and creates difficulty in the assembly process. The housing is made entirely out of E-fiberglass, which has a very high density.

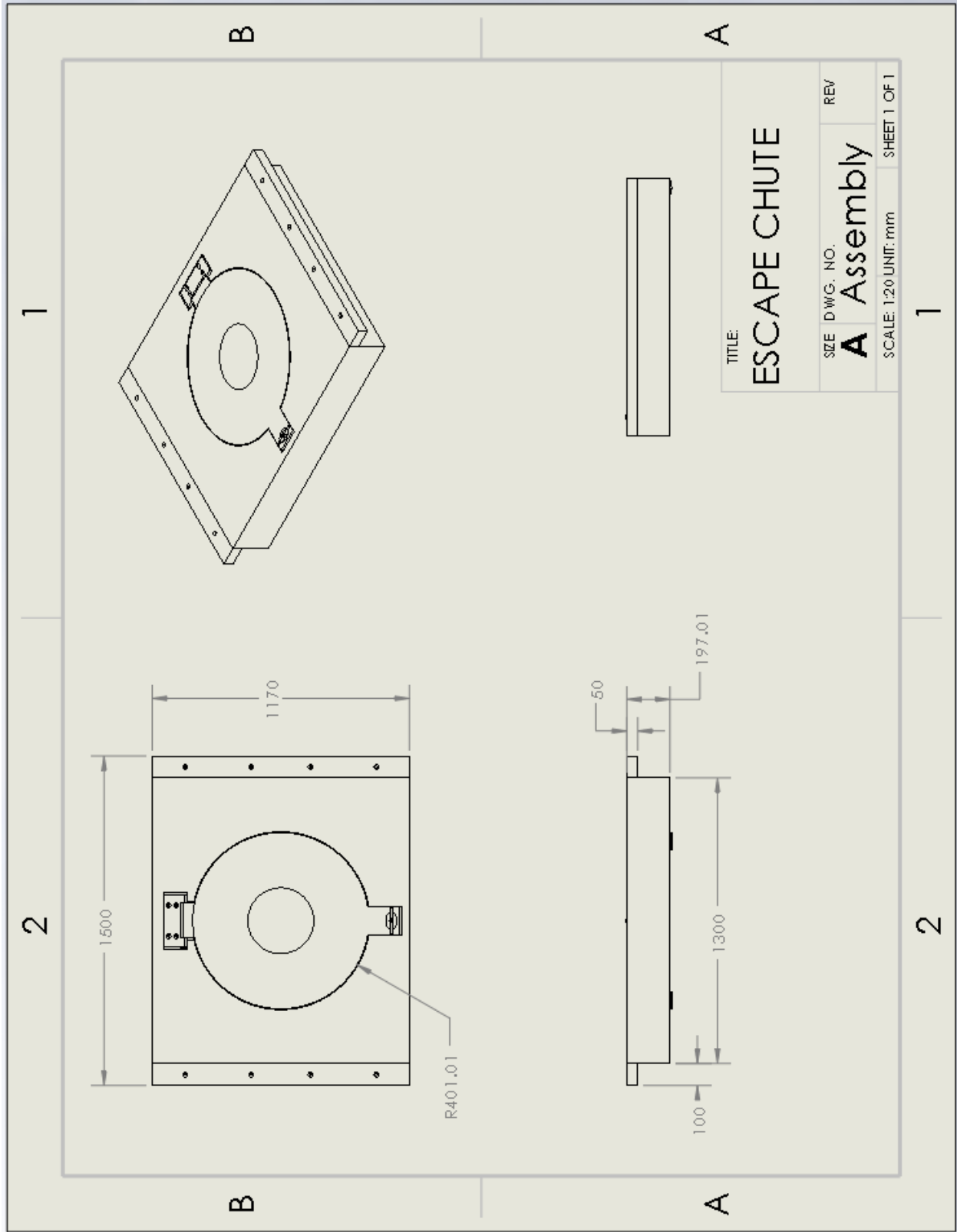


Figure 60. Third generation unit overall dimension. The overall dimensions of the complete assembly of the third generation model can be seen in the above image.

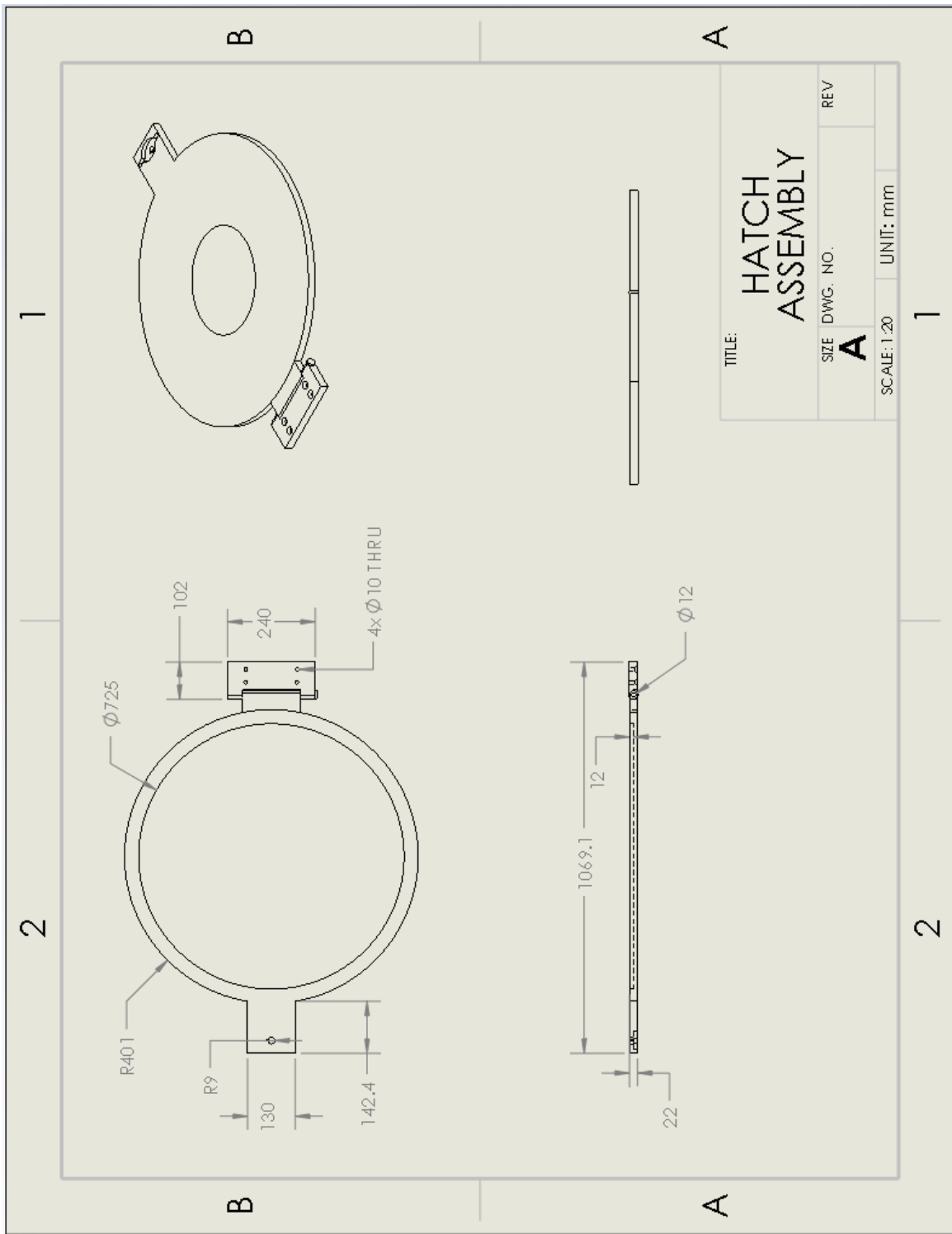


Figure 61. Third generation hatch drawing. This drawing represents the dimensions of the third generation hatch, which was entirely made out of E-glass fiber.

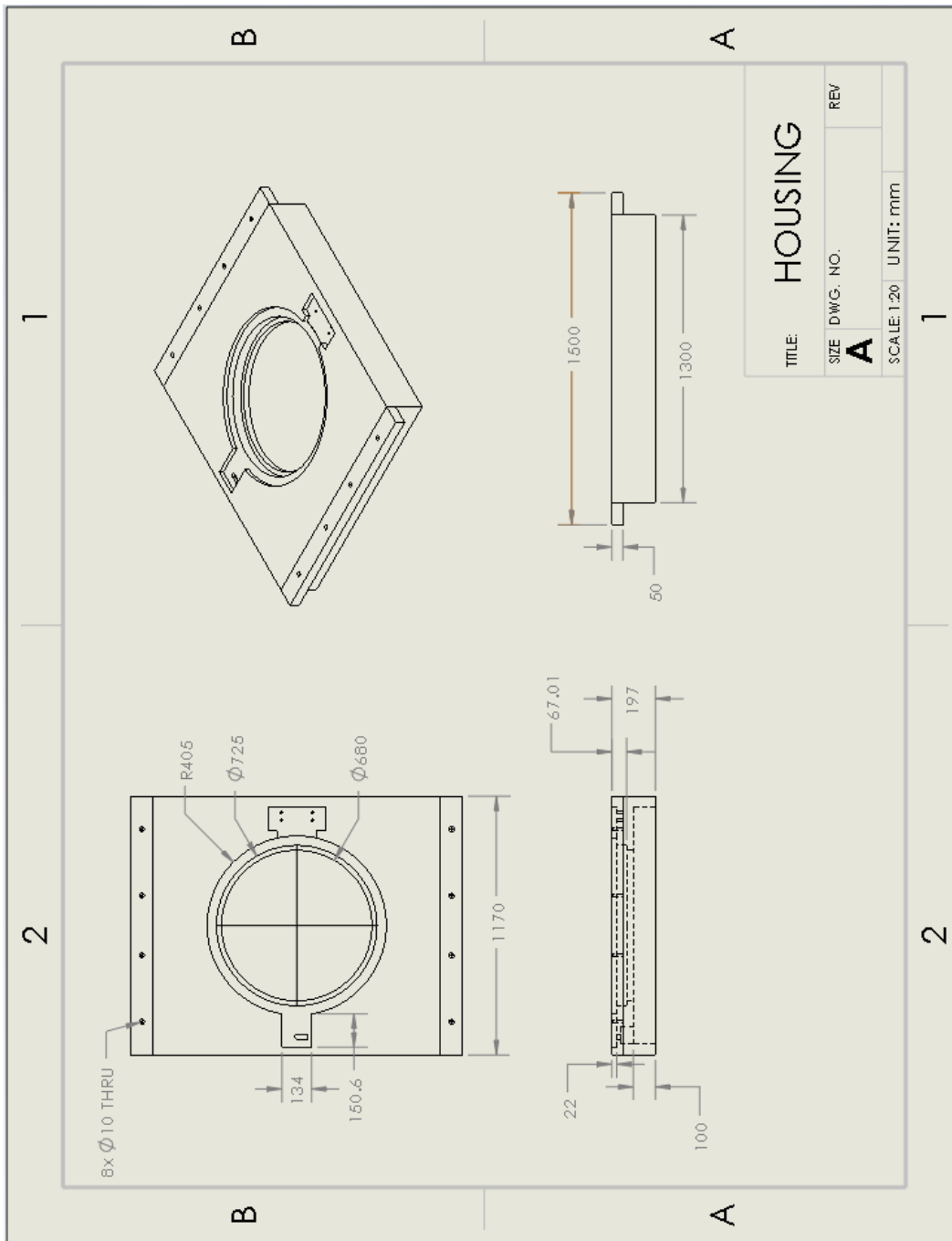


Figure 62. Third generation housing dimensions. The overall dimensions of the third generation housing can be seen in the above image. This hatch was made entirely out of E-glass fiber.

Table 9. E-glass fiber material properties (**E-Glass Fibre**). E-glass fiber was used for the design of the third generation hatch and housing.

<b>Property</b>	<b>Value</b>
Elastic Modulus (N/m <sup>2</sup> )	8.5e+10
Poisson's Ratio	0.23
Shear Modulus (N/m <sup>2</sup> )	3.6e+10
Mass Density (kg/m <sup>3</sup> )	2770
Tensile Strength (N/m <sup>2</sup> )	2.05e+9
Compressive Strength (N/m <sup>2</sup> )	5e+9
Yield Strength (N/m <sup>2</sup> )	2.875e+9
Thermal Expansion Coefficient (1/K)	5.1e-6
Thermal Conductivity (W/(m·K))	1.35
Specific Heat (J/(kg·K))	805

Table 10. Galvanized steel material properties (SolidWorks material properties). Galvanized steel was used to design the door and the release mechanism of the third generation unit.

<b>Property</b>	<b>Value</b>
Elastic Modulus (N/m <sup>2</sup> )	2e+11
Poisson's Ratio	0.29
Mass Density (kg/m <sup>3</sup> )	7870
Tensile Strength (N/m <sup>2</sup> )	356900674.5
Yield Strength (N/m <sup>2</sup> )	203943242.6



# CERTIFICATE

Management system as per  
**DIN EN ISO 9001 : 2015**

In accordance with TÜV NORD CERT procedures, it is hereby certified that

**Axel Thoms**  
Lebensrettungseinrichtungen GmbH  
Bimöhler Str. 32-36  
24576 Bad Bramstedt  
Germany

applies a management system in line with the above standard for the following scope

**Development, production, marketing, installation and  
service of life saving equipment**

**"Escape Chutes" (Mobile & stationary)**

Certificate Registration No. 07 100 990750  
Audit Report No. 3515 1397

Valid from 2018-01-25  
Valid until 2021-01-24  
Initial certification 1999



Certification body  
at TÜV NORD CERT GmbH

Essen, 2018-01-23

This certification was conducted in accordance with the TÜV NORD CERT auditing and certification procedures and is subject to regular surveillance audits.

TÜV NORD CERT GmbH

Langemarckstraße 20

45141 Essen

[www.tuev-nord-cert.de](http://www.tuev-nord-cert.de)



Figure 64. Axel Thom's certificate. The above mobile/stationary escape chute certificate was retrieved from one of Axel Thoms' employees.

## THOMS Escape chute – AT-1

### DIN 4102 B I

flame retardant standard – B I is highest standard for flammable fabrics, A II is the next higher, which is inflammable (e.g. Kevlar, fibre glass with the according disadvantages: UV resistance, breaking / folding)

### DIN 5510-2 S4

flame expansion speed

Standard used for textile fabrics in use for example in public transportation etc.

### DIN EN ISO 9001 : 2000

QM Managementsystem

### DIN 1055 Part 4

loading assumption for buildings, conformity to standard for frame and static analysis (and corresponding combination)

### DIN 31000 Richtlinie 95/16/EG

Technical safety standard, referring to safe user design (operation and use), 'Technical safety elaboration' – e.g. prevention to bruise one's finger etc.

### EN 294

safety measures and dimensions

Technical safety standards, referring to safe user design (operation and use), 'Technical safety elaboration' – e.g. prevention to bruise one's finger etc.

### DIN 53857

streight test for textile fabric – testing standard, results stated in fabric certificates

### DIN 3416/3418/3419

Technical standard for zippers, strength etc. (Mobile chute)

### DIN 18800-7

producer qualification for steel welding

### DIN 4131 Class E

process class for steel welding – related producer qualification required

### DIN 1876-1

Durability and strength tests at -40°C

Certified by 'Germanischer Lloyd' – globally responsible for shipping and offshore safety, performed for offshore use on Russian offshore platform

### GL 3.1 C

Approval for 'Germanischer Lloyd', referring to DIN 1876-1

### GPSG § 7(1)

Equipment and Product Safety Act

### M 48/8

TÜV testing program – certification for securing continuous conformity of products, production processes and production site to the ISO standards

Figure 65. Axel Thoms DIN explanation. This figure was retrieved from one of Axel Thoms' employees and describes some of the standards that were used during their chute manufacturing.